# Cosmological Observations in Braneworld Models

**Christophe Sebastian Rhodes**
**Jesus College**

Dissertation submitted for the degree of Doctor of Philosophy

University of Cambridge

October 2003

# Declaration

The material presented in this thesis is original and entirely my own except where explicitly stated in the text, and except for section 2.6 which contains work done in collaboration with Ian Vernon. Chapter 1 provides an overview of the scientific activities relevant to this thesis, and no claims of originality are made here. Chapter 2 is largely based on Journal of High Energy Physics 0111 (2001) 015 (with Dr. A.-C. Davis and Ian Vernon); portions of chapter 3 appeared as Physics Letters B531 (2002) 135–142 and Physical Review D65 (2002) 121501 (with Drs. Ph. Brax, C. van der Bruck and A.-C. Davis); chapter 4 is based on Physical Review D67 (2003) 023512 and Astrophys. Space Sci. 283 (2003) 627–632; chapter 5 is currently in press,to appear in Physical Review D (with the same co-authors). The work contained in chapter 6 is in preliminary form. Whilst these papers have been published in collaboration, I have included only my own contributions in this thesis.

To the best of my knowledge, the work presented as my own is original.

# Acknowledgements

I have greatly benefitted from discussions with Carsten van der Bruck, Philippe Brax, Stephen Davis, Chris Gordon, Fernando Quevedo, Neil Turok, and Ian Vernon. To the many people who have sacrificed their leisure time to proofread portions of this document, including Patrick Ashcroft, Francis Bursa, Jonathan Keeling, David Lewis, and Sam Webster, goes profound gratitude. My family – Tony, Elisabeth and Sophie – has provided great support at difficult times. Many musicians have provided a means of recreation and a way to escape, including the Lark Ensemble (Karl Sandeman, Leo Tsai, Nat Brown) and the Boys (Katie Hawks, Lewis Brown, Mark Dourish, Chris Jordinson, Anthony Smith, Matthew Lavy) among countless others. Eamonn Long, Sakura Schäfer-Nameki, and Ian Vernon, my officemates, deserve a vote of thanks for tolerating my bursts of whistling or song, and for providing a congenial atmosphere for day-to-day work. My thanks also go to Bill Newman, Dan Barlow and Alexey Dejneka for providing a completely different set of problems for after-hours.

These acknowledgements would be incomplete, however, without special mention of two people. Firstly, Anne-Christine Davis, whose advice and encouragement has been invaluable throughout my studies. Secondly, Jenni Hearn, who provided much-needed support – not to mention a critical eye and a red pen – deserves much gratitude, and probably a medal.

This work was supported by PPARC.

# Abstract

In this thesis we investigate the effects on cosmological observations due to extra dimensions. In particular, we consider braneworld models, wherein Standard Model fields are confined to a four-dimensional hypersurface embedded within a higher-dimensional space in which gravity is free to propagate, and derive several cosmological observational consequences from models under consideration. Models of higher-dimensional cosmology are sometimes invoked in attempts to resolve problems of the Standard Cosmology. We investigate one such attempt, and conclude that in a realistic cosmological model based on either of the Randall–Sundrum braneworld scenarios, we cannot solve the cosmological horizon problem in a simple manner, though our investigation does reveal possible signatures of extra dimensions observable in future gravitational wave experiments.

We go on to consider the form of the effective theory of gravity as it would be perceived by an observer confined to the hypersurface, showing that a supergravity model in five dimensions reduces to a theory which is of Brans–Dicke form, though with an extra gravitational scalar degree of freedom; we also demonstrate the presence of an attractor towards an effective Einsteinian General Relativity for certain initial configurations.

Following this, we examine the model under a more robust approximation for the derivation of the four-dimensional effective theory. We replicate our previous results, characterize the attractor towards four-dimensional General Relativity, and consider the possibility of deriving a model with varying fine-structure constant. We further examine possible phenomenological effects arising from the difference in coupling of gravity to normal and dark matter.

We then discuss the effect of the time evolution of extra dimensions on cosmic microwave background anisotropies, studying the impact of the effective theory scalar fields on the temperature anisotropy power spectrum. We show that when the coupling between these scalar fields and matter evolves over cosmological timescales, current observations of the CMB anisotropies can constrain primordial values of the fields in a manner complementary to local, late-time tests of gravity. We present the effect of these fields on the polarization anisotropy spectra and the growth of large-scale structure, showing that future CMB observations will constrain theories of the Universe involving extra dimensions even further.

# Contents

# Chapter 1

# Introduction

## 1.1 Twentieth Century Physics

The twentieth century saw not just one but several revolutions in our physical understanding of the world around us. At the century's very dawn, in 1900, the field of Quantum Physics was born with Max Planck's explanation of the black-body radiation spectrum; fifteen years later, Albert Einstein's General Theory of Relativity allowed us to view gravity with new eyes.

There exists a tension between these two physical models, however. The quantum theory of the electromagnetic field, QED, is a phenomenally successful theory in its domain; it has been used to calculate the gyromagnetic ratio of the electron to extraordinary precision and accuracy – famously, equivalent to measuring the distance "between Los Angeles and New York [...] exact to the thickness of a human hair" [1]. Other branches of Quantum Field Theory (or QFT) predicted the existence of hitherto-undetected particles and have shown similarities between apparently distinct interaction mechanisms, allowing the development of a unified theory of the electromagnetic, weak and strong forces (the Standard Model of particle physics). These theories are at their most useful when dealing with a small number of individual particles – at their root they deal in quanta, the smallest division of a quantity possible.

By contrast, Einstein's theory of General Relativity is a very successful theory on very large scales. Like QFT, it has been subjected to a large range of tests, from the amount of deflection of light by the Sun [2, 3] and the precession of Mercury's orbit to the decay rate in the orbits of binary pulsars and the expansion of the Universe [4]. If the evidence supporting General Relativity on large scales is more scant than that supporting QFT on small scales, it is mostly because of the technological difficulties in acquiring data from 'experiments' on such scales.

The tension becomes most evident when trying to combine these two theories, to provide a 'Grand Unified Theory' or a 'Theory of Everything'. Simply put, General Relativity, despite its being a local theory based on a symmetry principle like the other theories, resists being quantized – the theory obtained from a naïve quantization is non-renormalizable and hence useless. The first viable answer to this problem was the suggestion that the worst infinities arising could be avoided if, instead of point particles, one postulated that the fundamental building block of the theory should be a one-dimensional string.

This String Theory does allow a quantization of the gravitational field of General Relativity, but with a caveat: the resulting theory is only consistent if there are 10 spacetime dimensions. To explain the discrepancy between this and the four spacetime dimensions that we observe, we fall back to an idea due to Kaluza and Klein [5, 6] developed in a previous attempt at unifying gravity with electromagnetism: that the extra six dimensions are small and compact, and have stable radii. This means that, for experimental scales larger than these radii, the results of an experiment will appear to support the hypothesis that only four dimensions are present.

Nonetheless, General Relativity, along with the observations that can be made when twentieth century technology is brought to bear on the Universe, has founded the field of cosmology. Firstly, from purely theoretical grounds, an expanding Universe is a very natural solution to the equations of the Universe. Though Einstein's Cosmological Constant can be tuned to generate a static Universe, this solution is very special – any deviation from the tuned value leads inevitably to collapse or expansion. Since it was later observed [4] that the Universe in fact did seem to be expanding, the natural question to investigate was what happened earlier in the Universe's history. Following the evolution backwards, one is led[1] to surmise that the Universe early in its history must have been very hot – sufficiently so that its dynamics would have been dominated by the radiation content, rather than by matter.

This scenario, known today as the Big Bang model of the Universe, predicts that the remnants of this early radiation domination should be observable today, and indeed Penzias and Wilson [7] (serendipitously) discovered a faint radiation from the very background of

[1] Though not inevitably. Other paradigms of the Universe's history have largely fallen out of favour, due to the contortions that their proponents have to go through to justify them in the harsh light of today's evidence; the Steady State Universe, for instance, is not a serious contender to explain our Universe at present.

the sky, of equal intensity in all directions. This observation, of course, throws up its own problems, as clearly today's Universe is not homogeneous and isotropic. The fact that we observe the present Universe to be clumpy indicates that there must have been some perturbations away from homogeneity at some earlier point in the Universe's evolution: and indeed the COBE satellite team observed [8] that, though this radiation was very close to that of a black body at 2.7K, there were inhomogeneities distributed over the sky of magnitude about one part in $10^5$. This observation perhaps marked the beginning of a new stage in cosmology, as these inhomogeneities provide a view of the state of the universe at the time radiation and matter decoupled from each other. Thus we find a way of probing the result of interactions at higher energies than can be examined in current laboratory experiments, and so of testing theories of the early Universe.

## 1.2 Modern Cosmological Observations

### 1.2.1 The Equivalence Principle and tests of General Relativity

The Equivalence Principle as Einstein proposed it was that all non-gravitational laws of physics should be the same as measured in different local freely-falling frames, irrespective of their relative velocities. This principle lies behind the theory of General Relativity and also behind many of the competing classical theories of gravitation.

One example of such a competing theory is the scalar–tensor theory of Brans and Dicke [9]. Though by this point in time Brans–Dicke theory is unviable as a theory of gravitation distinct from General Relativity, after its development it spurred experimenters on to design and execute experiments aiming not just to measure General Relativistic effects, but to quantify them sufficiently to be able to distinguish between the different theories. The Brans–Dicke theory has not only a gravitational metric tensor, but also a gravitational scalar field, motivated by the need to have a varying gravitational 'constant' to conform to the Machian principle that objects accelerate with respect to the 'distant stars'.

Brans–Dicke theories are parametrized by a dimensionless coupling constant $\omega$ between the scalar field and the metric tensor, with the limit $\omega \to \infty$ leading to a theory indistinguishable from General Relativity. While this family is not not the only possible scalar–tensor theory of gravity, it is in some sense the next obvious candidate after General Relativity, and it is useful to examine how current experiments constrain the value of the Brans–Dicke parameter.

Tests of the Einstein Equivalence Principle, such as the Eötvös experiment (measuring the difference in gravitational acceleration between bodies of the same mass but different composition; see e.g. [10] for a review of this and many other gravitational experiments) do not allow us to distinguish between metric theories of gravity (or between possible values of the Brans–Dicke parameter), because all such theories incorporate the Einstein Equivalence Principle. However, these theories do give different predictions under the Strong Equivalence Principle, which extends the Einstein Principle by postulating that gravitational effects are the same in all freely-falling frames.

Treating the Solar System as a gravitational laboratory, then, can enable measurements to be made which are capable of distinguishing between metric theories of gravitation. Such measurements include that of the deflection of radio waves from quasars by the Sun's gravitational field; the time delay of light signals sent from spacecraft orbiting planets, such as the Mariner and Viking missions; and the precession of the perihelion of Mercury. Results from these experiments constrain the Brans–Dicke parameter to be greater than 250, which translates to differences in the predictions given by Brans–Dicke gravity and General Relativity of the order of 0.2% [10]. Though this constraint applies of course to all theories beyond General Relativity, any viable Brans–Dicke theory must be essentially indistinguishable from General Relativity for all time, not just at the present epoch, because in the Brans–Dicke theory the coupling function is a constant. Other scalar–tensor theories are not so constrained [11].

### 1.2.2 Cosmic Microwave Background Anisotropies

Twenty-eight years elapsed between the initial detection of the Cosmic Microwave Background Radiation [7] and the first observations of non-dipole[2] anisotropies [8]; this time difference, and the fact that the anisotropies were discovered at a level of one part in $10^5$, forces attention to the fact that the matter distribution in the Universe today is of a quantitatively different character from at the surface of last scattering: the matter perturbations away from uniformity today are strongly non-linear, as evidenced by the fact that we live on a solid ball of rock and iron. Matter inhomogeneities grow due to gravitational instability, but the same does not happen to radiation because of the inherent pressure. The smallness of the perturbations in the radiation allows us to use linear response theory in much of the analysis of CMB fluctuations, which means that few, if any, phenomenological parameters for non-linearities need to be introduced, greatly facilitating interpretation of the observations.

[2]Any dipole anisotropy can be explained by the proper motion of the observer [12].

The basic quantity observed in the CMB is its intensity at a given frequency. However, since the radiation is an extremely good black body with a fixed temperature $T$ over the sky, we can describe this observable in terms of a temperature fluctuation $\frac{\delta T}{T}$. With the further assumption of Gaussianity in these fluctuations, the multipole moments of the temperature field $a_{lm}$ are fully characterized by their power spectrum

$$\langle a^*_{lm} a_{l'm'} \rangle = \delta_{ll'} \delta_{mm'} C_l. \tag{1.1}$$

For small angular scales (corresponding to small regions of the sky, or high $l$) this harmonic analysis is simply Fourier analysis, and $l$ is the Fourier wavenumber, so what is generally plotted in results from CMB experiments or calculations is the power per logarithmic interval in $l$ (for large $l$),

$$\Delta_T^2 = \frac{l(l+1)}{2\pi} C_l T^2. \tag{1.2}$$

There is a fundamental limitation to the possible precision of observations of $C_l$: since (in our region of the Universe) we can in principle only have $2l+1$ samples of each multipole moment's power, we can only measure the power in a multipole $l$ to a precision of about $l^{-1}$ – 1% at $l = 100$. Added to this fundamental error will of course be any experimental, instrumental or astrophysical sources of error.

As a further complication, the radiation reaching observers on Earth will probably have a net polarization, due to Thomson scattering; the magnitude of a polarization anisotropy is expected to be of order 10% of the temperature anisotropy. Decomposing the polarization into scalar and pseudoscalar modes, there are then three additional multipole observables (again assuming Gaussianity): the scalar power spectrum, the pseudoscalar power spectrum, and the cross-correlation between the scalar and temperature anisotropies (other cross-correlations are zero by parity invariance).

It is relatively simple to understand how fluctuations lead to acoustic peaks in the anisotropy power spectrum. Fluctuations of a particular wavenumber $k$ obey a wave equation

$$\ddot{\Theta} + c_s^2 k^2 \Theta = 0, \tag{1.3}$$

with $c_s$ the sound speed. Initial perturbations thus evolve until recombination, at which point

$$\Theta(\eta) = \Theta(0) \cos(k s_*) \tag{1.4}$$

where $s_*$ is the distance that sound can travel before recombination time.

Thus, at large scales (small $k$), we probe the initial perturbation; at smaller scales, we expect to see oscillations, as any mode which is at a maximum or minimum of its oscillation at recombination will have higher power than its neighbours. We therefore expect to see harmonic peaks in the power spectrum of the Microwave Background.

Many other physical effects play their part in the determination of the CMB. It is beyond the scope of this overview to go into all of the effects; instead, we refer the reader to any of a number of reviews on the subject [13–16], and defer some details to chapter 5. One point should be highlighted here, however: namely, that the theory of the CMB does not address the question of the initial power spectrum, which is usually assumed to be a scale-invariant, curvature power spectrum. There are several motivations for this particular assumption, not least that it seems to agree very well with the observations we have; the inflationary paradigm, in particular, predicts a scale-invariant power spectrum [17], though other early-Universe models such as the recent ekpyrotic scenario [18] can generate such a spectrum. In any case, throughout this thesis, and in particular in chapter 5, we assume that the initial power spectrum of perturbations, whatever its source, is of scale-invariant density perturbations.

The inhomogeneities expected in the Cosmic Microwave Background Radiation can thus be calculated for a theory, given an initial perturbation spectrum. Various computational tools have been developed to enable this calculation to be made sufficiently quickly; the particular advance that had the greatest effect was precomputation of the purely geometrical portion of the calculation [19]. These calculated spectra can then be compared against observation where observations have already been made by experiments, and predictions made for data not yet available with today's experiments, in anticipation of the refinement of data from the MAP satellite [20] and ongoing refinement from existing ground-based experiments such as DASI [21], and in the medium term the launch of the Planck satellite of the European Space Agency (due in 2007).

### 1.2.3 Metal Abundances and Primordial Nucleosynthesis

One of the standard Big Bang model's most striking successes is in accounting for the observed abundances of light elements. In the very early Universe, by which we mean that for all particles under consideration $kT \gg mc^2$ and the timescales for interactions involving these particles is shorter than the age of the Universe, we can infer the equilibrium number densities of particle species from statistical mechanics as

$$n = \frac{4\pi g}{h^3} \int_0^\infty \frac{p^2 \mathrm{d}p}{e^{E/kT} \pm 1}, \tag{1.5}$$

with $g$ being the degeneracy of the particle, $p$ its momentum and the sign dependent on the statistical properties of the species. The relativistic limit of equation (1.5) yields a number density proportional to $T^3$. By contrast, the non-relativistic limit $kT \ll mc^2$ gives

$$n = g \left( \frac{mkT}{2\pi\hbar^2} \right)^{\frac{3}{2}} \exp\left( -\frac{mc^2}{kT} \right); \tag{1.6}$$

in other words, the contribution from these species is exponentially suppressed. In particular, applying this to the nucleon-neutrino system early in the evolution of the universe, at redshifts of about $10^{12}$, we find that since the protons and neutrons are non-relativistic, but electrons and neutrinos are, in equilibrium the abundances of neutrons and protons is given by

$$\left[ \frac{n}{p} \right] \sim \exp\left( -\frac{\Delta mc^2}{kT} \right). \tag{1.7}$$

This relative abundance 'freezes out' at a value of approximately 0.27 when the rate of the equilibrium-maintaining reactions drops below the Hubble rate, at a time of about 1 second after the Big Bang. Nucleosynthesis can then begin through the ordinary nuclear reactions familiar from stellar nucleosynthesis, leading to the production of one $^4$He nucleus for every two primordial neutrons.

To obtain a precise prediction for the primordial abundance of Helium, more detailed calculations must be made, because over the timescale of primordial nucleosynthesis some of the neutrons, being unstable to weak interactions, will decay spontaneously. The thermal history of the Universe was worked out in [22], following earlier calculations of the same sort, showing that most of the nucleosynthesis occurs at a time of around 300s into the Universe's history; this gives [23] an expected relative helium mass abundance of 0.25. One can also calculate the expected primordial abundances of other species, such as deuterium, helium-3 and lithium-7.

The deuterium and $^3$He abundances provide constraints on the baryon fraction of the Universe. To see this, first note that the abundance of $^4$He is essentially predicted by the equilibrium thermodynamics of the Universe; the amount generated is a function of the neutrino decoupling temperature. By contrast, the intermediate products will be present in abundances dictated by the subsequent thermal history: if the baryon density is high, then the nucleosynthesis rate will be sufficiently high to ensure that all of the intermediate products react to form $^4$He; on the other hand, a low baryon density means that there are correspondingly more intermediate products left over when the temperature of the Universe drops below the nucleosynthetic range. Thus, primordial abundances of light elements can measure the present baryon density of the Universe.

Computation of the expected abundances of light elements have been done [24] as a function of $\Omega_B$ (really $\Omega_B h^2$, where $h$ is Hubble's constant $H_0$ in units of 100km s$^{-1}$ Mpc), and, comparing with recent observations of abundances as measured by the Hubble Space Telescope and other experiments, gives even using very conservative values for $h$ a constraint for $\Omega_B < 0.2$ (see [25] for a thorough discussion).

This analysis, of course, depends on various physical constants that we measure today being the same at the epoch of nucleosynthesis; for example, since the mass difference between the proton and neutron is probably electro-magnetic in origin, our calculated value for the freeze-out ratio of proton to neutron abundances and hence the amount of primordial $^4$He is extremely sensitive to the value of the fine structure constant. It turns out that our models of nucleosynthesis strongly constrain the allowed variation of fundamental constants between the epoch of nucleosynthesis and today's values [24], which will be relevant in the following chapters.

## 1.3 Modern models with extra dimensions

We have seen, then, that though Standard Cosmology successfully explains many of the modern cosmological observations, there remain problems in the framework. The clearest theoretical problem lies in the quantization of Gravity: if, as we suspect, superstring theory or something like it is the answer to this problem, then models of the Universe must include extra dimensions.

Many frameworks exist for working with cosmology in extra dimensions; the present work will concentrate on objects known as 'branes'. The origin of this term is as a generalization of 'membrane' (on which more in section 1.3.1); we will be describing our Universe as a '3-brane' (or, sometimes, a brane with co-dimension 1).

The exact nature of a brane depends to some extent on the model of which the theory in question is viewed as a reduction; however, we shall consider a 3-brane to be an entity with three space and one time dimensions as normal, and infinitesimal extent in other dimensions. Further, we shall assume that the Standard Model fields are confined to the brane, but that gravity propagates everywhere in the four spacetime dimensions of our Universe and in all other dimensions, according to Einstein's theory of General Relativity trivially adapted to the higher dimensionality.

This means that, viewed from a higher-dimensional perspective, the stress–energy–momentum tensor of the Universe can be decomposed into parts $T_{AB}^{\text{bulk}}$, representing the bulk fields' contribution, and $\delta(\mathbf{y})S_{AB}$, which accounts for the matter on the brane (assuming the brane to live at the 0 coordinate in the extra dimensions $\mathbf{y}$).

### 1.3.1 M-theory

M-theory is the name given to the theory that overarches the five known String theories; it is believed that the String theories are limits of the M-theory in certain circumstances. The 'M' in the name is a slightly ambiguous initial; it was named thus because M-theory might, or might not, have a direct connection with the theory of membranes. For our purposes, however, we shall mainly be concerned with the identification [26, 27] of the $E_8 \times E_8$ heterotic string theory in the strong coupling limit as a solution to eleven-dimensional supergravity on an $R^{10} \times S^1/Z_2$ orbifold. This theory can then consistently be reduced to a five-dimensional one, using the standard Kaluza–Klein dimensional reduction, giving a Minkowski spacetime with one extra dimension.

At the ends of the orbifold, cancellation of quantum anomalies requires that there be boundary branes. Making the identification of one of these boundary branes with our Universe can directly lead [28] to a description of cosmology within eleven-dimensional supergravity. This model is interesting in itself, and has also sparked interest in models with extra dimensions in general, as we shall see in the following sections.

### 1.3.2 The hierarchy problem

One unsolved problem in modern high-energy physics is the hierarchy problem, which can be expressed as follows: why do there seem to be two relevant energy scales in the Universe?

The electroweak scale, of order $m_{\text{EW}} \sim 10^3\text{GeV}$, and the Planck (gravitational) scale $M_{\text{Pl}} \sim 10^{18}\text{GeV}$ seem, to current theories, both to be fundamental energy scales of nature. However, if we make the (philosophically appealing) assumption that there is one underlying, unifying theory in the Universe, then we would expect to have one essential energy scale, and be able to derive one or both of the electroweak and Planck scales from details of the unifying theory.

A purely phenomenological model [29–31] based on extra dimensions can resolve this problem in a simple way. A $4+n$ dimensional model was considered, with a (fundamental) Planck mass ${}^{(4+n)}M_{\mathrm{Pl}}$, and with Standard Model fields confined to a 3-brane; the $n$ extra dimensions are taken as compact, with radius $R$. Then, for a four-dimensional observer, the gravitational potential due to a test mass $m$ would be

$$V(r) \sim \frac{m}{{}^{(4+n)}M_{\mathrm{Pl}}^{n+2}} \frac{1}{r^{n+1}} \tag{1.8}$$

for distances $r$ much less than the extra-dimensional radius $R$, as the gravity would 'see' all of the dimensions. Over larger distances, however, the compact nature of the extra dimensions interferes with the propagation of gravity, and so the potential for $r \gg R$ is given by

$$V(r) \sim \frac{m}{{}^{(4+n)}M_{\mathrm{Pl}}^{n+2} R^n} \frac{1}{r}, \tag{1.9}$$

giving the usual $1/r$ potential, and an effective four-dimensional Planck mass

$${}^{(4)}M_{\mathrm{Pl}}^2 \sim {}^{(4+n)}M_{\mathrm{Pl}}^{n+2} R^n. \tag{1.10}$$

At present, gravitational experiments have not detected any deviations from Gauss' Law (in four dimensions) at scales higher than 0.1mm [32, 33]; therefore, the upper bound on the extra-dimensional radius $R$ is of the order of this length. If we wish to solve the hierarchy problem using this technique, we require the fundamental Planck mass to be equal to the electroweak energy scale; when this is done [29], we obtain for the radius of the extra dimensions

$$R \sim 10^{\frac{30}{n}-19}\mathrm{m} \times \left(\frac{1\mathrm{TeV}}{m_{\mathrm{EW}}}\right)^{1+\frac{2}{n}}. \tag{1.11}$$

For only one extra dimension, putting $n = 1$ gives $R \sim 10^{11}$m, which is comfortably ruled out by measurements of gravitational interactions in the Solar System. A larger number of extra dimensions, however, remains a possibility given the current data.

This idea, while solving the hierarchy problem in one sense, leaves open a related question: why should the extent of the extra dimensions be 'large' (compared to the fundamental scale) and stable? The next section shows a resolution to this question by invoking a warped bulk spacetime.

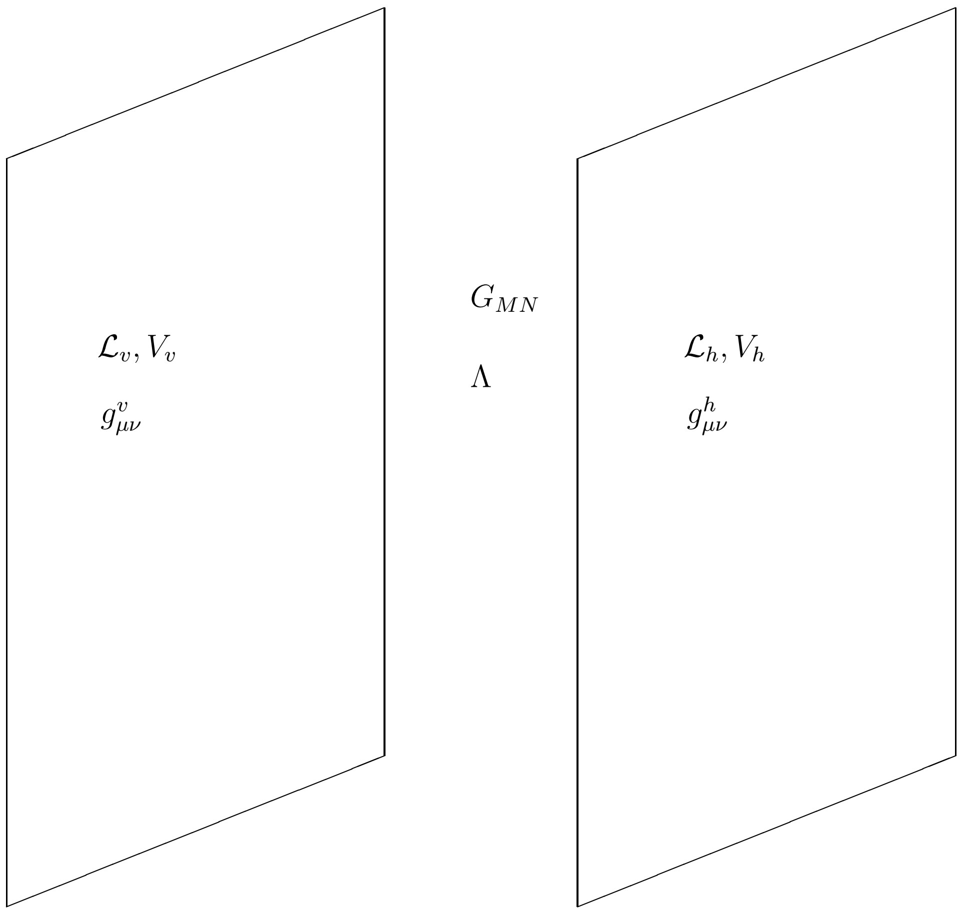


Figure 1.1: The Randall–Sundrum braneworld setup

### 1.3.3 Warped geometries

The notion of our universe as a domain wall in a warped background is not new, either. Warped compactifications have been studied [34, 35] in an attempt to solve other cosmological problems, with extensions to self-gravitating domain walls [36, 37]. Recently, interest in this idea was rekindled by the demonstration [38, 39] (inspired by the Hořava-Witten model discussed in section 1.3.1) that one can have a static four-dimensional domain wall in a negatively curved five-dimensional bulk.

The first scenario proposed by Randall and Sundrum [38] was, like the model presented in section 1.3.2, an attempt to solve the hierarchy problem by invoking extra dimensions.

The setup in figure 1.1 encapsulates the essential features for the so-called Randall–Sundrum braneworld scenario. We have a five-dimensional spacetime slice, bounded by two 'branes': the 'visible' brane (which we identify with our own visible Universe) and an 'invisible' brane at the other end of the spacetime. The boundary conditions for Randall–Sundrum are those of periodicity: we specify that the branes are at the fixed points of an orbifold product of Minkowski spacetime with $S^1/Z_2$.

The action for the system is then

$$S = \int \mathrm{d}^4x \left( \int \mathrm{d}z\sqrt{-G}(-\Lambda + 2M^3 R) + \sqrt{-g^v}(\mathcal{L}_v - V_v) + \sqrt{-g^h}(\mathcal{L}_h - V_h) \right), \tag{1.12}$$

giving Einstein equations which, under the metric Ansatz (satisfying four-dimensional Poincaré invariance)

$$ds^2 = e^{2\sigma(z)}\eta_{\alpha\beta}dx^\alpha dx^\beta + dz^2 \tag{1.13}$$

reduce to

$$6\sigma'^2 = \frac{-\Lambda}{4M^3} \tag{1.14}$$

and

$$3\sigma'' = \frac{V_h}{4M^3}\delta(z - z_h) + \frac{V_v}{4M^3}\delta(z - z_v). \tag{1.15}$$

The solution to equation 1.14 must be consistent with the orbifold symmetry, and is therefore given by

$$\sigma = |z|\sqrt{\frac{-\Lambda}{24M^3}}; \tag{1.16}$$

inserting this into equation 1.15 implies that $\Lambda$ and the two brane potentials $V_v$ and $V_h$ must, for a solution to exist, be related by

$$V_h = -V_v = 24M^3\sqrt{\frac{-\Lambda}{24M^3}} = 24M^3\mu, \tag{1.17}$$

under which condition the metric solution is

$$ds^2 = e^{-2\mu|z|}\eta_{\alpha\beta}dx^\alpha dx^\beta + dz^2. \tag{1.18}$$

This exponential 'warp factor' $\mu$ can then be coupled to a relatively natural size of the extra dimension, with the caveat that our universe corresponds to the brane with negative energy density, because the effective Planck mass is given in terms of the fundamental Planck mass by

$${}^{(4)}M_{\mathrm{Pl}} = e^{\mu R}M, \tag{1.19}$$

where $M$ can be taken to be naturally of the TeV scale. It thus requires $\mu R$ to be only about 50, rather than an unnaturally large number, to solve the hierarchy problem.

The second scenario due to Randall and Sundrum [39] is perhaps even more intriguing; in it, only one 3-brane is present, and the extra dimension is infinite in extent, though it has a $Z_2$ symmetry imposed about the brane position and is negatively curved; conceptually, this scenario may be obtained from that presented in figure 1.1 by moving one brane to infinity. Somewhat surprisingly, the modification to the gravitational potential of a test mass can be made, with a suitable choice of the $\mathrm{AdS}_5$ radius of curvature $\mu$, to be indistinguishable with current data from the four dimensional Gauss' Law; by considering fluctuations around the background metric 1.18, the potential was found to be given by

$$V(r) \sim G_N \frac{m}{r}\left(1+\frac{1}{\mu^2 r^2}\right). \tag{1.20}$$

This scenario, unlike their previous one discussed above, does not intrinsically solve the hierarchy problem. However, it is a viable theory of extra dimensions without many of the philosophical problems of most of the others, as there is no extra-dimensional length that *a priori* needs to be stabilized.

It is conceivable that laboratory gravitational experiments could one day give precise enough measurements of the force due to gravity between two test masses that this deviation from Gauss' Law could be measured. It seems more fruitful, at least at present, to examine the cosmological consequences of these and other extra-dimensional models, in an attempt to distinguish viable from unviable theories of the Universe, and to make predictions of observations that could be made in the near future.

### 1.3.4 Supergravity in singular spaces

The embedding of the scenarios due to Randall and Sundrum [38, 39] in a supersymmetric theory was not initially clear, as the brane objects represent singularities. A no-go theorem was established [40] that demonstrated the impossibility of localizing gravity on the brane in a particular ($N = 2$) supergravity. However, a consistent extension to supersymmetry in 'singular spaces' – in spaces where the curvature has $\delta$-function singularities – was eventually found [41]. A new singlet field is needed to ensure that the total energy of supersymmetric configurations vanishes at each brane.

The braneworld presented by this supergravity in singular spaces scenario, then, adds an extra scalar field to the setup shown in figure 1.1. This extra scalar field is a 'bulk' scalar field – it exists everywhere in the spacetime, not just confined to the branes like Standard Model matter – and couples to ordinary matter through the brane potentials $V_h$ and $V_v$, which are now dependent on this scalar field. In general, the bulk cosmological constant $\Lambda$, too, is no longer constant but is a function of the bulk scalar.

A 'fixed scalar domain wall' solution was found, with

$$(\psi^x)' = 0, \qquad \left(\frac{\partial U_B}{\partial \psi^x}\right) = 0 \qquad , \frac{a'}{a} = -g\epsilon(y)U_B, \tag{1.21}$$

for scalar fields $\psi^x$ and superpotential $U_B$. This gives rise to a metric solution

$$ds^2 = e^{-2gU_B|y|}dx^\mu dx^\nu \eta_{\mu\nu} + (dy)^2, \tag{1.22}$$

which, for positive $gU_B$ yields the Randall–Sundrum solution of section 1.3.3. Further, [42] it was shown that a generalization of the Randall–Sundrum solution is achievable when there is one scalar field (see figure 3.1 for the braneworld setup). In that case, the equations of motion for a metric Ansatz

$$ds^2 = e^{-A/2}dx^\mu dx^\nu \eta_{\mu\nu} + dy^2 \tag{1.23}$$

read, with $U(\psi)$ given by $U = \frac{\partial U_B}{\partial \psi}^2 - U_B^2$:

$$\begin{aligned} A'' &= \psi'^2 + 2U_B(\psi)\delta_y \\ A'^2 &= \psi'^2 - U(\psi) \\ \psi'' - A'\psi' &= \frac{1}{2}\frac{\partial U}{\partial \psi} + 2\frac{\partial U_B}{\partial \psi}\delta_y \end{aligned} \tag{1.24}$$

or, in BPS form,

$$\begin{aligned} \psi' &= \frac{\partial U_B}{\partial \psi} \\ A' &= U_B. \end{aligned} \tag{1.25}$$

For the choice of superpotential $U_B = \xi e^{\alpha\psi}$, the solution to these equations is, for the metric

$$ds^2 = (1 - \alpha^2\xi|y|)^{\frac{1}{2\alpha^2}} dx^\mu dx^\nu \eta_{\mu\nu} + dy^2 \tag{1.26}$$

with the scalar field profile given by

$$\psi = -\frac{1}{\alpha}\ln(1-\alpha^2\xi|y|). \tag{1.27}$$

Clearly, there is a singularity in this spacetime at $y_* = (\alpha^2\xi)^{-1}$; the above solution must break down in the vicinity of this point. We are free to exclude it by positioning our boundary branes such that the interval between them does not contain this value of $y$, and in particular supergravity ensures that it must lie outside the physical spacetime; in a cosmological scenario the spacetime will evolve, and we must beware of the possibility of the evolution bringing in a singular region. We will examine this further in chapter 4.

The values $\frac{1}{\sqrt{3}}$ and $\frac{-1}{2\sqrt{3}}$ for $\alpha$ are of particular interest in this scenario, as they are the solutions resulting from the underlying supergravity theory for the superpotential [42]. We shall see in chapters 3 and 4 that the choice of superpotential strongly affects the predictions of the theory on cosmological observables.

## 1.4 Cosmological Extension

The extension to cosmologically realistic theories of these scenarios at the very least involves allowing the spatial scale factor on the brane to vary. The Randall–Sundrum scenarios described in section 1.3.3 can be extended to the cosmological domain by making a less restrictive choice of Ansatz for the background metric. A natural choice of Ansatz [43] is

$$ds^2 = -n^2(t,y)dt^2 + a^2(t,y)\gamma_{ij}dx^i dx^j + b^2(t,y)dy^2, \tag{1.28}$$

where $y$ is the fifth dimension, and the 3-brane of our Universe is the hypersurface defined as $y=0$. These 'brane-based' coordinates are, of course, an arbitrary choice; a different, though fundamentally equivalent, perspective can be obtained by treating the bulk as fixed and allowing the brane to move through this bulk.

The non-vanishing components of the five-dimensional Einstein tensor under the Ansatz (1.28) are given by (denoting $t$-derivatives with a dot and $y$-derivatives with a prime):

$$\begin{aligned} G_{00} &= 3\left[\frac{\dot a}{a}\left(\frac{\dot a}{a}+\frac{\dot b}{b}\right) - \frac{n^2}{b^2}\left(\frac{a''}{a}+\frac{a'}{a}\left(\frac{a'}{a}-\frac{b'}{b}\right)\right)\right], \qquad (1.29)\\ G_{ij} &= \frac{a^2}{b^2}\delta_{ij}\left[\frac{a'}{a}\left(\frac{a'}{a}+2\frac{n'}{n}\right) - \frac{b'}{b}\left(\frac{n'}{n}+2\frac{a'}{a}\right) + 2\frac{a''}{a} + \frac{n''}{n}\right] \end{aligned}$$

$$+\frac{a^2}{n^2}\delta_{ij}\left[\frac{\dot{a}}{a}\left(-\frac{\dot{a}}{a}+2\frac{\dot{n}}{n}\right)-2\frac{\ddot{a}}{a}+\frac{\dot{b}}{b}\left(-2\frac{\dot{a}}{a}+\frac{\dot{n}}{n}\right)-\frac{\ddot{b}}{b}\right], \tag{1.30}$$

$$G_{05} = 3\left(\frac{n'}{n}\frac{\dot{a}}{a}+\frac{a'}{a}\frac{\dot{b}}{b}-\frac{\dot{a}'}{a}\right), \tag{1.31}$$

$$G_{55} = 3\left[\frac{a'}{a}\left(\frac{a'}{a}+\frac{n'}{n}\right)-\frac{b^2}{n^2}\left(\frac{\dot{a}}{a}\left(\frac{\dot{a}}{a}-\frac{\dot{n}}{n}\right)+\frac{\ddot{a}}{a}\right)\right], \tag{1.32}$$

and Einstein's equations read

$$G_{AB} = \kappa^2 T_{AB}. \tag{1.33}$$

We assume that the bulk energy–momentum tensor represents a (negative) cosmological constant

$$T^A_B|_{\text{bulk}} = \text{diag}(-\Lambda,-\Lambda,-\Lambda,-\Lambda,-\Lambda), \tag{1.34}$$

and the matter on the brane is a homogeneous, isotropic four-dimensional matter distribution (as is usual in cosmology)

$$T^A_B|_{\text{brane}} = \delta(y)S^A_B = \delta(y)\text{diag}(-\tilde{\rho},\tilde{p},\tilde{p},\tilde{p},0). \tag{1.35}$$

The metric (and so the functions $n$, $a$ and $b$) must be continuous across the brane at $y=0$, but the delta function source in the matter distribution implies that the first derivatives are discontinuous, so that there is a delta function in the second derivative terms in equations (1.29) and (1.30). Matching these delta functions to the delta function sources yield the junction conditions

$$\begin{aligned}\frac{[a']}{a_0 b_0} &= -\frac{\kappa^2}{3}\rho\\ \frac{[n']}{n_0 b_0} &= \frac{\kappa^2}{3}(3p+2\rho)\end{aligned} \tag{1.36}$$

Using these relations to solve the remaining Einstein equations (1.31) and (1.32) then yields [43], assuming a $Z_2$ symmetry about the brane (a condition that can be relaxed, as for instance in [44]), a modified Friedman equation

$$H_0^2 \equiv \left(\frac{\dot{a}_0}{a_0}\right)^2 = \frac{\kappa^4}{36}\tilde{\rho}^2+\frac{\Lambda}{6}-\frac{k}{a_0^2}+\frac{C}{a_0^4}. \tag{1.37}$$

The squared dependence of the Hubble parameter on the brane energy density is typical of five-dimensional braneworld models, and initially appears to be in direct conflict with observation. However, by interpreting the energy density $\tilde{\rho}$ as the sum of a brane tension and an energy density of Standard Model fields $\tilde{\rho} = \sigma + \rho$, standard cosmology (with the Hubble parameter $H_0$ proportional to $\sqrt{\rho}$) can be recovered [45] at late times. There will, of course, be consequences of this interpretation for cosmology at early times, some of the effects of which are investigated in chapters 2 and 5.

The description of the brane world models as embedded inside a supersymmetric theory (as in section 1.3.4 above) is likewise open to cosmological expansion. Though the analysis in [41] is general, cosmological solutions for models based on this with one scalar field were found [42, 46], and observables based on these models can be computed; however, they were not realistic cosmological extensions, in that they did not include Standard Model matter fields, and consequently could not be a proper description of our Universe. The cosmological implications of the models of supergravity in singular spaces are considered in more depth in chapters 3 and 4.

## 1.5 Overview

We have seen that extra dimensional models provide a fertile field for extension of our investigation of cosmology – indeed, the above-discussed models are the simplest fraction of the bewildering number of scenarios that have been proposed in recent years.

To distinguish between them, one must look at the models' consequences for four-dimensional observers. In some cases, the models will make predictions that are clearly testable in particle accelerators (for instance, predicting new particle interactions); these models can live or die on the evidence that, once gathered, will either support the model or remove its viability. Those models which do not predict new particle phenomena are nonetheless not philosophically unscientific, though their falsifiability is a little more indirect; in general, they predict new effects in the cosmological domain (as for example the non-standard dependence on the energy density of the Hubble parameter as discussed in section 1.4 above).

In chapter 2 we examine the causal structure of braneworld models generalized from the Randall–Sundrum model by a breaking of the $Z_2$ symmetry about the brane, motivated by a suggestion [47] that an extra dimensional scenario might provide a framework in which to solve the cosmological horizon problem. We analyze this effect in realistic cosmological braneworld models, derived from the Randall–Sundrum models with both one and two branes.

Deducing other expected cosmological consequences of a model depends on deriving from it an effective four-dimensional description of gravity. Chapter 3 contains an analysis of a family of braneworld models [42, 46, 48] motivated by supergravity in singular spaces, generating an effective description of the gravitational field, and examining the consequences and the viability of this theory. The effective theory at low energies is shown to resemble a scalar–tensor theory.

In chapter 4, the results from the analysis of a four dimensional effective theory of chapter 3 are examined for their cosmological effects. In particular, we examine the possibility of cosmological variation of notional constants (such as the electromagnetic fine-structure constant) and also of the presence in the system of an attractor driving the evolution of the system towards a theory with consequences for local observations indistinguishable from those of General Relativity.

Following this, in chapter 5, we present work investigating the perturbations of the Cosmic Microwave Background Radiation in braneworld models. We examine the possibility of using current CMB anisotropy measurements to constrain the parameters and field evolutions of braneworld models, and consider the prospects of improving these through refinements of existing measurements and data from planned observations. Finally, we discuss avenues for further work and draw overall conclusions in chapter 6.

# Chapter 2

# Causality in braneworlds

## 2.1 Introduction

As we have discussed in chapter 1, the possibility that various cosmological problems could be solved in an extra-dimensional scenario has been examined by several authors; for instance, a suggestion that could possibly resolve the cosmological horizon problem was made in [47], where a variety of simple metrics were used to demonstrate that gravity signals, propagating either purely in the extra dimension or via a second hidden brane, could connect regions of our four-dimensional universe that a four-dimensional observer might naïvely think to be causally unconnected. Such a mechanism would have important cosmological consequences as it could greatly alter the size of the particle horizon, as well as possibly providing a viable method for experimental confirmation of the existence of extra dimensions.

The aim of this chapter is to investigate in detail both the one and the two brane mechanisms proposed in [47], in a much more general, physically acceptable braneworld scenario: that of a non-$Z_2$ symmetric cosmological model with a non-zero Weyl tensor component [44, 49–53].

In the single brane case we examine numerically the nature of null geodesics leaving our 3-brane at various times in the universe: whether they return to our 3-brane or freeze out at the horizon; their apparent speed relative to that of light as viewed by a four-dimensional observer; and how these attributes depend on the initial velocity of the geodesics. The effect on the geodesics of breaking the $Z_2$ symmetry and of varying the Weyl tensor component is also investigated fully. We have therefore considerably generalized the previous work done on the subject [54–56], showing that there are only significant deviations from Lorentz invariance at early times.

The second case, where signals travel along a hidden brane, has not previously been investigated in any realistic scenario: the metrics used in prior studies [47] were not solutions to Einstein's equations. In order to examine the two brane case fully, the non-linear equation of motion of the inter-brane distance (otherwise known as the cosmological radion $\mathcal{D}$ [57]) is concisely derived and is used to evaluate the relative speeds of signals on the second brane compared to the first, quantitatively for the stationary case and qualitatively for the moving brane case. It is found that although signals can in some situations propagate along the second brane significantly faster than along ours, it is not a large enough effect to solve the horizon problem; on the other hand we do get significant violations of Lorentz invariance at late times, such that the gravitational horizon is larger than the particle horizon. This could lead to signals in future gravitational wave detector experiments.

This chapter is organized as follows: the general setup and geodesic equations are derived in section 2.2; section 2.3 contains a brief discussion of geodesics in the normal Randall–Sundrum model [54]. We continue, in section 2.4, by investigating non-cosmological (i.e. static) solutions of Einstein's equations, with the Randall–Sundrum model extended by admitting [44] the possibility of $Z_2$-symmetry breaking across the brane, as well as deviations from perfect tuning; the behaviour of null geodesics in the five-dimensional theory is examined both analytically and numerically. We then extend the investigation in section 2.5 to fully cosmological solutions of Einstein's equations without mirror symmetry, numerically investigating the possibilities for solving the horizon problem in a similar fashion to [56]. In section 2.6 we consider the possible acausality in a two brane scenario where in general the second brane is moving. Our conclusions are discussed in section 2.7.

## 2.2 Geodesics in five-dimensional Einstein Gravity

Throughout this chapter we investigate the behaviour of geodesics, in a variety of different braneworld scenarios. In this section we describe both the general setup and the assumptions that have been made, as well as giving the equations from which all the results in the chapter are derived.

In each scenario investigated, it is assumed that the five-dimensional spacetime satisfies three-dimensional homogeneity and isotropy as we are mainly interested in realistic cosmological models. We choose to work in a 'brane-based' coordinate system as it will facilitate physical interpretation of the results. We therefore assume that the four-dimensional universe in which we reside is situated on a 3-brane which we place at the origin of the extra dimension ($y = 0$). This implies that the most general metric must have the form

$$\mathrm{d}s^2 = -n^2(t,y)\mathrm{d}t^2 + a^2(t,y)\gamma_{ij}\mathrm{d}x^i\mathrm{d}x^j + \mathrm{d}y^2, \tag{2.1}$$

where $t$ is the cosmic time on our brane, $x^i$ represents the three spatial dimensions of our brane, and $y$ is the coordinate of the extra dimension. $\gamma_{ij}$ is the maximally symmetric three-dimensional metric with $k = -1, 0, 1$ parameterizing the spatial curvature, although throughout most of this chapter $k$ will be set to zero. The bulk is assumed to be empty except for a cosmological constant $\Lambda$, and therefore the metric is obtained by solving the five-dimensional Einstein's equations[1],

$$G_{AB} \;-\; \Lambda g_{AB} \;=\; \kappa^2 T_{AB}, \tag{2.2}$$

where we define $\kappa^2 \equiv 1/\widetilde{M}_5^3$, $\widetilde{M}_5$ being the fundamental (reduced) five-dimensional Planck Mass. In the single brane scenario, the energy-momentum tensor $T_{AB}$ takes the form

$$T^A_B \;=\; \delta(y)\mathrm{diag}(-\rho_0, P_0, P_0, P_0, 0), \tag{2.3}$$

and for the two brane scenario,

$$T^A_B \;=\; \delta(y)\mathrm{diag}(-\rho_0, P_0, P_0, P_0, 0) \;+\; \delta(y - \mathcal{D}(t))\mathrm{diag}(-\rho_2, P_2, P_2, P_2, 0), \tag{2.4}$$

where we follow the notation used in [57] by defining $\rho_0$ and $\rho_2$ to be the energy density of our brane and of the second brane respectively, and by defining the pressures $P_0$ and $P_2$ similarly. The position of the second brane, given by $y = \mathcal{D}(t)$, is in general time dependent.

In sections (2.4) and (2.5) we use solutions of Einstein's equations that do not possess a $Z_2$ symmetry (or mirror symmetry) across the brane. For a full discussion of this topic see [44, 49–53].

[1] Throughout this thesis, we use the standard braneworld convention in that lower-case Roman indices (such as $i$, $j$) run across the normal space dimensions (1 to 3); Greek indices ($\mu$, $\nu$) run across time and normal space (0 to 3), while capital Roman indices ($A$, $B$) cover all space and time dimensions (0 to 3 and 5).

### 2.2.1 Geodesic Equations

Here we derive the necessary geodesic equations corresponding to the metric given by equation (2.1). In what follows the notation is such that dots indicate differentiation with respect to the affine parameter and dashes with respect to the fifth dimension, $y$, leaving $\frac{\partial}{\partial t}$ as the differentiation operator with respect to coordinate time. Starting from the variational principle

$$\delta S = \delta \int \mathcal{L} \mathrm{d}s = 0, \tag{2.5}$$

with

$$\mathcal{L} = \sqrt{g_{AB}\dot{x}^A \dot{x}^B}, \tag{2.6}$$

we can derive the equations of motion for test particles. We shall principally be concerned here with lightlike geodesics, which means that we can consider the variation of $\int \mathcal{L}^2 \mathrm{d}s$, so that the effective Lagrangian density is $-n^2(t,y)\dot{t}^2 + a^2(t,y)\dot{x}_i\dot{x}_i + \dot{y}^2$, giving Euler-Lagrange equations:

$$\begin{aligned} \ddot{t} &= \frac{1}{n}\left(\frac{\partial n}{\partial t}\dot{t}^2 - 2\dot{n}\dot{t} - \frac{\partial a}{\partial t}\frac{\theta_i\theta_i}{a^3 n}\right) \\ \dot{x}_i &= \frac{\theta_i}{a^2} \\ \ddot{y} &= -\frac{\theta_i\theta_i}{a^2}\left(\frac{n'}{n} - \frac{a'}{a}\right) - \frac{n'}{n}\dot{y}^2, \end{aligned} \tag{2.7}$$

where the $\theta_i$ are integration constants. For null geodesics, with which we shall be exclusively concerned in this study, we have the additional constraint that the test particle must move at the speed of light; this tells us that the first integral of the $t$ equation above must be of the form

$$n^2\dot{t}^2 = \dot{y}^2 + \frac{\theta_i\theta_i}{a^2}. \tag{2.8}$$

These equations will be used extensively throughout sections 2.3, 2.4 and 2.5 to evaluate possible shortcuts through the bulk.

## 2.3 Geodesics in the Randall–Sundrum Model

### 2.3.1 The Randall–Sundrum Metric

The Randall–Sundrum model, as initially presented [38, 39], is not a cosmological one; rather, it is included here as a simple model to develop the reasoning employed in rather more complicated cases. It may be derived from the above, general, metric Ansatz given in equation (2.1) by taking $n(\not{t}, y) = a(\not{t}, y) = a(y)$, and then solving Einstein's equations while assuming a $Z_2$ symmetry across each brane. Provided that the bulk cosmological constant $\Lambda$ is less than zero, and that the energy densities of each of the branes are tuned such that

$$\kappa^2\rho_0 \;=\; -\kappa^2\rho_2 \;=\; \sqrt{-6\Lambda}, \tag{2.9}$$

the familiar Randall–Sundrum metric is recovered:

$$\mathrm{d}s^2 = e^{-2\mu|y|}\eta_{\mu\nu}\mathrm{d}x^\mu\mathrm{d}x^\nu + \mathrm{d}y^2, \tag{2.10}$$

which implies that

$$n(y) = a(y) = e^{-\mu|y|}. \tag{2.11}$$

$\mu$ is the inverse of the $\mathrm{AdS}_5$ curvature radius and is given by $\mu = \sqrt{-\Lambda/6}$.

### 2.3.2 Randall–Sundrum Geodesics

We can immediately see that the Randall–Sundrum model is not going to help us solve the horizon problem. The local speed of light is everywhere the same, because $n(y) = a(y)$, and so even if off-brane null geodesics can return to the brane, they will return with an effective sub-luminal velocity.

However, the Randall–Sundrum model does not exhibit even this kind of behaviour. As shown in [54], the geodesic follows the path given by

$$e^{2\mu y} = e^{2\mu y_0} + 2\mu\dot{y}_0 e^{2\mu y_0} t - v^2\mu^2 t^2, \tag{2.12}$$

with $v^2 = \eta_{\mu\nu}\dot{x}^\mu\dot{x}^\nu$.

As a side note, $v^2 = 0$ does not necessarily correspond to a lightlike geodesic, as claimed in section 2 of [54], as the condition for lightlike behaviour is $g_{AB}\dot{x}^A\dot{x}^B = 0$, which includes an extra $\dot{y}^2$.

## 2.4 Geodesics in Other Static Braneworld Models

### 2.4.1 Obtaining the Metric

We relax some of the assumptions made in the Randall–Sundrum model; specifically, we no longer impose strict $Z_2$ symmetry, nor do we fine-tune the bulk cosmological constant. Further to the relaxation of fine-tuning and $Z_2$ symmetry, we must also adapt the Ansatz, making $n(y)$ no longer equal to $a(y)$, in order to be able to obtain a self-consistent solution.

The $G_{00}$ equation (1.29) yields

$$a^2(y) = \cosh(2\mu y) + A \sinh(2\mu y), \tag{2.13}$$

where we have implicitly scaled so that $a_0 \equiv a|_{y=0} = 1$. To consider the loss of $Z_2$ or mirror symmetry, when we apply the Israel junction condition

$$[a'(y)] = -\frac{\kappa^2}{3}\rho, \tag{2.14}$$

where $[f] = f(0^+) - f(0^-)$, we make the assumption that $a'(0^+) = -a'(0^-) + d_a$, giving

$$\mu A = -\frac{\kappa^2}{6}\rho + \frac{d_a}{2}; \tag{2.15}$$

$d_a = 0$ for $Z_2$-symmetric braneworlds. Then, parameterizing the lack of fine-tuning by

$$r = \frac{\kappa^2 \rho}{6\mu} \tag{2.16}$$

and the $Z_2$ symmetry breaking by

$$d = \frac{d_a}{2\mu}, \tag{2.17}$$

we obtain

$$a(y) = \sqrt{\cosh(2\mu|y|) + (d-r)\sinh(2\mu|y|)}. \tag{2.18}$$

The $G_{55}$ equation (1.32) then yields

$$n(y) = \frac{\sinh(2\mu|y|) + (d-r)\cosh(2\mu|y|)}{(d-r)\sqrt{\cosh(2\mu|y|) + (d-r)\sinh(2\mu|y|)}}, \tag{2.19}$$

which has again been scaled so that $n(y=0) = 1$; this solution may then be substituted into the other Einstein equations and junction conditions (1.36) to check the self-consistency of this solution.

### 2.4.2 Geodesics in Static Non-$Z_2$ Braneworlds

Since the Lagrangian density $\mathcal{L}$ given by equation (2.5) does not depend explicitly on coordinate time $t$, we can immediately obtain a further first integral of the form

$$\dot{t} = \frac{\theta_0}{n^2(y)}, \tag{2.20}$$

and so straight from the Lagrangian constraint for lightlike geodesics we have

$$\dot{y}^2 = \frac{\theta_0^2}{n^2(y)} - \frac{\theta_i\theta_i}{a(y)^2}. \tag{2.21}$$

This is effectively a conservation of energy equation, with a kinetic term proportional to $\dot{y}^2$ and a potential of the form

$$V(y) = -\frac{\theta_0^2}{n^2(y)} + \frac{\theta_i\theta_i}{a(y)^2}. \tag{2.22}$$

We may therefore reason that firstly if a geodesic starts its life on our brane (at $y = 0$) then we have, since $\dot{y}^2 \geq 0$,

$$\theta_0^2 \geq \theta_i\theta_i. \tag{2.23}$$

Further, if the geodesic is ever to return, then $\dot{y}$ must at some point be zero, so

$$\theta_0^2 \left( \frac{1}{n^2(y)} - \frac{\gamma^2}{a^2(y)} \right), \tag{2.24}$$

where $0 < \gamma^2 = \frac{\theta_i\theta_i}{\theta_0^2} < 1$, must be zero at some positive value of $y$. Rearranging and substituting the above solution for the metric, we find that the positions at which $\dot{y} = 0$, denoted by $y_t^{\pm}$, satisfies

$$\cosh(2\mu y_t^{\pm}) + (d-r)\sinh(2\mu y_t^{\pm}) = \pm\gamma \frac{\sinh(2\mu y_t^{\pm}) + (d-r)\cosh(2\mu y_t^{\pm})}{(d-r)}, \tag{2.25}$$

or

$$y_t^{\pm} = \frac{1}{2\mu}\tanh^{-1}\left[\frac{(d-r)(\pm\gamma - 1)}{(d-r)^2 \mp \gamma}\right]. \tag{2.26}$$

However, there could be a horizon intervening between $y = 0$ and this point; a horizon will occur if either of $a(y)$ or $n(y)$ is equal to zero. We split the analysis into two parts, one for $(d-r) > -1$ and one for $(d-r) < -1$, reminding the reader that $(d-r) = -1$ corresponds to the Randall–Sundrum braneworld. Below, subscript $t$ refers to the geodesic turning point, while subscript $h$ to the position of the horizon.

**The $(d-r) > -1$ case:**

For $(d-r) > -1$, $a(y)$ (equation 2.18) is never zero because $\cosh(2\mu y) > \sinh(2\mu y)$ for all $y$. $n(y) = 0$ gives (from equation 2.19)

$$y_h^{>} = \frac{1}{2\mu}\tanh^{-1}(r-d). \tag{2.27}$$

Then $y_t^-$ (equation 2.26) is clearly greater than $y_h^{>}$ (as $(d-r)^2 < 1$); also $y_t^+$ is either greater than $y_h^{>}$ or is negative (the latter when $(d-r)^2 < \gamma$). Thus a geodesic leaving our brane in the positive $y$ direction for $(d-r) > -1$ will always reach a horizon at $y = y_h^{>}$, and will therefore, from the point of view of an observer on the brane, never return. See figures 2.1 and 2.2 for illustrations of a sample geodesic in this régime.

**The $(d-r) < -1$ case:**

For $(d-r) < -1$, $n(y)$ is never zero, and $a(y) = 0$ gives

$$y_h^{<} = \frac{1}{2\mu}\tanh^{-1}\left[\frac{1}{(r-d)}\right]. \tag{2.28}$$

This is always greater than $y_t^-$ which is the smaller of the two turning points, and so for $(d-r) < -1$, the geodesic will turn around at a $y$ value of

$$y_t = \frac{1}{2\mu}\tanh^{-1}\left[\frac{(r-d)(1-\gamma)}{(d-r)^2-\gamma}\right]. \tag{2.29}$$

Figures 2.3 and 2.4 similarly show a sample geodesic for $(d-r) < -1$.

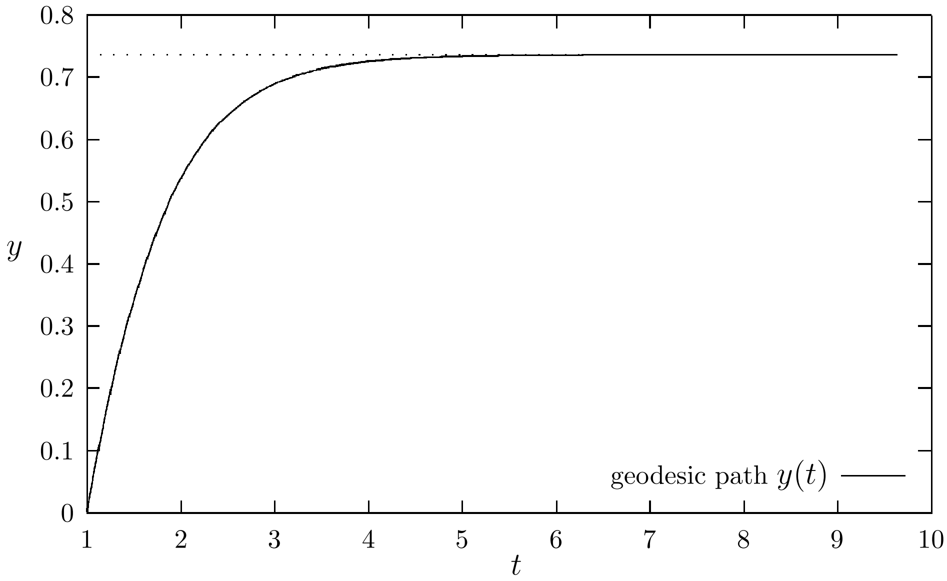


Figure 2.1: Graph of $y$ against coordinate time for a geodesic in a static, untuned $(d-r = -0.9)$ braneworld with $\dot{x}_0 = -0.5$. The dotted line represents the calculated $y_h^>$ horizon position.

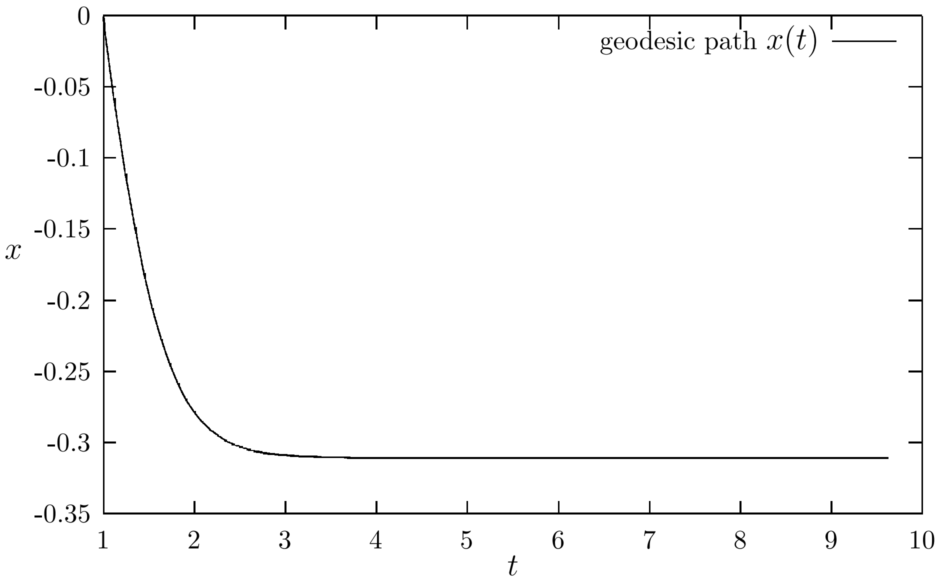


Figure 2.2: Graph of $x$ against coordinate time for a geodesic in a static, untuned $(d-r = -0.9)$ braneworld with $\dot{x}_0 = -0.5$. Note that as the geodesic goes towards the horizon its $x$-velocity decreases.

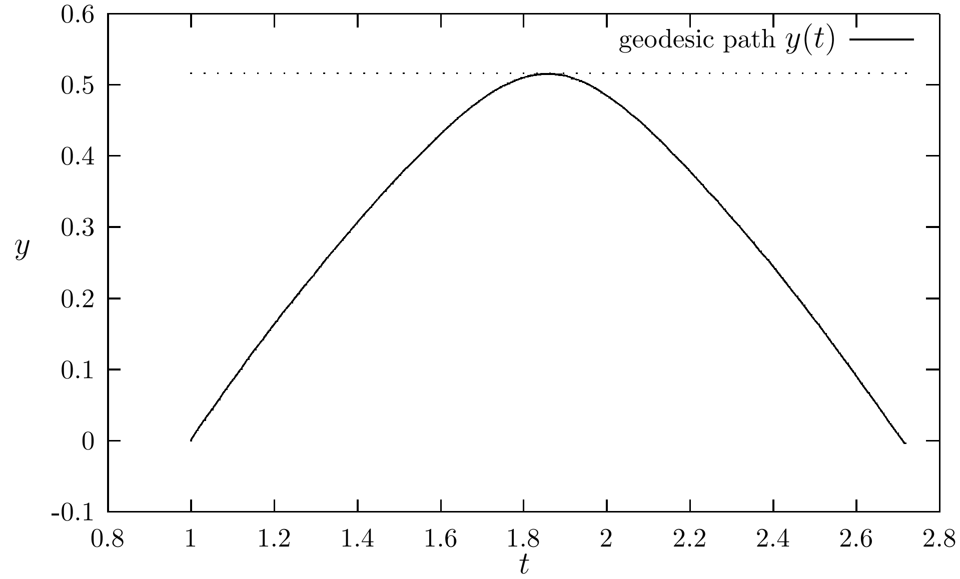


Figure 2.3: Graph of $y$ against coordinate time for a geodesic in a static, untuned ($d-r=-1.1$) braneworld with $\dot{x}_0=-0.5$. The dotted line represents the calculated $y$ turnaround position.

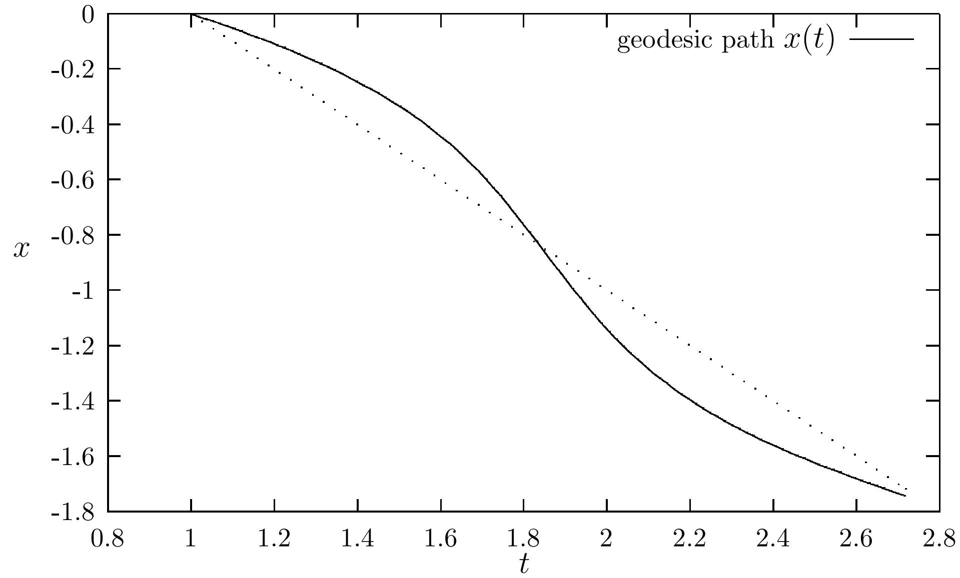


Figure 2.4: Graph of $x$ against coordinate time for a geodesic in a static, untuned ($d-r=-1.1$) braneworld with $\dot{x}_0=-0.5$. The dotted line represents a light ray moving on the brane. Note that the true null geodesic has covered a greater distance on return to the brane than the light ray in the same time $t$; lower magnitudes of $\dot{x}_0$ lead to higher superluminosities.

## 2.5 Cosmological Models

### 2.5.1 The non-$Z_2$ Symmetric Cosmological Metric

In this section we investigate the behaviour of geodesics in the full cosmologically realistic, non-$Z_2$ symmetric braneworld scenario (see [44] for more details). In order to obtain standard cosmology at late times we make the usual assumption, first noted by [45], that our brane possesses an energy density which is the sum of the brane tension $\sigma$ and a physical energy density $\rho$, and we assume that the brane tension and bulk cosmological constant are tuned to ensure that the effective four-dimensional cosmological constant is zero. The Friedman equation is then given by [44],

$$H_0^2 = \left(\frac{\dot{a}_0}{a_0}\right)^2 = \frac{\kappa^4\sigma}{18}\rho + \frac{\kappa^4}{36}\rho^2 - \frac{k}{a_0^2} + \frac{\mathcal{C}}{a_0^4} + \frac{F^2}{(\rho+\sigma)^2 a_0^8}, \tag{2.30}$$

where $a_0(t) = a(t,0)$, $\mathcal{C}$ is the dark radiation term corresponding to a non-zero Weyl tensor component, and $F$ represents the extent to which the $Z_2$ symmetry is broken. Motivated by previous work on geodesics [55] which suggests that more interesting effects are to be seen at earlier times, we assume a radiation dominated universe and therefore set

$$\rho = \frac{\lambda}{a_0(t)^4}, \tag{2.31}$$

where $\lambda$ is some constant. We can now use the bulk solutions to the metric Ansatz (2.1) which have been found for a single brane without reflection symmetry in an infinite fifth dimension [44], and are given by

$$a^2(t,y) = a_0^2(t)\left(A(t)\cosh 2\mu y + B(t)\sinh 2\mu y + C(t)\right), \tag{2.32}$$

where $\mu$ as before, is defined in terms of the bulk cosmological constant $\Lambda$ as $\mu = \sqrt{-\Lambda/6}$. The purely time dependent constants $A(t)$, $B(t)$, and $C(t)$ are given by

$$A(t) = 1 + (1+w)\frac{\rho}{\sigma} + \frac{1}{2}\frac{\rho^2}{\sigma^2} + \frac{f^2\rho^2}{2(\sigma+\rho)^2} \tag{2.33}$$

$$B(t) = -(1+\frac{\rho}{\sigma}) \pm \frac{f\rho}{(\sigma+\rho)} \tag{2.34}$$

$$C(t) = -(1+w)\frac{\rho}{\sigma} - \frac{1}{2}\frac{\rho^2}{\sigma} - \frac{f^2\rho^2}{2(\sigma+\rho)^2}. \tag{2.35}$$

Here $w$ and $f$ are dimensionless constants defined by $w \equiv 18\mathcal{C}/\kappa\sigma\lambda$ and $f \equiv 6F/\kappa^2\sigma\lambda$, and the $\pm$-signs in the expression for $B(t)$ give the different solutions on each side of the brane. The solution for $n(t,y)$ is given in terms of $a(t,y)$ as:

$$n(t,y) \quad = \quad \frac{\dot{a}(t,y)}{\dot{a}_0(t)}, \tag{2.36}$$

where from now the dots denote differentiation with respect to coordinate time.

To find $a_0(t)$, we must solve the Friedman equation (2.30); however, for $f \neq 0$, there is no analytical solution, and so it must be solved numerically; this presents a problem, however, due to the initial singularity. Therefore, to solve this equation we approximate the $f^2$ term for early times, when $\rho \gg \sigma$, as $f^2\sigma^2$; the solution is then, as in [44],

$$a_0 = \left\{\gamma f \left(\frac{1+w}{f\sigma}\left[\cosh\frac{2\sigma f}{3\tilde{M}_5^3}t - 1\right] + \frac{1}{\sigma}\sinh\frac{2\sigma f}{3\tilde{M}_5^3}t\right)\right\}^{\frac{1}{4}}. \tag{2.37}$$

This solution will be approximately valid to some time $t_0$; to estimate that time, we calculate the time at which $\rho = 4\sigma$, giving

$$\frac{1+w}{f}\left[\cosh\frac{2\sigma f}{3\tilde{M}_5^3}t_0 - 1\right] + \sinh\frac{2\sigma f}{3\tilde{M}_5^3}t_0 = \frac{f}{4}, \tag{2.38}$$

or

$$t_0 = \frac{3\tilde{M}_5^3}{2\sigma f}\log\left\{\frac{\frac{1+w}{f} + \frac{f}{4} + \sqrt{(\frac{1+w}{f} + \frac{f}{4})^2 - (\frac{1+w}{f})^2 + 1}}{\frac{1+w}{f} + 1}\right\}. \tag{2.39}$$

Over the range of values of interest ($0 < w < 0.2$, $0 < f < 60$), $t_0 > \frac{1}{20}\frac{3\tilde{M}_5^3}{2\sigma f}$, (see figure 2.5) and so we may safely take the initial conditions for numerical integration of the Friedman equation as our approximate solution at $t = \frac{1}{40}\frac{3\tilde{M}_5^3}{2\sigma f}$. This can then be numerically integrated using the full Friedman equation (2.30) to generate the solutions of the Einstein equations.

### 2.5.2 Geodesics

At late times, we would expect the behaviour of geodesics to be similar to the static case, assuming that the dynamical timescale is much smaller than the cosmological one. This appears broadly to be the case, though the position or cross-section of the horizon would need to be tuned for an adequate comparison. The main difference is that for large

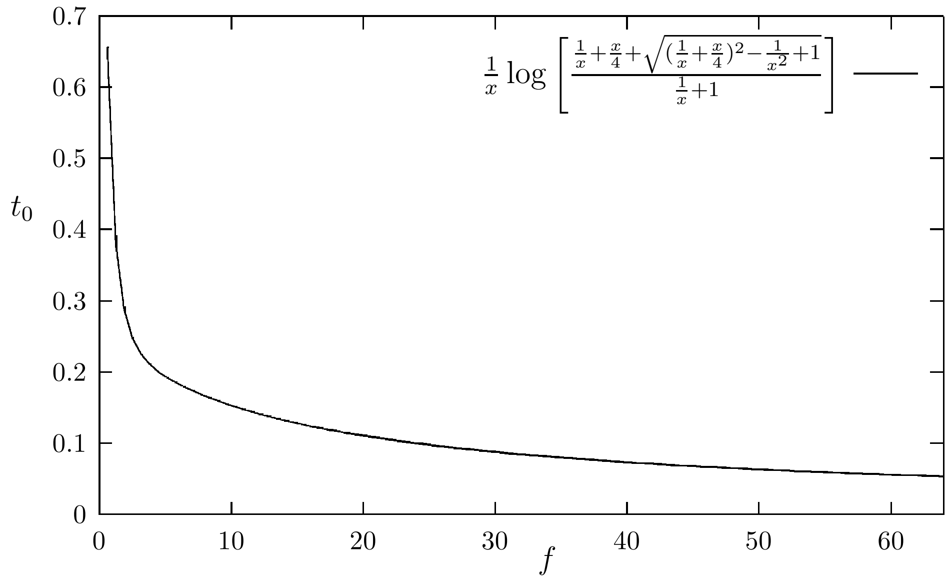


Figure 2.5: A graph of $t_0$ (for $w = 0$) over a range of values of $f$; this is used to determine the point at which numerical integration of the Friedman equation must begin.

dynamical times there will be a certain amount of asymmetry in the geodesic's path, due to the changing scale factor $a = a(t, y)$.

Consider figure 2.6, which shows null geodesics leaving the brane at a time $t_0$ such that $a_0(t_0) = 0.5$, when the $\rho^2$ term dominates in the Friedman equation[2]. In that figure, both geodesics have an initial $\dot{y}$ of 0.975 (where the speed of light is 1); the difference is that the dotted geodesic is in a braneworld with broken $Z_2$ symmetry ($f = 0.1$, in the notation of [44]). The graph has been cut off so that the path of the returning geodesic is clear; the $f = 0.1$ geodesic reaches the horizon in the bulk asymptotically (as $t$ tends to infinity). It is perhaps slightly clearer when viewed in conjunction with figure 2.7, which shows that when the geodesic in the $f = 0.1$ world reaches $x$ of about 290 it is at the horizon, at which point it will move with the horizon in the $y$ direction.

Let us next examine figures 2.8 and 2.9, in which we have taken a number of geodesics as in figures 2.6 and 2.7, and examined the superluminosity of the returning signal; in other words, how much faster than light, which is constrained to travel along the brane with speed $\frac{1}{a_0(t)}$, is the true null geodesic.

The results are perhaps surprising at first sight. Conceptually there are two separate effects here. One is that space is 'warped'; loosely, there is an $e^{\mu y}$ factor warping space in

[2]Though extensive tests have shown that there is no particular difference in between the régimes.

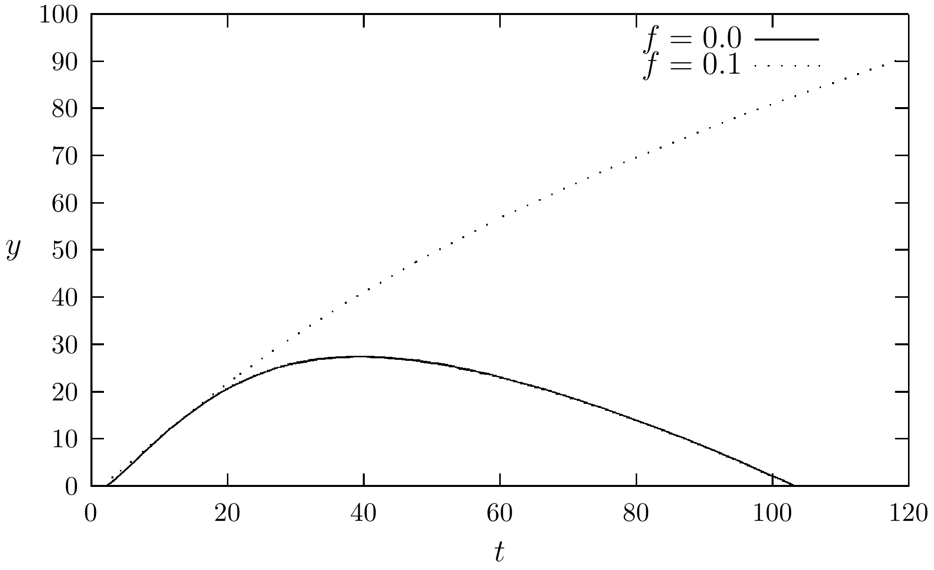


Figure 2.6: Graph of $y$ against coordinate time for a geodesic in a cosmological braneworld with $\dot{y}_0 = 0.975$. The returning geodesic is in a $Z_2$-symmetric braneworld, while the one tending towards the horizon has $f = 0.1$. The geodesics were set off at $a_0 = 0.5$

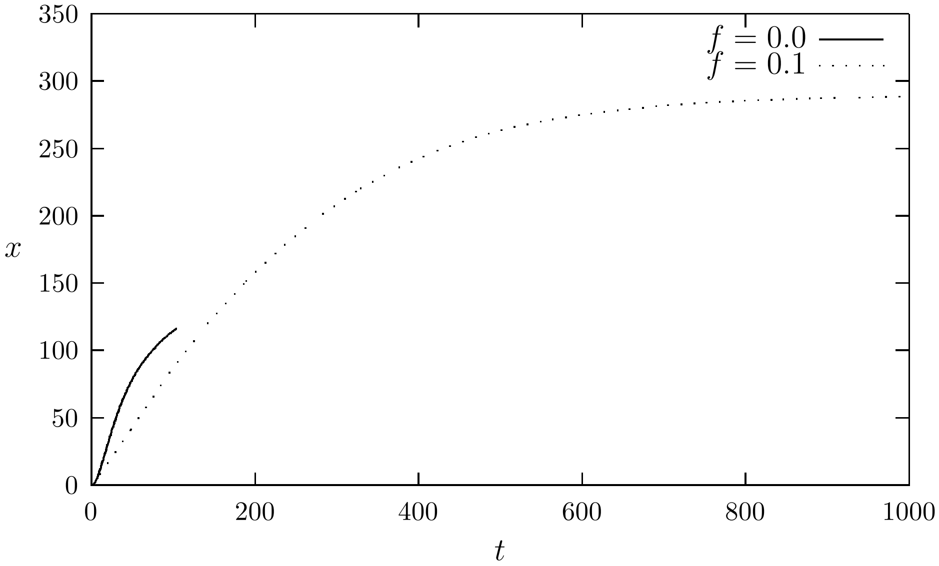


Figure 2.7: Graph of $x$ against coordinate time for a geodesic in a cosmological braneworld with $\dot{y}_0 = 0.975$. The geodesics are the same as in Figure 2.6. Note that the $f = 0.1$ geodesic asymptotically tends to a maximal $x = x(\tau_H)$, where $\tau_H$ is the value of the affine parameter when the geodesic crosses the horizon.

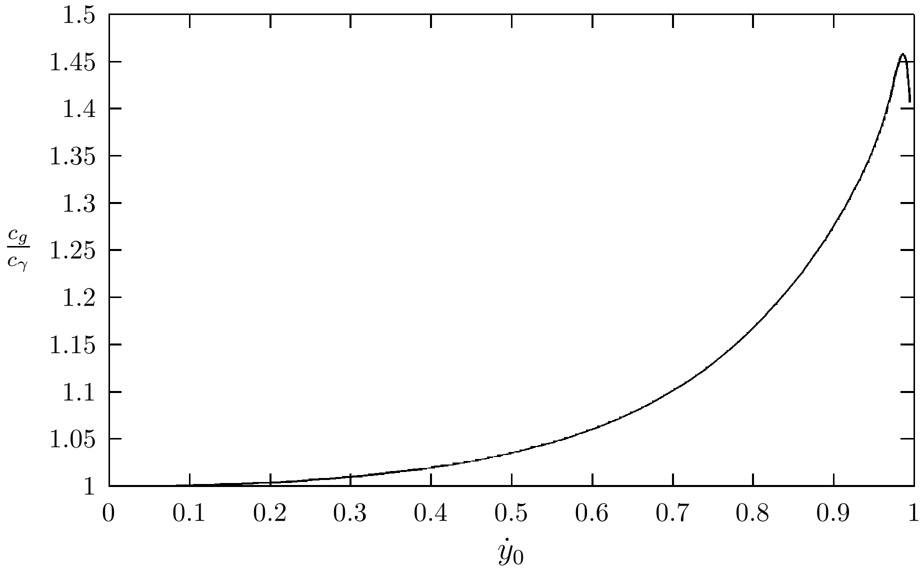


Figure 2.8: The ratio of gravitational to electromagnetic speeds, as a function of the initial component of velocity in the fifth dimension, in a $Z_2$-symmetric braneworld. $a_0(t_0) = 0.5$.

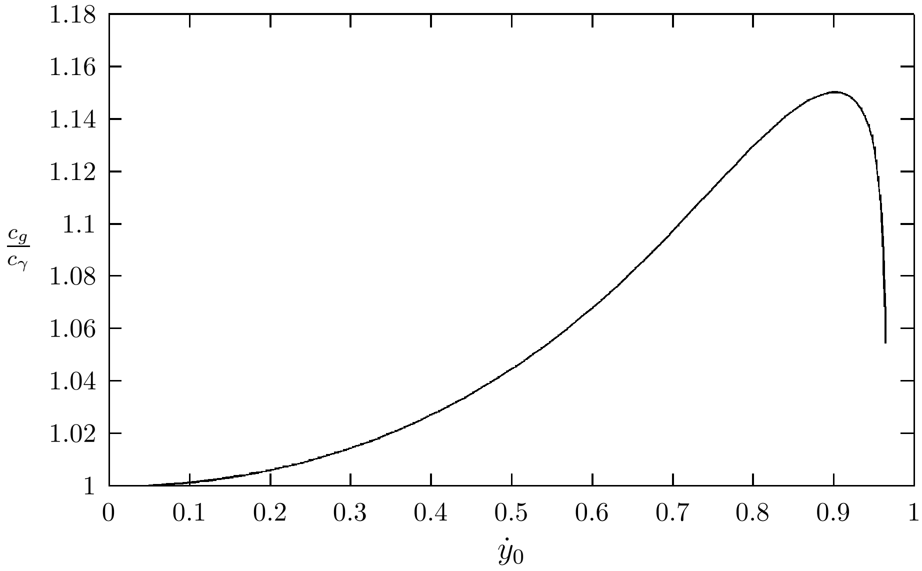


Figure 2.9: The ratio of gravitational to electromagnetic speeds, as a function of the initial component of velocity in the fifth dimension, in a non-$Z_2$-symmetric braneworld ($f = 0.1$). Note firstly that the maximum has moved leftwards, and also that some geodesics from our samples no longer return.

the bulk, meaning that null geodesics can effectively cover much greater distances. Thus, the farther into the bulk that the geodesic penetrates, the more superluminal the geodesic will be. However, there is a competing effect due to the presence of a horizon in the bulk; the horizon is only a coordinate singularity, but since it is a singularity in the physical brane coordinates it is nevertheless of physical relevance, in that, from the point of view of an observer on the brane, geodesics which reach the horizon never return.

Null geodesics that have too large a velocity component in the fifth dimension will not be able to escape the horizon, and thus, at very high $\dot{y}_0$, the geodesics will not return to the brane before the end of the universe. Null geodesics with small initial $\dot{y}$, however, will be confined to the brane.

In between these two régimes, what will happen? At some critical angle, the effect of the horizon will begin to dominate over the effect of the warped spacetime, and consequently there will be a maximum of the ratio of gravitational to electromagnetic effective speeds.

As discussed in [55], the maximal superluminal effect will be obtained when the hierarchy is the most pronounced experimentally allowed value, and the null geodesic is set off at the earliest physical time possible (of the order of $M_5^{-1}$): not because of any particularly stronger warping at this earlier time, but rather because the geodesic can spend much 'longer' in the warped area before returning to the brane. There is thus no discrepancy in principle[3] between the relatively low superluminal values shown here and the figure of $10^3$ quoted in [55].

It appears from figures 2.8 and 2.9 that the effect of including asymmetry[4] is to increase the horizon cross-section, for geodesics leaving at equivalent times (taken as equal redshifts, or, what amounts to the same thing, equal energy densities), and also to decrease the ratio of the speeds even for geodesics that do not go anywhere near the horizon.

The effect of the start time on the superluminosity is such that when the $\rho^2$ term dominates, at early times, the superluminosity is increased (see figure 2.10). A corresponding late-time graph is not shown, as the cross-section of the horizon has increased to such an extent that almost all geodesics hit the horizon and do not return, from which we note that the acausality in this model is maximal at early time, with energy leakage from the brane at later times.

Including dark radiation likewise dampens the superluminosity; figure 2.11 shows the

[3] Unfortunately it is not possible without extensive code writing to investigate this figure numerically in this framework, as the maximal superluminosity will be obtained with an initial $\dot{y}$ of somewhere between $1 - 10^{-15}$ and 1.

[4] We have shown here results with positive $f$ only, as results with $f < 0$ are physically similar.

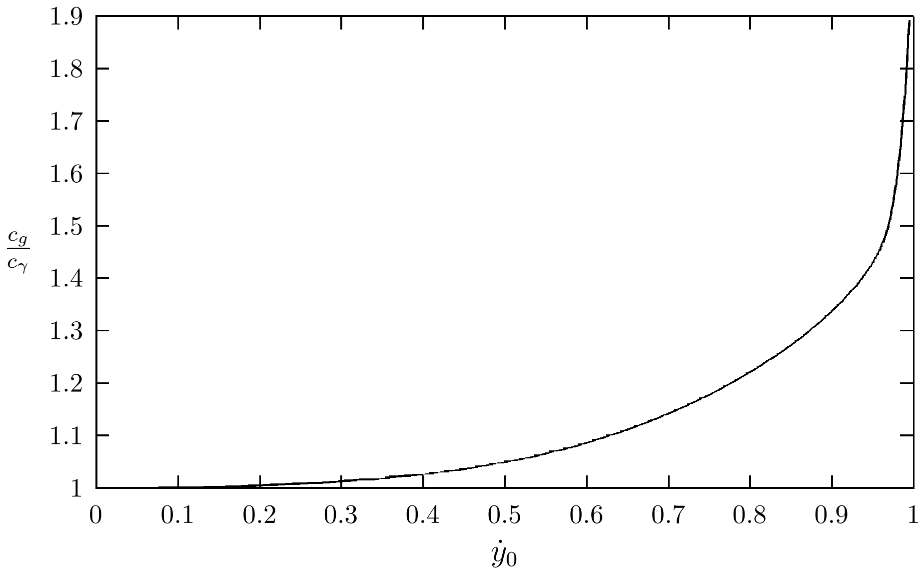


Figure 2.10: The ratio of gravitational to electromagnetic speeds, as a function of the initial component of velocity in the fifth dimension, in a $Z_2$-symmetric braneworld. $a_0(t_0) = 0.125$ (earlier time than Figure 2.8).

effect of including a dark radiation term $w = 2$ in the calculation. Note that this value of $w$ is well outside the nucleosynthesis bound [58], and is tested in our investigation only so as to exaggerate any possible visible effect.

## 2.6 The Two Brane Model

It would seem, from the above results, that the possibility of null signals taking shortcuts through the bulk in the single brane scenario cannot solve the well known cosmological horizon problem, as the apparent speeds of such signals are not significantly greater than the speed of light signals confined to the brane. Therefore, we now investigate an alternative suggestion made by [47]: that a two brane scenario could provide a solution to the horizon problem. By investigating a variety of 'toy' metrics, it was shown in [47] that apparently acausal signals could be sent between different points on our brane, via the second hidden brane. These signals would, as before, bring in to causal contact regions of our Universe that would have otherwise been unable to communicate.

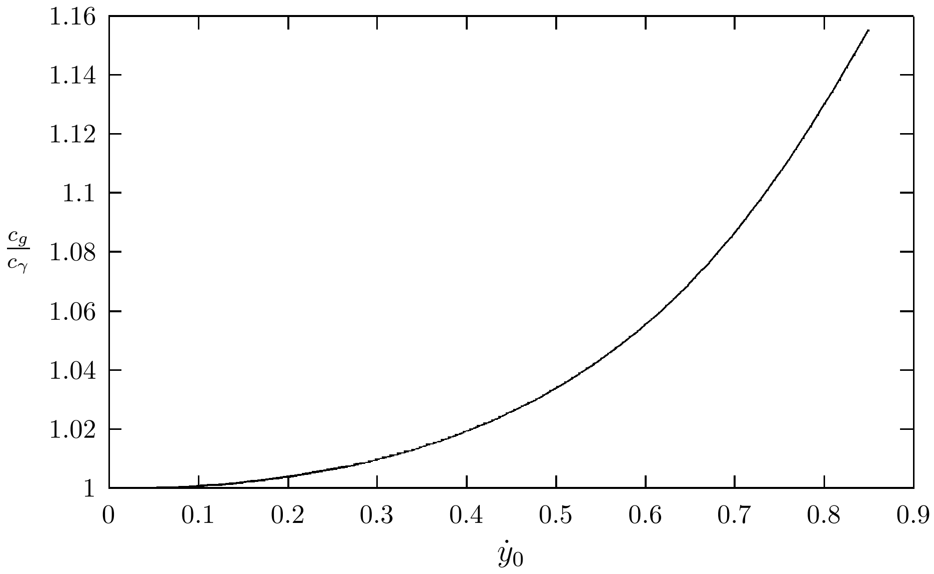


Figure 2.11: The ratio of gravitational to electromagnetic speeds, as a function of the initial component of velocity in the fifth dimension, in a $Z_2$-symmetric braneworld. $w = 2.0$ (same time as Figure 2.8). Note that some previously-returning geodesics no longer return.

In order for this method to work, a metric of the following form was assumed:

$$\mathrm{d}s^2 = \mathrm{d}t^2 - e^{-2\mu y} a^2(t)\mathrm{d}x^2 - \mathrm{d}y^2, \tag{2.40}$$

where $y$ corresponds to one extra spatial dimension; our brane and the hidden brane were assumed to be at $y = 0$ and $y = \mathcal{D}$ respectively. The distance $s_{AE}$ travelled by a null signal on our brane in time $t_f$ is then (see figure 2.12)

$$s_{AE} = \int_0^{t_f} \frac{\mathrm{d}t}{a(t)}. \tag{2.41}$$

However, if it is possible for a null signal to leave our brane, interact with and therefore travel along the hidden brane, before eventually returning to our world, we can then ask how far it would have appeared to have travelled $s_{AD}$, in time $t_f$. If it takes a time $t_c$ to cross between the branes, this distance would be given by

$$s_{AD} = e^{\mu\mathcal{D}} \int_{t_c}^{t_f - t_c} \frac{\mathrm{d}t}{a(t)}. \tag{2.42}$$

Therefore, if $e^{\mu\mathcal{D}} \gg 1$, then $s_{AD} \gg s_{AE}$ and we have a mechanism for solving the horizon

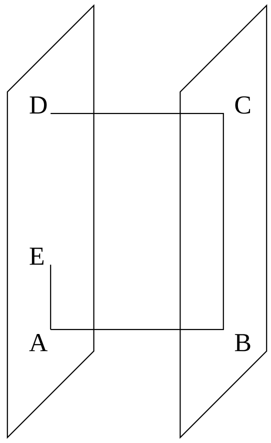


Figure 2.12: A Null signal that remains on our brane goes from A to E in time $t_f$, one which leaves the brane could travel between A, B, C and then return to our brane at D in the same time as the first signal reaches E.

problem.

The major problem with this suggestion as presented is that it involves metrics that are not realistic. It relies upon there being a conformal factor that affects the spatial part of the four-dimensional metric only. In typical Randall–Sundrum braneworld models, the metric is usually of the form

$$\mathrm{d}s^2 = e^{-2\mu y}\eta_{\mu\nu}\mathrm{d}x^\mu \mathrm{d}x^\nu - \mathrm{d}y^2, \tag{2.43}$$

and hence the above mechanism for solving the horizon problem is inapplicable.

### 2.6.1 A Cosmologically Realistic Metric

The above metrics (2.40) and (2.43) are static, and so are obviously not realistic descriptions of our Universe; it is therefore worthwhile to consider whether the above proposed solution to the horizon problem will work for a cosmological metric. If $w$, $f$ and $k$ are set to zero, the solutions to Einstein's equations given by (2.32) can be greatly simplified. Writing $a(t,y)$ in terms of exponentials gives

$$a(t,y)^2 = \frac{a_0^2 e^{-2\mu y}}{4}\left[\frac{\rho}{\sigma}e^{2\mu y} - (\frac{\rho}{\sigma}+2)\right]^2, \tag{2.44}$$

further simplified to give

$$a(t,y) \quad = \quad a_0\left(\cosh\mu y - \eta_0 \sinh\mu y\right), \tag{2.45}$$

which can be used with equation (2.36) to give

$$n(t,y) \quad = \quad \left(\cosh\mu y - \tilde{\eta}_0 \sinh\mu y\right), \tag{2.46}$$

We have defined

$$\eta_0 \quad = \quad 1+\frac{\rho}{\sigma}, \qquad \tilde{\eta}_0 \quad = \quad \eta_0 + \frac{\dot{\eta}_0}{H_0}. \tag{2.47}$$

Here, $H_0$ is the Hubble constant on the brane at $y=0$, given by equation (2.30), and can now be written in the form

$$H_0^2 \quad = \quad \frac{\kappa^4}{36}\rho_0^2 + \frac{\Lambda}{6} \quad = \quad \mu^2\left(\eta_0^2 - 1\right). \tag{2.48}$$

In order for there to be a significant difference in the relative 'speeds' of null signals travelling along the two branes, we require that $n/a$ is larger for some $y$ than it is for $y=0$, i.e. that

$$\frac{n(t,y)}{a(t,y)} \gg \frac{n(t,0)}{a(t,0)} \quad \Leftrightarrow \quad \frac{\cosh\mu y - \tilde{\eta}_0 \sinh\mu y}{a_0(\cosh\mu y - \eta_0 \sinh\mu y)} \gg \frac{1}{a_0}. \tag{2.49}$$

An acceptable equation of state on our brane demands that $\rho \propto a_0^{-q}$ implying that $\tilde{\eta}_0 = \eta_0 - q\rho/\sigma$ and therefore that $\tilde{\eta}_0 < \eta_0$. The ratio $n/a$ will therefore diverge as $y \to y_h$, where $y_h$ is the position of the horizon defined by $a(t,y_h)=0$ and is given by

$$\tanh\mu y_h \quad = \quad \frac{1}{\eta_0}. \tag{2.50}$$

This suggests that null signals may travel along the second brane at much greater 'speeds' than on our brane, provided the second brane is close to the horizon. To calculate the difference in speeds correctly, we must turn our attention to the motion of the second brane with respect to the one at $y=0$.

### 2.6.2 General Behaviour of the Inter-brane Distance

In this section we use a simple non-perturbative method to derive the general equation of motion for the inter-brane distance otherwise known as the cosmological radion and denoted by $\mathcal{D}(t)$, which was first derived by [57]. For alternative approaches to this topic see [59–62].

We first note that if the second brane follows a trajectory given by $y = \mathcal{D}(t)$, then the induced four-dimensional metric on the second brane is given by

$$\begin{aligned} \mathrm{d}s^2 &= -\left[n^2(t, \mathcal{D}(t)) - \dot{\mathcal{D}}^2\right] \mathrm{d}t^2 + a^2(t, \mathcal{D}(t))\mathrm{d}x^2 && (2.51) \\ &= -\mathrm{d}\tau^2 + a_2^2(\tau)\mathrm{d}x^2, && (2.52) \end{aligned}$$

where $\tau$ has been defined as the proper time as seen by an observer on the second brane. The expansion rate of the second brane as seen by an observer on our brane is simply

$$H_2(t) = \frac{1}{a_2}\frac{\mathrm{d}a_2}{\mathrm{d}t} = \left(\frac{\dot{a}}{a} + \frac{a'}{a}\dot{\mathcal{D}}\right)_2, \tag{2.53}$$

and as seen by an observer on the second brane itself

$$\begin{aligned} \mathcal{H}_2(\tau) &= \frac{1}{a_2}\frac{\mathrm{d}a_2}{\mathrm{d}\tau} = H_2(t)\frac{\mathrm{d}t}{\mathrm{d}\tau} && (2.54) \\ &= \left(\frac{\dot{a}}{a} + \frac{a'}{a}\dot{\mathcal{D}}\right)\left(n^2 - \dot{\mathcal{D}}^2\right)^{-1/2}. && (2.55) \end{aligned}$$

The significance of this equation for $\mathcal{H}_2$ is that it relates the expansion rate of the second brane (with respect to proper time) to $\mathcal{D}$ and $\dot{\mathcal{D}}$. It does not seem so useful at first sight, as calculating $\mathcal{H}_2$ could remain difficult; however, we know that the braneworld Friedman equation given by (2.48) is derived from a purely local analysis, and that should we have chosen the second brane to be stationary and at $y = 0$, we would have derived the equivalent Friedman equation with $\rho$ replaced by $\rho_2$. This means that $\mathcal{H}_2(\tau)$ must have the form

$$\mathcal{H}_2^2(\tau) = \frac{\kappa^4}{36}\rho_2^2 - \frac{\Lambda}{6} = \mu^2\left(\eta_2^2 - 1\right), \tag{2.56}$$

where we have defined $\eta_2 = \rho_2/\sigma$.

Equation (2.56) ensures that the second brane is $Z_2$ symmetric and that it evolves according to the junction conditions of the extrinsic curvature tensor, just as equation (2.48) ensures similar behaviour for our brane. At this point we use the following identity[5]

[5]Note that although the derivation is done here for $f = k = w = 0$, this method generalizes to braneworlds with non-zero values of these parameters with the use of the appropriate Friedman equation for equation (2.56) and identity for equation (2.57).

which is obtained from the Einstein equations and is derived in [58]:

$$\left(\frac{\dot{a}}{na}\right)^2 = \frac{a'^2}{a^2} - \mu^2, \tag{2.57}$$

giving

$$\mathcal{H}_2^2 = \left(\frac{\dot{a}}{na}\right)^2 - \frac{a'^2}{a^2} + \mu^2\eta_2^2. \tag{2.58}$$

Substituting (2.58) into (2.54) and rearranging finally gives the first order equation for $\dot{\mathcal{D}}$:

$$\dot{\mathcal{D}} = n\left(-\frac{a'\dot{a}}{a^2 n} \pm \mu^2\eta_2\sqrt{\eta_2^2 - 1}\right)\left(\frac{\dot{a}^2}{n^2a^2} + \mu^2\eta_2^2\right)^{-1}. \tag{2.59}$$

This can be rewritten in the form found by [57]

$$\frac{a'}{a} + \frac{\dot{a}}{n^2 a}\dot{\mathcal{D}} = \mu\eta_2\left(1 - \frac{\dot{\mathcal{D}}}{n^2}\right)^{1/2}. \tag{2.60}$$

In order to investigate acausal signals we will be interested in a stationary second brane, and therefore need an equation for $\ddot{\mathcal{D}}$. [57] have shown that by differentiating (2.60) with respect to time, considering the three-dimensional symmetries of the bulk energy momentum tensor, and the $Z_2$-symmetry of the branes, it is possible to derive that

$$\frac{\ddot{\mathcal{D}}}{n^2} + \frac{n'}{n}\left(1 - 2\frac{\dot{\mathcal{D}}^2}{n^2}\right) - \frac{\dot{n}}{n}\frac{\dot{\mathcal{D}}}{n^2} = -(2\mu\eta_2 + 3\mu p_2)\left(1 - \frac{\dot{\mathcal{D}}^2}{n^2}\right)^{3/2}. \tag{2.61}$$

Equations (2.59) and (2.61) govern the evolution of $\mathcal{D}$ and will be used in the next two sections to evaluate the difference in the speeds of null signals travelling along each brane.

### 2.6.3 Acausal Signals: Stationary Branes

The simplest solutions to equations (2.59) and (2.61) are those describing a stationary second brane; in this section we will investigate the appropriate conditions and the ratio of distances travelled on each brane in a certain time interval. Setting $\dot{\mathcal{D}} = \ddot{\mathcal{D}} = 0$ in (2.60) and (2.61) trivially gives the well known conditions on $\eta_2$ and $p_2 \equiv P_2/\sigma$ which ensure that the second brane does not move:

$$\eta_2 = \frac{\sinh\mu\mathcal{D} - \eta_0\cosh\mu\mathcal{D}}{\cosh\mu\mathcal{D} - \eta_0\sinh\mu\mathcal{D}}, \tag{2.62}$$

$$p_2 = -\frac{1}{3}\frac{\sinh\mu\mathcal{D} - \tilde{\eta}_0\cosh\mu\mathcal{D}}{\cosh\mu\mathcal{D} - \tilde{\eta}_0\sinh\mu\mathcal{D}} - \frac{2}{3}\eta_2. \tag{2.63}$$

Note that if we demand standard cosmology on our brane at late times then this requires that both $\eta_0$ and $\tilde{\eta}_0$ tend to 1 (not zero as [57] have suggested). This results in the equation of state for matter on the second brane becoming $-\eta_2 = p_2 = 1$ which is equivalent to $-\rho_2 = P_2 = 6\mu/\kappa^2$, the conditions in the original Randall–Sundrum two brane scenario.

Assuming the above form for the energy and pressure densities on the second brane, it only remains to evaluate the distances travelled by null signals between times $t_1$ and $t_2$ on either brane:

$$s_1 = \int_{t_1}^{t_2}\frac{1}{a_0}\mathrm{d}t, \qquad s_2 = \int_{t_1}^{t_2}\frac{\sqrt{n^2(t,\mathcal{D}(t)) - \dot{\mathcal{D}}^2}}{a^2(t,\mathcal{D}(t))}\mathrm{d}t : \tag{2.64}$$

though, since we have assumed a stationary second brane, $s_2$ simplifies to become

$$s_2 = \int_{t_1}^{t_2}\frac{n(t,\mathcal{D}(t))}{a(t,\mathcal{D}(t))}\mathrm{d}t = \int_{t_1}^{t_2}\frac{\cosh\mu\mathcal{D} - \tilde{\eta}_0\sinh\mu\mathcal{D}}{a_0(\cosh\mu\mathcal{D} - \eta_0\sinh\mu\mathcal{D})}\mathrm{d}t. \tag{2.65}$$

As discussed in 2.6.1, a standard equation of state on our brane leads to $\tilde{\eta}_0$ having the form $\tilde{\eta}_0 = \eta_0 - q\rho/\sigma$ and therefore,

$$s_2 = \int_{t_1}^{t_2}\left[\frac{1}{a_0} + \frac{(q\rho/\sigma)\sinh\mu\mathcal{D}}{a_0(\cosh\mu\mathcal{D} - (1+\rho/\sigma)\sinh\mu\mathcal{D})}\right]\mathrm{d}t \tag{2.66}$$

$$= s_1 + \Delta s. \tag{2.67}$$

Rewriting the Friedman equation for our brane in terms of $\rho/\sigma$ gives $H_0^2 = \mu^2 q^2((\rho/\sigma)^2 + 2\rho/\sigma)$. This, and the fact that $\rho = \lambda/a_0^q$ allows the $\Delta s$ integral to be converted into the form

$$\Delta s = \frac{A(\mathcal{D})}{\mu(\sigma\lambda)^{1/q}}\int_{u_1}^{u_2}\frac{\mathrm{d}u}{u^{1/q}\sqrt{2u+1}(u - A(\mathcal{D}))} \tag{2.68}$$

where $u = \sigma/\rho$ and all the information on the second brane's position has been grouped into $A(\mathcal{D}) = \sinh\mu\mathcal{D}/(\cosh\mu\mathcal{D} - \sinh\mu\mathcal{D})$. The integral in (2.64) can be similarly converted, and we then obtain the ratio of the extra distance travelled on the second brane, divided by the distance travelled on our brane in the same time,

$$\frac{\Delta s}{s_1} = qA(\mathcal{D})\left(\int_{u_1}^{u_2}\frac{\mathrm{d}u}{u^{1/q}\sqrt{2u+1}(u-A(\mathcal{D}))}\right)\left(\int_{u_1}^{u_2}\frac{\mathrm{d}u}{u^{1/q}\sqrt{2u+1}}\right)^{-1}. \tag{2.69}$$

We now need to determine the possible limits on $u_1$ and $u_2$. Obviously the contribution of the integral to $\Delta s$ for values of $u$ greater than $(q+1)A(\mathcal{D})$ will be less than the corresponding contribution to $s_1$ and so we set an upper limit of $u_2$ to be $(q+1)A(\mathcal{D})$, as a larger $u_2$ is of no interest. The minimum possible value of $u_1$ is slightly harder to find as it is constrained by the requirement that the energy densities of both branes remain below the five-dimensional Planck mass limit

$$\rho \le M_5^4 \quad \Rightarrow \quad u = \frac{\sigma}{\rho} \le \frac{6M_5^2}{M_4^2} = \frac{6}{M}, \tag{2.70}$$

where we have defined $M$ to be the dimensionless ratio of the squares of the four- and five-dimensional Planck masses $M \equiv M_4^2/M_5^2$. Demanding a similar constraint on $\rho_2$ and using the stability condition given by (2.62), results in the condition

$$|\rho_2| \le M_5^4 \quad \Rightarrow \quad |\eta_2| = \frac{|\rho_2|}{\sigma} \le \frac{M}{6} \tag{2.71}$$

$$\Rightarrow \quad \frac{\eta_0\cosh\mu\mathcal{D}-\sinh\mu\mathcal{D}}{\cosh\mu\mathcal{D}-\eta_0\sinh\mu\mathcal{D}} \le \frac{M}{6}; \tag{2.72}$$

this can be rearranged and expressed in terms of $u$ using the fact that $\eta_0 = 1+1/u$, to give the constraint on $u$ that ensures that $|\rho_2|$ is always less than $M_5^4$:

$$u \ge \frac{M\tanh\mu\mathcal{D}+6}{(M-6)(1-\tanh\mu\mathcal{D})}. \tag{2.73}$$

In the next two sections we will use this constraint to determine $u_1$ which corresponds to the earliest possible time that a null signal can set off along the second brane. We examine both the near brane ($\mu\mathcal{D} \ll 1$) and the far brane ($\mu\mathcal{D} \gg 1$) limits.

### 2.6.4 Near-brane Limit

We now evaluate the integral expression for $\Delta s/s_1$ given by (2.69), in the small $\mu\mathcal{D}$ limit. The minimum possible value of the inter-brane distance $\mathcal{D}$ will be the inverse of the 5D Planck mass, $\mathcal{D} \ge 1/M_5$, and for a cosmologically realistic brane $\mu$ is given by $\mu = M_5^3/M_4^2$, leading to the relation

$$\mu\mathcal{D} \quad \geq \quad \frac{M_5^2}{M_4^2} \quad = \quad \frac{1}{M}. \tag{2.74}$$

If we therefore assume that $1/M \leq \mu\mathcal{D} \ll 1$, we find that in this limit $A(\mathcal{D}) \simeq \mu\mathcal{D}$ and therefore that $u_1 < u_2 = (q+1)A(\mathcal{D}) \ll 1$. Equation (2.69) can then be approximated by

$$\frac{\Delta s}{s_1} \quad \simeq \quad qA(\mathcal{D}) \left( \int_{u_1}^{(q+1)A(\mathcal{D})} \frac{\mathrm{d}u}{u^{1/q}(u - A(\mathcal{D}))} \right) \left( \int_{u_1}^{(q+1)A(\mathcal{D})} \frac{\mathrm{d}u}{u^{1/q}} \right)^{-1}. \tag{2.75}$$

If we further assume that our brane is undergoing radiation dominance by setting $q = 4$, the first integral on the right hand side of (2.75) can be integrated to give

$$A^{\frac{1}{4}} \int_{u_1}^{u_2} \frac{\mathrm{d}u}{u^{1/4}(u - A(\mathcal{D}))} \quad =$$
$$2\arctan\left[\left(\frac{u_2}{A}\right)^{\frac{1}{4}}\right] \; - \; 2\arctan\left[\left(\frac{u_1}{A}\right)^{\frac{1}{4}}\right] \; + \; \ln\left[\frac{\left(\frac{u_2}{A}\right)^{\frac{1}{4}} - 1}{\left(\frac{u_1}{A}\right)^{\frac{1}{4}} - 1} \cdot \frac{\left(\frac{u_1}{A}\right)^{\frac{1}{4}} + 1}{\left(\frac{u_2}{A}\right)^{\frac{1}{4}} + 1}\right],$$

and the second integral is trivially given by

$$\int_{u_1}^{u_2} \frac{\mathrm{d}u}{u^{1/4}} \quad = \quad \frac{4}{3}(u_2^{\frac{3}{4}} - u_1^{\frac{3}{4}}). \tag{2.76}$$

From above we take $u_2 = (q+1)A(\mathcal{D}) = 5A(\mathcal{D})$, and therefore it only remains to evaluate $u_1/A(\mathcal{D})$ in the small $\mu\mathcal{D}$ limit using equation (2.73):

$$\frac{u_1}{A(\mathcal{D})} \quad = \quad \frac{M\tanh\mu\mathcal{D} \; + \; 6}{(M \; - \; 6)\tanh\mu\mathcal{D}} \quad \simeq \quad 1 \; + \; \frac{3}{2M\mu\mathcal{D}}. \tag{2.77}$$

Replacing the values for $u_1$ and $u_2$ into the expression for $\Delta s/s_1$ and ignoring all subdominant terms finally gives the ratio of the maximum extra distance travelled by a null signal on the second brane compared with the first in the near brane limit as

$$\frac{\Delta s}{s_1} \quad \simeq \quad 1.28\ln(M\mu\mathcal{D}). \tag{2.78}$$

The value of $M_5$ is constrained by nucleosynthesis such that $M_5 \geq 30$TeV. This gives the corresponding constraint on the dimensionless ratio $M$ as

$$M = \frac{M_4^2}{M_5^2} < 10^{29}. \tag{2.79}$$

In order for the above approximations to be valid, $\mu\mathcal{D}$ must satisfy $\mu\mathcal{D} < 10^{-2}$, and therefore (2.78) becomes

$$\frac{\Delta s}{s_1} \simeq 80. \tag{2.80}$$

This shows that any seemingly acausal effects due to signals travelling on the second brane as opposed to our brane are too small to solve the cosmological horizon problem in the ($\mathcal{D} \ll 1/\mu$) limit. Another important point is that $\Delta s$ is only significantly greater than $s_1$ for a very brief time, shortly after the big bang; if the signals were to travel for longer periods, say until $u_2 = 1$, then the distance ratio would become much less than unity: $\Delta s/s_1 \simeq \mu\mathcal{D}\ln(M\mu\mathcal{D})$ as can be seen from (2.75).

### 2.6.5 Far-brane Limit

In this section we investigate the behaviour of null signals travelling on the second brane when the inter-brane distance is large ($\mathcal{D} \gg 1/\mu$). The fact that the second brane has to be closer to our brane than the horizon implies that we will be examining signals that are travelling at late times with respect to our Universe, as opposed to the previous section where the interesting situations occurred only at early times.

In the $\mathcal{D} \gg 1/\mu$ limit, the function $A(\mathcal{D})$ becomes very large and can be approximated by

$$A(\mathcal{D}) = \frac{\tanh\mu\mathcal{D}}{1-\tanh\mu\mathcal{D}} \simeq \frac{1}{2}e^{2\mu\mathcal{D}}. \tag{2.81}$$

As before, we will require the ratios $u_2/A(\mathcal{D}) = (q+1)$ and $u_1/A(\mathcal{D})$ which is obtained from equation (2.73) and is approximately given by

$$\frac{u_1}{A(\mathcal{D})} = \frac{M\tanh\mu\mathcal{D} + 6}{(M - 6)\tanh\mu\mathcal{D}} \simeq 1 + \frac{12}{M}. \tag{2.82}$$

Therefore both $u_1$ and $u_2$ are exponentially large and so the expression for $\Delta s/s_1$ given by equation (2.69) can be simplified in the large $\mathcal{D}$ limit to

$$\frac{\Delta s}{s_1} \simeq qA(\mathcal{D})\left(\int_{(1+\frac{12}{M})A(\mathcal{D})}^{(q+1)A(\mathcal{D})} \frac{\mathrm{d}u}{u^{\frac{1}{q}+\frac{1}{2}}(u-A(\mathcal{D}))}\right)\left(\int_{(1+\frac{12}{M})A(\mathcal{D})}^{(q+1)A(\mathcal{D})} \frac{\mathrm{d}u}{u^{\frac{1}{q}+\frac{1}{2}}}\right)^{-1}. \tag{2.83}$$

Assuming radiation dominance, the first integral on the right hand side of (2.83) can be solved to give

$$A^{\frac{3}{4}}\int_{u_1}^{u_2}\frac{\mathrm{d}u}{u^{3/4}(u-A(\mathcal{D}))} = $$
$$-2\arctan\left[\left(\frac{u_2}{A}\right)^{\frac{1}{4}}\right] + 2\arctan\left[\left(\frac{u_1}{A}\right)^{\frac{1}{4}}\right] + \ln\left[\frac{\left(\frac{u_2}{A}\right)^{\frac{1}{4}}-1}{\left(\frac{u_1}{A}\right)^{\frac{1}{4}}-1}\cdot\frac{\left(\frac{u_1}{A}\right)^{\frac{1}{4}}+1}{\left(\frac{u_2}{A}\right)^{\frac{1}{4}}+1}\right],$$

which when combined with (2.83) and (2.82), and after all subdominant terms are neglected, results in the following expression for the extra distance travelled on the second brane in the far brane limit:

$$\frac{\Delta s}{s_1} \simeq 2\ln(M); \tag{2.84}$$

note that if instead of radiation domination we had chosen matter domination and set $q = 3$, the leading term given in equation (2.84) would have been unaltered. Finally, substituting the maximum permissible value of $M \simeq 10^{29}$ into 2.84 leads to the final result

$$\frac{\Delta s}{s_1} \simeq 130. \tag{2.85}$$

Unlike when $\mathcal{D} \ll 1/\mu$, here $\Delta s$ is significantly greater than $s_1$ for an extended period of time. Solving the Friedman equation gives the late-time relation between $u$ and the cosmic time $t$ as measured on our brane to be $u \simeq \mu^2 q^2 t^2/2$. This implies that $\Delta s > s_1$ during a time interval of

$$\Delta t \simeq (M_4^2/2M_5^3)\exp(\mu\mathcal{D}) = 10^{27}\exp(\mu\mathcal{D})\mathrm{TeV}^{-1}. \tag{2.86}$$

However, as can be seen from equation (2.83), if limits for the integral for $\Delta s/s_1$ are such that $u_2 \gg u_1$, then any acausal effect becomes negligible. Taking $u_1$ to be just before recombination and $u_2$ at the present day leads to $u_1 \sim 10^{12}$ and $u_2 \sim 10^{21}$, and therefore the horizon problem cannot be solved in this manner, though this effect may have important consequences in other areas of cosmology such as structure formation. One should note that the effectiveness of the acausality would also be lessened by the time taken for signals to cross between the branes.

### 2.6.6 Acausal Signals: Moving Branes

Until now we have been examining the possibility of acausal signals travelling along stationary branes. It is, however, of interest to consider the possible effects of allowing the branes to move. For a general cosmological scenario the equation of motion of the second brane is very difficult to solve; various qualitative features can, however, be investigated and will be discussed in this section. We start with the equation for the time dependent inter-brane spacing $\mathcal{D}(t)$, derived previously in equation (2.60):

$$\frac{\dot{\mathcal{D}}}{n} = \left(-\frac{a'\dot{a}}{a^2 n} + \mu^2\eta_2\sqrt{\eta_2^2-1}\right)\left(\frac{\dot{a}^2}{n^2a^2}+\mu^2\eta_2^2\right)^{-1}. \tag{2.87}$$

This can be rewritten using equations (2.56), (2.58), (2.45) and (2.46) as

$$\frac{\dot{\mathcal{D}}}{n} = \frac{H_0(\eta_0\cosh\mu\mathcal{D}-\sinh\mu\mathcal{D})+\mu\eta_2\mathcal{H}_2(\cosh\mu\mathcal{D}-\eta_0\sinh\mu\mathcal{D})^2}{(\eta_0\cosh\mu\mathcal{D}-\sinh\mu\mathcal{D})^2+\mathcal{H}_2^2(\cosh\mu\mathcal{D}-\eta_0\sinh\mu\mathcal{D})^2}. \tag{2.88}$$

For the trivial case where $\eta_2$ is constant and therefore $\mathcal{H}_2 = 0$, equation (2.88) can easily be solved numerically as was done in [57]. For a cosmologically realistic case where $\eta_2$ is time dependent, the solution is less easily obtained. If, for example, we assume a standard equation of state on the second brane: $P_2 = \omega_2\rho_2$ which provided $\omega_2 > -1$, implies that $\rho_2 \propto 1/a_2^{q_2}$, we can then solve the Friedman equation

$$\mathcal{H}_2^2 = \frac{1}{a_2^2}\left(\frac{\mathrm{d}a_2}{\mathrm{d}\tau}\right)^2 = \frac{1}{q_2^2\eta_2^2}\left(\frac{\mathrm{d}\eta_2^2}{\mathrm{d}\tau}\right)^2 = \mu^2(\eta_2^2-1), \tag{2.89}$$

to give $\eta_2 = -1/\sin(q_2\mu\tau)$ and $\mathcal{H}_2 = \mu^2/\tan(q_2\mu\tau)$. However, to solve equation (2.88) we need to know $\eta_2$ and $\mathcal{H}_2$ in terms of $t$: our cosmic time, which is related to the second brane's cosmic time $\tau$ by

$$\mathrm{d}\tau = \sqrt{n^2-\dot{\mathcal{D}}^2}\,\mathrm{d}t. \tag{2.90}$$

This makes it much more difficult to solve for $\dot{\mathcal{D}}$ and due to this added level of complexity we leave a more general study of (2.88) to future work. We now examine the situation qualitatively and argue that acausality in the moving brane model is not appreciably greater than in the static case.

From equation (2.87) it can be seen immediately that since $a' < 0$ for $0 < \mathcal{D} < y_h$, if $\eta_2 > 0$, then $\dot{\mathcal{D}} > 0$ for all $\mathcal{D}$ and the second brane will move away from our brane and freeze out at the horizon, which has a time dependent position given by $y_h = \arctan(1/\eta_0)$.

If $\eta_2 < 0$, then $\dot{\mathcal{D}} = 0$ only when

$$\mu\eta_2 = \frac{a'(t,\mathcal{D})}{a(t,\mathcal{D})}. \tag{2.91}$$

Requiring also that $\ddot{\mathcal{D}} = 0$ gives the conditions for stationary branes as discussed previously. The stability of a stationary second brane has been investigated in [57] where it was shown that if both branes are de Sitter the equilibrium position is unstable, while if both branes are anti-de Sitter it is stable. For our purposes, we only need to examine the case where the second brane moves in the positive $y$ direction and freezes out at the horizon, as the other possibilities are that the second brane approaches our brane and collides with it which is physically unacceptable, or that the second brane is stable: the case which has been examined previously.

If the second brane does freeze out, then $\mathcal{D} \to y_h$ and $\dot{\mathcal{D}} \to n(t,\mathcal{D})$, as can be verified from equation (2.87). The expression for the distance travelled on the second, moving, brane is

$$s_2 = \int_{t_1}^{t_2} \frac{\sqrt{n^2(t,\mathcal{D}(t)) - \dot{\mathcal{D}}^2}}{a^2(t,\mathcal{D}(t))}\mathrm{d}t, \tag{2.92}$$

which will therefore tend to zero as $\dot{\mathcal{D}} \to n(t,\mathcal{D})$. Another problem is the distance that signals have to travel to return. In order for there to be a significant acausal effect, the null signal must travel on the second brane for a substantial amount of time, and will therefore be a large distance away from our brane when starting to return. The combination of these two effects – the distance travelled by a null signal on the second brane frozen at the horizon tending to zero, and the large distance returning signals would have to travel – suggest that any experiments aiming to detect acausal effects on our brane would have to have impractically high sensitivity.

## 2.7 Conclusions

We have investigated the behaviour of null geodesics in several five-dimensional braneworld scenarios. In the single brane case it was shown that apparent causality violations caused by such signals taking shortcuts through the bulk were small. The ratio of the speed of five-dimensional gravity signals to the speed of four-dimensional light $c_g/c_\gamma$ was found to be in general not more than two. The effects of introducing a non-zero Weyl tensor component and of relaxing the mirror (or $Z_2$) symmetry were examined and shown in general to decrease the observed acausality.

It was found that during early times in the Universe many geodesics could have returned to our brane, in contrast to late times when most of the geodesics leaving our brane freeze out at the horizon. This is understandable, as at late times ($\rho \to 0$) the cosmological metrics that were considered tend to the standard Randall–Sundrum metric which, as previously discussed, results in geodesics not returning. The behaviour of these geodesics could be used in conjunction with the temperature dependent production rate of gravitons to determine exactly the amount of energy lost to the bulk throughout the history of the Universe as is discussed in [63].

Analysis of the two brane scenario (with $w = f = k = 0$) shows that signals can in some situations travel along the second brane significantly faster than along our brane. This effect, however, would only last for a certain time depending on the position of the second brane. In the near brane limit ($\mu\mathcal{D} \ll 1$) this period is very brief and any acausal effects would become negligible when longer time intervals are considered. In the far brane limit ($\mu\mathcal{D} \gg 1$) however, the period of interest can last for $\Delta t \simeq 10^{27}\exp(\mu\mathcal{D})\mathrm{TeV}^{-1}$and it was found that the apparent speeds of null signals were approximately 130 times faster on the second brane than on the first. It should be noted that a non-zero $w$ and $f$ would lessen the above effect as the crucial ratio $n(t,\mathcal{D})/a(t,\mathcal{D})$ is largest only when $w = f = 0$. Another factor that would detract from the effectiveness of this mechanism in the far brane limit is the time taken for signals to travel between the two branes.

In neither one nor two brane scenarios are the possible acausal effects significant enough to enable us to solve the cosmological horizon problem. The increase in the gravitational particle horizon could, however, have important effects on other areas of cosmology such as the initial conditions of inflation, structure formation and the production of topological defects. It would also technically be possible to measure the time delay between the detection of gravitational waves and light waves from a particular cosmic event; however, we believe that this would require significant advances in gravitational wave detector technology.

In the following chapter, we shall investigate the effective theory of gravity that applies to a four-dimensional observer located on a 3-brane. We shall use as our basis another extension of the Randall–Sundrum scenario, motivated by supergravity solutions in singular spaces [41, 42], and examine the gravitational perturbations around the background model.

# Chapter 3

# A four-dimensional view of a braneworld

## 3.1 Introduction

In the previous chapter, we considered the causal structure of a cosmological braneworld scenario. We examined the behaviour of geodesics in a generalization of the Randall–Sundrum solutions, considering both systems with only one brane present and those with two branes. In the latter case, the behaviour of the radion (the distance between the branes) was found to influence the behaviour of the geodesics substantially. We now turn to the investigation of the dynamics of a braneworld scenario with two branes in the presence of a bulk scalar field. The second brane is separated from the first brane by a distance $r_c$. From the viewpoint of the four-dimensional theory the radion is another scalar degree of freedom; the dynamics of the radion in isolation have been discussed in chapter 2 and in many papers (see [57, 59, 60, 64–70] and references therein).

In this chapter we start by studying the coupling of the radion to the bulk scalar field. To do so we focus on linear perturbations around a static solution, solving the equations of motion for the scalar and gravitational perturbations. As usual we isolate two types of gravitational degrees of freedom: the first type comprises the gravitons and their imprints on the brane; the second springs from the existence of two branes and leads to the radion modulus parameterizing the proper distance between the branes. In the models considered here, the coupling between the bulk scalar field and the radion ensures that there is essentially only one scalar degree of freedom in the four-dimensional effective theory. We then compute the metric perturbation due to matter on the brane, and compare the low-energy limit to the Brans–Dicke theories; see [71].

The chapter is organized as follows. In section 3.2 we outline the theory used and

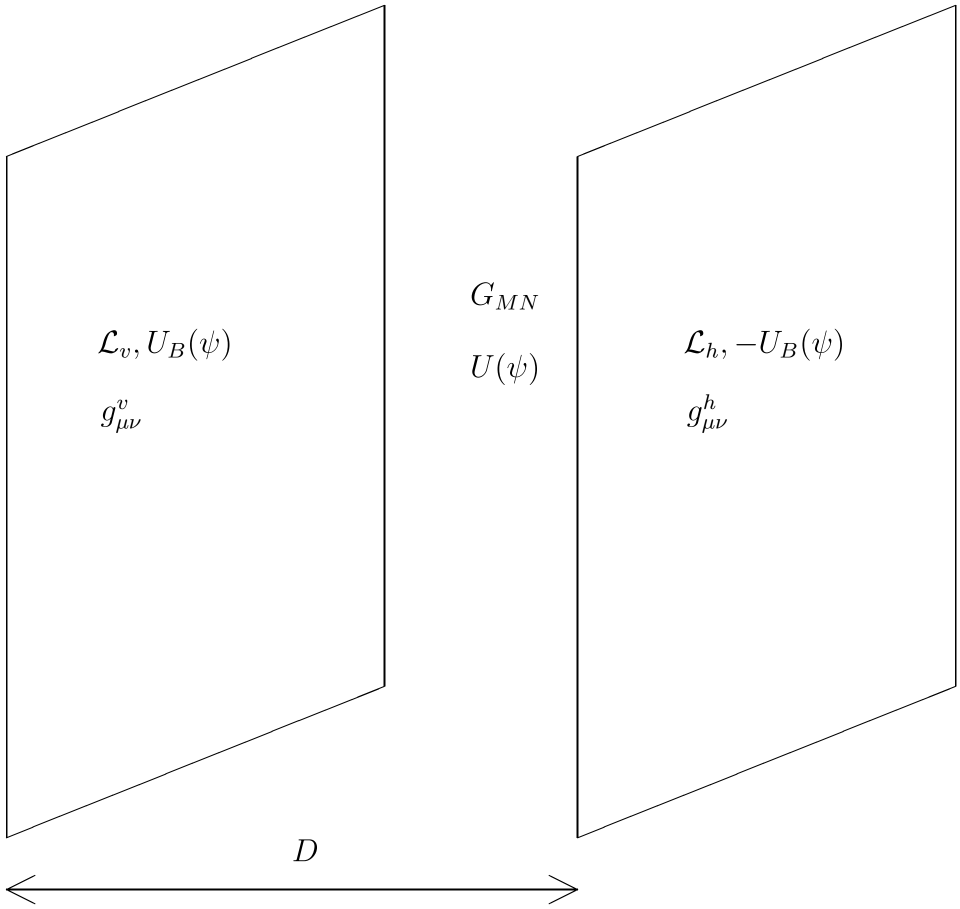


Figure 3.1: The braneworld setup. $U_B$ and $U$ are the superpotential and bulk potential for the bulk scalar field $\psi$; $D$ represents the physical distance between the branes.

the corresponding graviton wave function. In section 3.3 we discuss the fluctuation of the distances between the branes and its coupling to the bulk scalar field. We examine the effect of adding matter sources on the branes in section 3.4 and then, in section 3.5, compute the Brans–Dicke parameter that would be observed on the positive-tension brane in the low energy limit, and show that General Relativity is an attractor in rather general cases. We draw our conclusions in section 3.6.

## 3.2 The Graviton and the Scalar Field Zero Mode

In this section we describe the brane world configuration, and describe the graviton and scalar field zero modes; see figure 3.1.

### 3.2.1 The Background Configurations

We consider a bulk Lagrangian consisting of two terms which describe gravity and the bulk scalar field, respectively:

$$S_{\text{bulk}} = \frac{1}{2\kappa_5^2}\int d^5x\sqrt{-g_5}\left(\mathcal{R} - \frac{3}{4}\left((\partial\psi)^2 + U\right)\right). \tag{3.1}$$

The boundary terms read

$$S_{\text{brane}} = -\frac{3}{2\kappa_5^2}\int d^5x\sqrt{-g_5}(\delta(z) - \delta(z - r_c))U_B \tag{3.2}$$

where $U_B$ is the superpotential related to the potential as

$$U = \left(\frac{\partial U_B}{\partial\psi}\right)^2 - U_B^2. \tag{3.3}$$

We also include the Gibbons-Hawking boundary term

$$S_{\text{GH}} = \frac{1}{\kappa_5^2}\int_\delta d^4x\sqrt{-g^B}K \tag{3.4}$$

where $\delta = \delta(z) - \delta(z - r_c)$ is the boundary of spacetime, while $g^B$ is the boundary metric and $K$ the extrinsic curvature. At the positions of the branes we impose a $Z_2$ symmetry.

We investigate solutions which are obtained from BPS–like equations, which are given by [42, 46]

$$\frac{a'}{a} = -\frac{U_B}{4},\ \psi' = \frac{\partial U_B}{\partial\psi} \tag{3.5}$$

where $' = d/dz$ for a metric of the form

$$ds^2 = dz^2 + a^2(z)\eta_{\mu\nu}dx^\mu dx^\nu. \tag{3.6}$$

We will focus on the case where

$$U_B = 4ke^{\alpha\psi}, \tag{3.7}$$

with $\alpha = 1/\sqrt{3}$ or $-1/\sqrt{12}$, which was obtained in a theory of supergravity in singular spaces [42]. In that case the solution for the scale factor $a(z)$ reads

$$a(z) = (1 - 4k\alpha^2 z)^{\frac{1}{4\alpha^2}}, \tag{3.8}$$

while the scalar field solution is

$$\psi = -\frac{1}{\alpha}\ln\left(1 - 4k\alpha^2 z\right). \tag{3.9}$$

Note that in the $\alpha \to 0$ limit we retrieve the anti–de Sitter profile for the scale factor

$$a(z) = e^{-kz}, \tag{3.10}$$

and that in that case the scalar field decouples altogether.

In the following analysis we will assume that the conditions (3.5) are valid everywhere.

### 3.2.2 Absence of the Scalar Field Zero Mode

We now consider perturbations around the background metric (3.6). It was shown in [59] that in order to understand the origin of the radion mode, it is essential to analyze the possible gauge choices which preserve the Gaussian normal coordinates (see also section 3.3 below); in this section we therefore concentrate on the bulk scalar field perturbation and its transformation under infinitesimal coordinate transformations under this constraint.

Consider a brane located at

$$z = f(x^\mu) \tag{3.11}$$

where the bulk metric has the form (3.6), i.e. it reads

$$ds_0^2 = dz^2 + a^2(z)\eta_{\mu\nu}dx^\mu dx^\nu. \tag{3.12}$$

We consider perturbations of this background metric for which the perturbed metric has the form of a Gaussian normal coordinate system, i.e.

$$\delta g_{zz} = 0 = \delta g_{\mu z}. \tag{3.13}$$

When perturbing this background metric, one can change coordinates while preserving the Gaussian normal coordinate system and bringing the brane back to the origin of coordinates. This is achieved by considering vector fields $\xi$ (transforming $z \to z+\xi^z$, $x^\mu \to x^\mu+\xi^\mu$) which satisfy

$$\xi^z \equiv f(x^\mu),\ \xi^\mu = -\int \frac{dz}{a^2}\eta^{\mu\nu}\partial_\nu\xi_z + \eta^{\mu\nu}\epsilon_\nu(x^\mu). \tag{3.14}$$

Such a change of coordinates shifts the brane position to $z = 0$.

We still have five gauge degrees of freedom, specified by $\xi^z$ and $\epsilon^\mu$. In such a coordinate system the metric reads

$$ds^2 = ds_0^2 - \frac{U_B}{2}a^2(z)\xi_z dx^\mu dx_\mu - 2a^2\left(\int \frac{dz}{a^2}\right)\partial_\mu\partial_\nu\xi_z dx^\mu dx^\nu \tag{3.15}$$

where we have put $\epsilon_\mu = 0$. Such a change of metric corresponds to gravitational modes which lead to the existence of a radion mode.

Let us now consider the case of a perturbed four-dimensional part of the metric

$$ds^2 = dz^2 + a^2(z)dx^\mu dx_\mu + h_{\mu\nu}dx^\mu dx^\nu \tag{3.16}$$

when the brane is still located at $z = \xi_z$. In the Gaussian system at the origin we can write down the boundary conditions using

$$K_{\mu\nu} = \frac{1}{2}\partial_z g^B_{\mu\nu} \tag{3.17}$$

where $g^B$ is the brane metric. The Israel junction conditions can be expressed as the identity

$$K_{\mu\nu} - g^B_{\mu\nu}K = \frac{1}{2}T^B_{\mu\nu} \tag{3.18}$$

evaluated on the brane, where $T^B$ denotes the brane energy–momentum tensor.

In the coordinate system where the brane is at the origin, the perturbed metric reads

$$\hat{h}_{\mu\nu} = h_{\mu\nu} - \frac{U_B}{2}a^2(z)\xi_z\eta_{\mu\nu} - 2a^2\left(\int \frac{dz}{a^2}\right)\partial_\mu\partial_\nu\xi_z, \tag{3.19}$$

while the perturbation of the scalar field is

$$\delta\hat{\psi} = \delta\psi + \frac{\partial U_B}{\partial\psi}\xi_z, \tag{3.20}$$

where $\delta\psi$ is the intrinsic part of the scalar field fluctuation as measured when the brane is at $z = \xi_z$. Notice that the perturbed metric and perturbed scalar field have two sources. The boundary condition evaluated at the origin leads to

$$\partial_z h_{\mu\nu}|_0 + \frac{U_B}{2}h_{\mu\nu}\bigg|_0 = 2\partial_\mu\partial_\nu\xi_z - \frac{a^2}{2}\frac{\partial U_B}{\partial\psi}\eta_{\mu\nu}\delta\psi \tag{3.21}$$

while the scalar field boundary condition reads

$$\partial_z \delta\psi|_0 = \frac{\partial^2 U_B}{\partial\psi^2}\delta\psi\bigg|_0 ; \tag{3.22}$$

these equations tell us that the brane fluctuation $\xi_z$ acts as a source of gravitation on the brane.

Let us now describe the equations of motion in the bulk. We first concentrate on the Klein-Gordon equation

$$\Box\delta\psi + \frac{1}{2}h'\psi' = \frac{1}{2}\frac{\partial^2 U}{\partial\psi^2}\delta\psi \tag{3.23}$$

where $h = h^\mu_\mu$. The Klein-Gordon equation admits a solution

$$\delta\psi(x^\mu, z) = \frac{\partial U_B}{\partial\psi}\hat{\psi}(x^\mu), \tag{3.24}$$

with $h = 0$, for any four-dimensional massless $\hat{\psi}(x^\mu)$. It satisfies the boundary condition identically. Moreover we find that for these solutions the four-dimensional metric perturbation is traceless. Of course, there may be other solutions for which the trace does not vanish; but these solutions would not be zero modes, which are under consideration here.

We shall now analyze the Einstein equations to first order. They are best described by using the second order variation of the action. We consider the coordinate system where the brane is at $z = \xi_z$ and therefore write the metric perturbation as $h_{AB}$, where $h_{55} = 0 = h_{\mu 5}$, as we consider Gaussian normal coordinates. The second order variation of the gravitational Lagrangian reads [72]

$$\begin{aligned} \delta^{(2)}S_g &= \frac{1}{2\kappa_5^2}\int d^5x\sqrt{-g_0}\left(\frac{1}{2}D_A h^{AB}D_C h^{CB} - \frac{1}{4}D_A h_{BC}D^A h^{BC}\right. \\ &- \left.\frac{\mathcal{R}}{4}h_{AB}h^{AB} + \frac{1}{2}\mathcal{R}_{AB}h^A_C h^{BC} - \frac{1}{2}\mathcal{R}_{ABCD}h^{AD}h^{BC}\right) \end{aligned} \tag{3.25}$$

while the scalar Lagrangian gives

$$\delta^{(2)}S_\psi = -\frac{3}{8\kappa_5^2}\int\sqrt{-g_0}\left(\frac{\mathcal{L}_\psi}{3}h_{AB}h^{AB} + (\partial\delta\psi)^2 + \frac{1}{2}\frac{\partial^2 U}{\partial\psi^2}\delta\psi^2 + 2h^{AB}\partial_A\delta\psi\partial_B\psi\right) \tag{3.26}$$

where

$$\mathcal{L}_\psi = -\frac{3}{4}\left[(\partial\psi_0)^2 + U\right]. \tag{3.27}$$

Notice that there is a contribution to the gravitational part from the transverse part of the gravitational field. We can simplify these actions using Einstein's equations

$$\mathcal{R}_{AB} = T_{AB} - \frac{1}{3} T g_{AB} \tag{3.28}$$

and

$$\mathcal{R}_{ABCD} = -\frac{U_B^2}{16}\left(g^0_{AB}g^0_{CD} - g^0_{AD}g^0_{CB}\right) + \frac{1}{4}\left(\frac{\partial U_B}{\partial \psi}\right)^2 \left(p_A g^0_{[CD}p_{B]} - p_C g^0_{A[D}p_{B]}\right), \tag{3.29}$$

where $p_a = \delta_{a5}$. The bulk Einstein equations are then

$$\Box h_{ab} + \frac{U_B^2}{8} h_{ab} - D_{\{a}D_c \bar{h}^c_{b\}} = \frac{3}{4}\partial_{\{a}\delta\psi\partial_{b\}}\psi_0 \tag{3.30}$$

Notice the unconventional appearance of the transverse part of the metric perturbation.

Let us focus on the (55) component of the Einstein equations. It leads to

$$\partial_z \delta\psi = 0, \tag{3.31}$$

implying that $\delta\psi$ is a function of $x^\mu$ only. This is not compatible with the solution of the Klein-Gordon equation unless

$$\delta\psi \equiv 0, \tag{3.32}$$

and therefore the scalar field perturbation vanishes altogether in the coordinate system where the brane position fluctuates according to $\xi_z$. Finally, the ($\mu 5$) component of the Einstein equations gives

$$D_\nu h^\nu{}_\mu = 0, \tag{3.33}$$

and the metric perturbation is therefore found to be transverse–traceless. This finding will be used in the following section to identify the graviton wave function.

### 3.2.3 The Graviton

Now we consider the gravitational equation in order to discuss the graviton modes. The field equation for the graviton simplifies to

$$\Box h_{\mu\nu} + \frac{U_B^2}{8} h_{\mu\nu} = 0 \tag{3.34}$$

together with the boundary condition

$$\partial_z h_{\mu\nu}|_0 + \frac{U_B}{2} h_{\mu\nu}\bigg|_0 = 0 \tag{3.35}$$

where we impose $\xi_z = 0$. We decompose the solution into a product of a $z-$dependent part and a $x^\mu-$dependent part:

$$h_{\mu\nu} = g(z)\chi_{\mu\nu}(x^\mu). \tag{3.36}$$

The Laplacian operator acting on the gravitational perturbation can be obtained by writing

$$\Gamma^\alpha_{5\beta} = -\frac{U_B}{4}\eta^\alpha_\beta, \ \Gamma^5_{\alpha\beta} = \frac{U_B}{4} g^0_{\alpha\beta}, \tag{3.37}$$

where the BPS conditions (3.5) have been used; this leads to

$$\Box h_{\mu\nu} = (\partial_z^2 g)\chi_{\mu\nu} + g\Box\chi_{\mu\nu} \tag{3.38}$$

and eventually

$$\Box\chi_{\mu\nu} = a^{-2}\Box^{(4)}\chi_{\mu\nu} + \left(\left(\frac{\partial U_B}{\partial\psi}\right)^2 - \frac{3}{8}U_B^2\right)\chi_{\mu\nu}. \tag{3.39}$$

We consider the zero modes of the gravitational perturbation only; i.e. we select

$$\Box^{(4)}\chi_{\mu\nu} = 0, \tag{3.40}$$

implying that the graviton profile $g$ satisfies

$$\partial_z^2 g + \left(\frac{1}{2}\left(\frac{\partial U_B}{\partial\psi}\right)^2 - \frac{1}{4}U_B^2\right) g = 0. \tag{3.41}$$

This is a Schrödinger equation with a non-trivial potential. In the Randall-Sundrum case the brane potential is constant $U_B = 4k$, leading to

$$g_{RS} = a^2 \tag{3.42}$$

which satisfies the boundary condition.

To find the solution in the general case it is convenient to define the conformal coordinate

$$du = \frac{dz}{a}; \tag{3.43}$$

with such a choice and putting

$$g = \sqrt{a}\phi \tag{3.44}$$

we obtain the graviton equation

$$-\frac{d^2\phi}{du^2} + \frac{1}{a^{3/2}}\frac{d^2 a^{3/2}}{du^2}\phi = 0. \tag{3.45}$$

This is of the form of a supersymmetric quantum mechanics problem with

$$Q^\dagger Q\phi = 0 \tag{3.46}$$

where

$$Q = -\frac{d}{du} + \frac{d\ln a^{3/2}}{du},\ Q^\dagger = \frac{d}{du} + \frac{d\ln a^{3/2}}{du}: \tag{3.47}$$

the two zero modes are easily found to be

$$\phi_1 = a^{3/2} \tag{3.48}$$

and

$$\phi_2 = a^{3/2}\int \frac{du}{a^3}. \tag{3.49}$$

The boundary condition can be reexpressed in terms of $\phi$

$$\frac{d(\phi a^{-3/2})}{du} = 0 \tag{3.50}$$

implying that the graviton profile is given by $\phi_1$, i.e. that

$$g(z) = a^2. \tag{3.51}$$

Notice that this is the generalization to models with a bulk scalar field of the Randall-Sundrum result. The graviton is then described by

$$h_{\mu\nu} = a^2\chi_{\mu\nu}, \tag{3.52}$$

where $\chi_{\mu\nu}$ is a four-dimensional massless field. Now notice that we can use the residual gauge freedom specified by $\epsilon_\mu(x)$ to retrieve the fact that $\chi_{\mu\nu}$ possesses only two independent polarizations and therefore qualifies as the four-dimensional graviton. This result guarantees that the low energy effective action will be a scalar–tensor theory. We shall now discuss the appearance of an independent scalar mode whose coupling to gravity will be studied.

## 3.3 The Radion

So far we have discussed transverse–traceless modes with $\xi_z = 0$. In this section we include fluctuations of the brane positions and discuss their dynamics.

### 3.3.1 Brane Fluctuations

Coming back to the gravitational equation (3.30), we can investigate modes with $\xi_z \neq 0$: the boundary condition for such modes reads

$$\partial_z h_{\mu\nu}|_0 + \frac{U_B}{2} h_{\mu\nu}\Big|_0 = 2\partial_\mu\partial_\nu\xi_z \tag{3.53}$$

Taking the trace of the boundary condition and using the tracelessness of the gravitational perturbation $h_{\mu\nu}$ we find

$$\Box^{(4)}\xi_z \equiv \eta^{\mu\nu}\partial_\mu\partial_\nu\xi_z = 0, \tag{3.54}$$

implying that the brane fluctuation corresponds to a massless four-dimensional field. It is a mode which complements the graviton and leads to a scalar–tensor theory at low energy. We can solve the gravitational equation with the Ansatz

$$h_{\mu\nu} = a^{1/2}\phi_\xi(z)\partial_\mu\partial_\nu\xi_z \tag{3.55}$$

where $\phi_\xi$ satisfies (3.45); the boundary condition reads

$$\frac{d(\phi_\xi a^{-3/2})}{du}\Big|_0 = \frac{2}{a}\Big|_0 \tag{3.56}$$

We can identify the solution with

$$\phi_\xi = 2a_0^2\phi_2(z) \tag{3.57}$$

leading to

$$h_{\mu\nu} = 2a_0^2 a^2 \left( \int \frac{dz}{a^4} \right) \partial_\mu \partial_\nu \xi_z \tag{3.58}$$

It is conspicuous that the two zero modes of the gravitational equation are transcribed in the two types of physical modes, the graviton and the brane fluctuation.

### 3.3.2 Including a Second Brane

So far, we have not used the existence of the second brane. However, as we shall see in the following, a second brane must be included in this setting. The rôle of the second brane is two-fold: on the one hand, the existence of the second brane is crucial in order to preserve a consistent supersymmetric setting; on the other hand, the second brane screens off the naked singularity from the first brane [73].

The metric tensor which is a solution of the gravitational equation can be rewritten as

$$\hat{h}_{\mu\nu} = a^2 \chi_{\mu\nu} + 2a_0^2 a^2 \left( \int \frac{dz}{a^4} \right) \partial_\mu \partial_\nu \xi_z - 2a^2 \left( \int \frac{dz}{a^2} \right) \partial_\mu \partial_\nu \xi_z - \frac{U_B}{2} a^2 \xi_z \eta_{\mu\nu}, \tag{3.59}$$

where we recognize the graviton and the brane fluctuation. Such a solution can be defined in the vicinity of each brane. In the following we shall denote by $a_+$ and $\xi_z^+$ the scale factor and the brane fluctuation on the positive tension brane (respectively $a_-$ and $\xi_z^-$ on the negative tension brane). In each patch surrounding each brane the metric tensor is single-valued. We still have to construct a metric tensor which is single-valued throughout the bulk.

To do so we first impose that the brane fluctuation solution of (3.45) be single-valued. This is achieved by requiring

$$a_+^2 \xi_z^+ \equiv a_-^2 \xi_z^- \equiv \xi \tag{3.60}$$

where $\xi$ is a four-dimensional massless field. Notice that this mode is intrinsically non-local, relating the fluctuations on one brane to the fluctuations on the other brane. The metric tensor is now

$$\hat{h}^+_{\mu\nu} = a^2 \xi_{\mu\nu} + 2a^2 \left( \int \frac{dz}{a^4} \right) \partial_\mu \partial_\nu \xi - 2\frac{a^2}{a_+^2} \left( \int \frac{dz}{a^2} \right) \partial_\mu \partial_\nu \xi - \frac{U_B}{2} \frac{a^2}{a_+^2} \xi \eta_{\mu\nu} \tag{3.61}$$

in the patch surrounding the positive tension brane; in the second patch close to the negative tension brane, the metric tensor is similar:

$$\hat{h}^{-}_{\mu\nu} = a^2\xi_{\mu\nu} + 2a^2\left(\int\frac{dz}{a^4}\right)\partial_\mu\partial_\nu\xi - 2\frac{a^2}{a_-^2}\left(\int\frac{dz}{a^2}\right)\partial_\mu\partial_\nu\xi - \frac{U_B}{2}\frac{a^2}{a_-^2}\xi\eta_{\mu\nu} \tag{3.62}$$

Obviously the metric tensor cannot be patched up in this form as the two expressions in the two patches are different.

However, we can perform a change of coordinates which preserves the Gaussian normal coordinates and translates the second brane. In the second patch it reads

$$z \to z - \left(\frac{1}{a_-^2} - \frac{1}{a_+^2}\right)\xi, \tag{3.63}$$

which transforms $h^{-}_{\mu\nu}$ into $h^{+}_{\mu\nu}$; the negative tension brane now sits at

$$T(x) = r_c - \left(\frac{1}{a_-^2} - \frac{1}{a_+^2}\right)\xi. \tag{3.64}$$

Now the bulk metric is single-valued and given by (3.61).

Notice that the position of the second brane fluctuates according to fluctuations of the massless field $\xi$. Moreover, the field $T(x)$ can now be interpreted as the radion measuring the size of the extra dimension. The radion is also a four-dimensional massless field. In particular the radion measures the brane bending of the second brane.

We would like to obtain the metric tensor in a form where the size of the interval does not fluctuate, i.e. where the radion would appear as a fluctuation of the metric. This can be achieved thanks to a new change of coordinates defined by

$$z \to z + \left(\frac{1}{a^2} - \frac{1}{a_+^2}\right)\xi, \tag{3.65}$$

which rescales the size of the bulk in such a way that the second brane sits at $z = r_c$. Imposing the requirement that no $(\mu z)$ component appears in the metric tensor means that one must also transform

$$x^\mu \to x^\mu + \xi^\mu \tag{3.66}$$

where

$$\xi_\mu = -\frac{a^2}{a_+^2}\int dz\left(\frac{a_+^2}{a^4} - \frac{1}{a^2}\right)\partial_\mu\xi. \tag{3.67}$$

This implies that the metric tensor becomes

$$\hat{h}_{\mu\nu} = a^2\chi_{\mu\nu} - \frac{U_B}{2}\frac{a^2}{a_+^2}\xi\eta_{\mu\nu}. \tag{3.68}$$

Let us now write the full metric including both the background and the perturbation

$$\begin{aligned} ds^2 &= a^2\left(z + \left(\frac{1}{a^2} - \frac{1}{a_+^2}\right)\xi\right)dx^\mu dx_\mu \\ &+ \left(1 + \partial_z\left(\frac{1}{a^2} - \frac{1}{a_+^2}\right)\xi\right)^2 dz^2 + \left(a^2\chi_{\mu\nu} - \frac{U_B}{2}\frac{a^2}{a_+^2}\xi\eta_{\mu\nu}\right)dx^\mu dx^\nu \end{aligned} \tag{3.69}$$

This can be simplified to

$$ds^2 = a^2(G(z,x))g_{\mu\nu}dx^\mu dx_\nu + (\partial_z G)^2 dz^2 \tag{3.70}$$

to linear order. We have defined

$$G(z,x) = z + \frac{\xi}{a^2}, g_{\mu\nu} = \eta_{\mu\nu} + \chi_{\mu\nu}. \tag{3.71}$$

This is the generalization of the metric Ansatz proposed by Charmousis, Gregory and Rubakov [59].

Let us now derive the fluctuation of the scalar field in the various coordinate systems. When the two branes are translated we have $\delta\psi = 0$. Shifting the first brane to the origin implies that

$$\delta\psi^+ = \frac{U_B'}{a_+^2}\xi \tag{3.72}$$

in the first patch and

$$\delta\psi^- = \frac{U_B'}{a_-^2}\xi \tag{3.73}$$

in the second patch. Performing the local change of coordinates in the second patch (3.63) defines a single-valued scalar field fluctuation which coincides with $\delta\psi^+$ throughout the bulk. The change of coordinates (3.65) leads to a single-valued fluctuation

$$\delta\psi = U_B'\frac{\xi}{a^2}, \tag{3.74}$$

which, combined with the background scalar field, leads to

$$\psi(z,x) = \psi_0(G(z,x)). \tag{3.75}$$

Notice that the scalar field is now a function of the brane fluctuation parameter $\xi$, i.e. the radion. There are no scalar field dynamics *per se*.

## 3.4 Adding matter sources on the branes

The effect of adding matter on the branes is to induce a bending of the brane. This leads to a shift in the position of both branes which sit at

$$z_+ = \xi^+, \ z_- = r_c + \xi^-. \tag{3.76}$$

We can perform local changes of coordinates around both branes which both preserve the Gaussian normal coordinates and shift the two branes to the origin and $r_c$ respectively. After such changes of coordinates the metric is

$$h^+_{\mu\nu} = h_{\mu\nu} - \frac{U_B}{2} a^2(z)\xi^+\eta_{\mu\nu} - 2a^2(z)\int_0^z \frac{dy}{a^2(y)}\partial_\mu\partial_\nu\xi^+ \tag{3.77}$$

in the vicinity of the origin and

$$h^-_{\mu\nu} = h_{\mu\nu} - \frac{U_B}{2} a^2(z)\xi^-\eta_{\mu\nu} - 2a^2(z)\int_{r_c}^z \frac{dy}{a^2(y)}\partial_\mu\partial_\nu\xi^- \tag{3.78}$$

in the vicinity of the second brane.

We can now study these perturbations. To do so we come back to the gravitational equation; it is convenient to work in the conformal gauge, defining

$$du = \frac{dz}{a} \tag{3.79}$$

and

$$h_{\mu\nu} = \sqrt{a}\tilde{h}_{\mu\nu}. \tag{3.80}$$

We denote by $u_+$ and $u_-$ the location of both branes in the conformal coordinate system.

The gravitational equations then read

$$-\frac{d^2\tilde{h}_{\mu\nu}}{du^2} + \frac{1}{a^{3/2}}\frac{d^2 a^{3/2}}{du^2}\tilde{h}_{\mu\nu} = \Box^{(4)}\tilde{h}_{\mu\nu} \tag{3.81}$$

or

$$\left[Q^\dagger Q - \Box^{(4)}\right]\tilde{h}_{\mu\nu} = 0, \tag{3.82}$$

with

$$Q = -\frac{d}{du} + \frac{d\ln a^{3/2}}{du},\ Q^\dagger = \frac{d}{du} + \frac{d\ln a^{3/2}}{du},\ \Box^{(4)} = \eta^{\mu\nu}\partial_\mu\partial_\nu. \tag{3.83}$$

The boundary conditions are now

$$\partial_z h_{\mu\nu}|_{u_\pm} + \frac{U_B}{2}h_{\mu\nu}\Big|_{u_\pm} = -\kappa_5^2\Sigma^\pm_{\mu\nu} \tag{3.84}$$

where

$$\Sigma^\pm_{\mu\nu} = -\frac{2}{\kappa_5^2}\partial_\mu\partial_\nu\xi^\pm + (T^\pm_{\mu\nu} - \frac{1}{3}T^\pm g^\pm_{\mu\nu}) \tag{3.85}$$

and $T^\pm_{\mu\nu}$ is the matter energy-momentum tensor on both branes while $g^\pm_{\mu\nu}$ is the induced metric.

The equations of motion can be conveniently written as

$$Q^\dagger Q h_{\mu\nu} - \Box^{(4)}\tilde{h}_{\mu\nu} = \sum_{\sigma=\pm}\left(\frac{3}{4}U_B h^\sigma_{\mu\nu} + 2\kappa_5^2\sqrt{a}\Sigma^\sigma_{\mu\nu}\right)\delta(u-u_\sigma) \tag{3.86}$$

The brane equation of motion determining the brane bending is obtained by taking the trace of the previous equation. Using the tracelessness of $h_{\mu\nu}$ we conclude that

$$\Box^{(4)}\xi^\pm = -\frac{\kappa_5^2}{6}a_\pm^2 T^\pm \tag{3.87}$$

where $a_\pm = a(u_\pm)$.

Let us decompose the metric perturbation into Kaluza-Klein modes

$$\Box^{(4)}h_{\mu\nu} = -k^2 h_{\mu\nu}. \tag{3.88}$$

It is convenient to define the eigenstates of the positive operator $Q^\dagger Q$

$$Q^\dagger Q\psi_\lambda = \lambda^2\psi_\lambda, \tag{3.89}$$

and now consider the Green's function $G_{k^2}$ of the operator

$$H_{k^2} = Q^\dagger Q + k^2 - \frac{3}{4}U_B(\delta(u-u_+) + \delta(u-u_-)) \tag{3.90}$$

defined by

$$G_{k^2}(u,u') = \sum_\lambda \frac{\psi_\lambda(u)\psi_\lambda(u')}{\lambda^2 + k^2 + i\epsilon} \tag{3.91}$$

where each mode is normalized. The only mode with $\lambda = 0$ is proportional to $a^{\frac{3}{2}}$, as it is the only zero mode to satisfy the boundary conditions imposed by the delta functions. Moreover the spectrum is discrete due to the two boundary conditions.

We can now write the metric perturbation due to matter on both branes as

$$h_{\mu\nu}(u,x) = 2\kappa_5^2 \sum_{\sigma=\pm} \int d^4x' G(x,u;x',u_\sigma) a_\sigma^{1/2} a^{1/2}(u) \Sigma^\sigma_{\mu\nu}(x') \tag{3.92}$$

where

$$G(x,u;x',u') = \int \frac{d^4k}{(2\pi)^4} e^{ik.(x-x')} G_{k^2}(u,u') \tag{3.93}$$

This provides the solution to the Einstein equations in the bulk due to the brane bending.

### 3.4.1 The Scalar-Tensor Theory at Low Energy

Having described the independent low energy degrees of freedom of the theory with a bulk scalar field we are in a position to discuss the low energy scalar–tensor theory. We shall only examine two relevant terms: the Einstein–Hilbert term and the radion kinetic term.

The Einstein–Hilbert term can be seen to be

$$\int d^4x \sqrt{-g} \Phi \mathcal{R} \tag{3.94}$$

where $g_{\mu\nu}$ is the four-dimensional metric, and the effective Newton constant is

$$\Phi = \frac{1}{\kappa_5^2} \int_{\xi/a_+^2}^{r_c + \xi/a_-^2} a^2(y) dy. \tag{3.95}$$

Notice the explicit dependence on the radion field. Similarly the kinetic term for the radion field is

$$-\frac{3}{8\kappa_5^2} \int d^4x \sqrt{-g} K \left(\partial\xi\right)^2, \tag{3.96}$$

where

$$K = \int_0^{r_c} dz a^{-2} \left[ U_B^2 + 2 \left( \frac{\partial U_B}{\partial \psi} \right)^2 \right]. \tag{3.97}$$

Notice that this is always positive.

To focus finally on the $AdS_5$ case, we see that the scalar–tensor theory is here specified by

$$\Phi = \frac{1}{2k\kappa_5^2} (e^{-k\xi/a_+^2} - e^{-kr_c - k\xi/a_-^2}) \tag{3.98}$$

and

$$K = 8k(e^{2kr_c} - 1). \tag{3.99}$$

In the large $r_c$ limit and for small fluctuations of the radion $\xi$ this result coincides with the results of Garriga and Tanaka [74] on the Brans–Dicke parameter when coupling the theory to matter.

## 3.5 Gravity on the visible brane: the zero mode truncation

We concentrate first on the case where no matter is present on the second brane, and study gravity on the first brane. In the low energy limit we neglect the contribution of the Kaluza-Klein modes and retain the zero mode only. In this case the metric perturbation on the brane is

$$h_{\mu\nu} = -\frac{\kappa_5^2}{\int_0^{r_c} dz a^2} \frac{1}{\Box^{(4)}} (T_{\mu\nu}^+ - \frac{1}{3} T^+ \eta_{\mu\nu}) - \left. \frac{U_B}{2} \right|_0 \xi^+ \eta_{\mu\nu}, \tag{3.100}$$

where we have normalized $a_+ = 1$ and used a four-dimensional gauge transformation to remove the second derivative terms. This leads to

$$\Box^{(4)} h_{\mu\nu} = -\frac{\kappa_5^2}{\int_0^{r_c} dz a^2} (T_{\mu\nu}^+ - \frac{1}{3} T^+ \eta_{\mu\nu}) + \left. \frac{U_B}{12} \right|_0 \kappa_5^2 T^+ \eta_{\mu\nu}, \tag{3.101}$$

corresponding to the Brans–Dicke expression

$$\Box^{(4)} h_{\mu\nu} = -\frac{16\pi G_N}{\Phi} (T_{\mu\nu}^+ - \frac{1}{2} T^+ \eta_{\mu\nu}) - \frac{8\pi G_N}{\Phi(3 + 2\omega(\Phi))} T^+ \eta_{\mu\nu}, \tag{3.102}$$

where $\Phi$ is the Brans–Dicke field and $\omega(\Phi)$ the Brans–Dicke parameter. We identify

$$\kappa_5^2 = 16\pi G_N \int_0^{r_\infty} \frac{a^2}{a_+^2} dz, \tag{3.103}$$

where $r_\infty$ is the maximal range of the extra dimension – infinity for the Randall-Sundrum scenario, the position of the singularity when a bulk scalar field is present. Next, we identify

$$\Phi = \frac{\int_0^{r_c} a^2 dz}{\int_0^{r_\infty} a^2 dz}, \tag{3.104}$$

which varies between zero and one. Finally we obtain the Brans–Dicke parameter

$$\omega(\Phi) = \frac{3}{2}\left(-1 + \frac{1}{1 - \Phi \frac{U_B}{2}\Big|_0 \int_0^{r_\infty} \frac{a^2}{a_+^2} dz}\right). \tag{3.105}$$

We can now consider the specific exponential models, with $U_B = 4ke^{\alpha\psi}$. This leads to

$$\Phi = 1 - \left(1 - \frac{r_c}{r_\infty}\right)^{1+\frac{1}{2\alpha^2}}, \tag{3.106}$$

where $r_\infty = z_0 + 1/4k\alpha^2$. Similarly for the Brans–Dicke parameter

$$\omega(\Phi) = \frac{3}{2}\left(-1 + \frac{1}{1 - \Phi \frac{1+4k\alpha^2 z_0}{1+2\alpha^2}}\right). \tag{3.107}$$

In the $\alpha \rightarrow 0$ limit we retrieve that

$$\Phi = 1 - e^{-2kr_c} \tag{3.108}$$

and

$$\omega(\Phi) = \frac{3}{2}\left(-1 + e^{2kr_c}\right), \tag{3.109}$$

in agreement with [74].

A comment is perhaps advisable on the well known attractor mechanism for scalar–tensor theories in the context of the theory discussed so far. Damour and Nordtvedt [75] found that in the case of Brans–Dicke theory the dynamics of the scalar field evolve during the matter dominated epoch such that the Brans–Dicke parameter grows rapidly and thus that Einstein gravity is a cosmological attractor. It is easy to verify that this is the case in the theory above: first, it is convenient to go to the Einstein frame where $g_{\mu\nu} = g_{E,\mu\nu}/\Phi$. We then define a canonically normalized field $\sigma$ by $\partial a/\partial\sigma = \beta(\sigma)$ where $a(\sigma) = -\ln(\Phi)/2$ and $\beta^2(\sigma) = 1/(3 + 2\omega(\Phi))$, and find that

$$\beta^2(\sigma) = 1 - \frac{\Phi}{\Phi_0}, \tag{3.110}$$

where $\Phi_0 = (1 + 2\alpha^2)/(1 + 4\alpha^2 kz_0)$. This leads to

$$\sigma - \sigma_0 = \frac{1}{2}\ln\left(\frac{1+\beta}{1-\beta}\right). \tag{3.111}$$

Notice that $\beta \to 0$ and $\sigma \to \sigma_0$ as $\Phi \to \Phi_0$. The field $\sigma$ is attracted towards its value at $\beta = 0$, i.e. $\sigma$ is attracted towards $\sigma_0$. The minimum $\sigma = \sigma_0$ can only been reached when $\Phi_0 \leq 1$, i.e. for $z_0 \geq 1/2k$. In that case the field $\sigma$ is attracted towards the point where $\omega(\Phi) = +\infty$, recovering Einstein gravity.

In the opposite situation ($\Phi_0 > 1$), the Brans–Dicke parameter can only reach a maximal value

$$\omega_{\max} = \frac{3}{2}\frac{1 + 4\alpha^2 kz_0}{2\alpha^2\left(1 - 2kz_0\right)} \tag{3.112}$$

which, since $\Phi_0 > 1$ implies that $2kz_0 < 1$, is in general not large enough to escape the experimental bounds on the Brans–Dicke parameter (and tends to $\frac{3}{4\alpha^2}$ in the limit as $2kz_0 \to 0$).

We have therefore found that the Brans–Dicke parameter converges towards infinity as soon as the distances between the branes and the naked singularity are large enough, which should be the case for a realistic cosmology, because we expect both branes to expand; thus, they will move away from the singularity and so the attractor mechanism can operate. We shall investigate this matter further in chapter 4, where we consider in more detail the evolution of moduli fields and show the presence of the attractor towards General Relativity.

Let us finally discuss the case when there is also matter on the second brane, and study its effect on the gravitational field as seen on the first brane. It is to be expected that the leading effect will be due to the propagation of gravitons in the bulk, hence suppressed by the warping of the bulk. Following the same method as in the previous calculation we find that

$$\frac{1}{a_+^2}\Box^{(4)}h_{\mu\nu} = -\frac{16\pi G_N}{\Phi}(T_{\mu\nu} - \frac{1}{3}(T_{\rho\lambda}\eta^{\rho\lambda})\eta_{\mu\nu}) + \frac{U_B}{12}|_0(T^+_{\rho\lambda}\eta^{\rho\lambda})\kappa_5^2\eta_{\mu\nu}, \tag{3.113}$$

where the total energy momentum tensor is

$$T_{\mu\nu} = T^{+}_{\mu\nu} + \frac{a_-^2}{a_+^2} T^{-}_{\mu\nu}. \tag{3.114}$$

This can be recast in the form

$$\begin{aligned}\frac{1}{a_+^2}\Box^{(4)} h_{\mu\nu} &= -\frac{16\pi G_N}{\Phi}(T_{\mu\nu} - \frac{1}{2}(T_{\rho\lambda}\eta^{\rho\lambda})\eta_{\mu\nu}) - \frac{8\pi G_N}{\Phi(3+2\omega(\Phi))}(T_{\rho\lambda}\eta^{\rho\lambda})\eta_{\mu\nu} \\ &- \frac{k}{3}\frac{a_-^2}{a_+^2}\kappa_5^2(\eta^{\rho\lambda}T^{-}_{\rho\lambda})\eta_{\mu\nu},\end{aligned} \tag{3.115}$$

where $G_N$, $\Phi$ and $\omega(\Phi)$ are as defined above. Notice that there is a direct coupling to matter on the second brane which does not follow from Brans–Dicke theory. In particular this implies that gravity does not couple universally to matter; there is a violation of the Equivalence Principle with a strength proportional to the warping factor $a_-^2/a_+^2$.

## 3.6 Conclusions

In this chapter we have given a detailed discussion of the dynamics of a two–brane system with a bulk scalar field. We have investigated the coupling of the distance between the branes, which is a scalar degree of freedom, and four-dimensional gravity, and have further presented an analysis of the effective four-dimensional gravity at the positive tension brane.

When the BPS conditions (3.5) are imposed on the system, we have found that the bulk scalar field and the radion combine to give one independent scalar degree of freedom; i.e. the bulk scalar field does not give rise to an additional degree of freedom. In this static supergravity background, we have found that the effective low-energy theory is a Brans–Dicke theory. We have briefly discussed the attractor mechanism which attracts the theory towards general relativity during a matter dominated epoch. We have found that the conditions for this to happen can easily be fulfilled, as long as the singularity in the background spacetime is far away from both branes.

When matter is present on both branes, we have found that each matter type (visible and invisible) has its own coupling to gravity. Thus, we expect a violation of the Equivalence Principle for matter which lives on the shadow brane, but this violation is suppressed by a factor which can be very small when the branes are far apart. We expect these considerations to have very interesting consequences for cosmology, and these will be further investigated in chapter 4, where we consider the implications of our theory starting in a configuration leading to an effective theory different from four-dimensional General Relativity, but tending towards it at later times.

# Chapter 4

# Cosmology of a braneworld universe

## 4.1 Introduction

We have seen in chapter 3 that the four-dimensional effective theory at low energies of a class of braneworld model encompassing both the supergravitational description of M–theory and the Randall–Sundrum scenarios has much in common with multi-scalar–tensor theories, where the interbrane distance and the bulk scalar field degree of freedom play the rôle of scalar degrees of freedom in the gravitational sector of the effective four-dimensional theory (see also [57, 60, 71, 74, 76–78]). From the cosmological point of view it is interesting to investigate the consequences of these moduli. Although it is usually assumed that these moduli fields are stabilized by some unknown mechanism in the early universe [79–82], it is imaginable that they are not stabilized by some potential.

Instead, as was discussed in chapter 3, it might be that there is a cosmological attractor mechanism at work, similar to the one found in Brans–Dicke type theories, which drives the theory towards four-dimensional General Relativity during the cosmological evolution by generating very small matter couplings to the moduli fields [75, 83, 84]. If this is the case, there could be cosmological consequences of the time evolution of the moduli, such as varying constants, time-varying masses, etc., leading to observational consequences, for instance in the cosmic microwave background radiation, large scale structures, time-varying constants, Equivalence Principle violations, and so on. Indeed, there is another motivation for our work: namely, the claim of a measurement of time variation of the fine-structure constant made in [85, 86]. If this claim is confirmed by future observations, this would suggest that at least some moduli fields are not stabilized but slowly varying.

In this chapter we investigate the cosmological evolution of moduli fields arising in brane world models and address the question of whether there is a cosmological attractor for the brane world moduli. We also analyze the conditions under which such an attractor would be efficient enough for the theory to agree with local experiments in the laboratory and/or strong field limits [10]. We study these issues in a broad class of models encapsulating features from both the Randall–Sundrum models and heterotic M–theory, i.e. a warped background with a bulk scalar field.

The chapter is organized as follows: in the next section we discuss the five-dimensional theory and derive in detail the effective low-energy action from the moduli space approximation, giving also the resulting field equations in the Einstein frame. In section 4.3 we clarify the conditions under which the theory would predict time-varying coupling constants, such as the fine-structure constant, and investigate the constraints imposed by strong field limits. Cosmological considerations and solutions to the field equations are presented in section 4.4, and we conclude in section 4.5.

## 4.2 Moduli space approximation

In this section we derive the four-dimensional low-energy effective action using the moduli space approximation. For the gravitational sector, our derivation follows closely that in [87]. We begin by reminding the reader of the static configuration, which was originally derived from supergravity [42].

### 4.2.1 The static configuration

The bulk action describes gravity and the bulk scalar field dynamics, and is given by equation (3.1). Further, our setup contains two branes. One of these branes has a positive tension, while the other has a negative tension. They are described by contributions to the action

$$S_{\rm brane1} = -\frac{3}{2\kappa_5^2}\int d^5x\sqrt{-g_5}U_B\delta(z_1), \tag{4.1}$$

$$S_{\rm brane2} = +\frac{3}{2\kappa_5^2}\int d^5x\sqrt{-g_5}U_B\delta(z_2) \tag{4.2}$$

where we note that in these expressions, $z_1$ and $z_2$ are the (arbitrary) positions of the two branes, and as in chapter 3 $U_B$ is the superpotential; the bulk potential energy of the scalar field $U$ is given by equation 3.3. We shall also need the Gibbons–Hawking boundary term, equation 3.4, and as before impose a $Z_2$ symmetry at the brane positions.

The solution of the system was discussed in section 3.2.1; points of importance for the discussion in this chapter are that we consider a superpotential of the form of equation (3.7), where $\alpha$ takes the values $\frac{1}{\sqrt{3}}$ and $\frac{-1}{\sqrt{12}}$ [42], and that there is a singular point in the bulk at $z_* = 1/4k\alpha^2$, for which the scale factor vanishes. This will be important for the discussion on the cosmological evolution in section 4.4.

In the following we will discuss the moduli space approximation. We will put matter on the branes as well as supersymmetry breaking corrections to the brane potentials. Two of the moduli of the system are the brane positions. That is, in the solution we use (discussed in section 3.2.1) the brane positions are arbitrary. In the moduli space approximation, these moduli are assumed to be dependent on space and time. We denote the position of brane one with $z_1 = \phi(x^\mu)$ and the position of brane two with $z_2 = \sigma(x^\mu)$. We consider the case where the evolution of the brane is slow. This means that in constructing the effective four-dimensional theory we neglect terms like $(\partial\phi)^3$.

In addition to the brane positions, we need to include the graviton zero mode, which can be done by replacing $\eta_{\mu\nu}$ with a spacetime-dependent tensor $g_{\mu\nu}(x^\mu)$. Thus, we have two scalar degrees of freedom, namely the positions of the two branes which we shall denote with $\phi(x^\mu)$ and $\sigma(x^\mu)$, and the graviton zero mode $g_{\mu\nu}$ (see chapter 3 and [88]). As we shall see below, in the coordinate system in which the branes move, the kinetic terms of the moduli come from the boundary terms alone.

It would also be possible to consider another coordinate system, in which the branes are fixed. Then, the moduli are a spacetime-dependent part which can be added to the bulk scalar field solution of equation (3.9), and the (55) component of the metric tensor becomes a four-dimensional effective field; in addition, we have the graviton zero–mode. Thus, the number of moduli fields is independent of the coordinate system.

Note that the moduli space approximation is only a good approximation if the time variation of the moduli fields is small. This should be the case for late-time cosmology well after the epoch of nucleosynthesis in which we are particularly interested. Similarly, for energy densities much higher than the brane tension it has been noted [43] that the expansion of the four-dimensional brane universe is not governed by the usual four-dimensional Einstein equations, according to which the expansion rate $H$ is proportional to the matter density $\sqrt{\rho}$; instead, it was found that the dependence of $H$ on $\rho$ is $H \propto \rho$. This behaviour was observed in one–brane scenarios [43] but was shown to hold in two–brane scenarios as well (see in particular [89] and [90]). However, for densities much less than the brane tension, which certainly holds at and after the epoch of nucleosynthesis, the usual law $H \propto \sqrt{\rho}$ can be recovered, albeit with some corrections coming from the scalar fields associated with the bulk dynamics. (See also [91, 92] for other uses of the moduli space approximation in the context of brane worlds).

### 4.2.2 Moduli space approximation: the gravitational sector

Let us first consider the bulk action. Replacing $\eta_{\mu\nu}$ with ${}^{(4)}g_{\mu\nu}(x^\mu)$ in (3.6) we have for the Ricci scalar $\mathcal{R} = \mathcal{R}^{(4)}/a^2 + \tilde{\mathcal{R}}$, where $\tilde{\mathcal{R}}$ is the Ricci–scalar of the background (3.6). We explicitly use the background solution (3.8) and (3.9), and so we see that $\tilde{\mathcal{R}}$ will not contribute to the low-energy effective action. Also, in this coordinate system, in which the branes are not fixed, there is no contribution from the part of the bulk scalar field. Collecting everything we therefore have

$$S_{\rm bulk} = \frac{1}{2\kappa_5}\int dzd^4xa^4\sqrt{-g_4}\frac{1}{a^2}\mathcal{R}^{(4)} = \int d^4x\sqrt{-g_4}f(\phi,\sigma)\mathcal{R}^{(4)}, \tag{4.3}$$

with

$$f(\phi,\sigma) = \frac{1}{\kappa_5^2}\int_\phi^\sigma dza^2(z). \tag{4.4}$$

We remind the reader that $a(z)$ is given by (3.8).

We now turn to the boundary terms. It is clear that the integrals (4.1) and (4.2) do not contribute to the effective action for the same reason that $\tilde{\mathcal{R}}$ does not contribute. Let us therefore now turn our attention to the Gibbons–Hawking boundary terms.

First, it is not difficult to construct the normal vectors to the brane:

$$n^\mu = \frac{1}{\sqrt{1+(\partial\phi)^2/a^2}}\left(\partial^\mu\phi/a^2, 1\right). \tag{4.5}$$

Then the induced metric on each brane is given by

$$g_{\mu\nu}^{\rm ind,1} = a^2(\phi)g_{\mu\nu}^4 - \partial_\mu\phi\partial_\nu\phi, \tag{4.6}$$

$$g_{\mu\nu}^{\rm ind,2} = a^2(\sigma)g_{\mu\nu}^4 - \partial_\mu\sigma\partial_\nu\sigma. \tag{4.7}$$

Thus,

$$\sqrt{-g^{\rm ind,1}} = a^4(\phi)\sqrt{-g_4}\left[1 - \frac{1}{2a^2(\phi)}(\partial\phi)^2\right], \tag{4.8}$$

$$\sqrt{-g^{\mathrm{ind},2}} \quad = \quad a^4(\sigma)\sqrt{-g_4}\left[1 - \frac{1}{2a^2(\sigma)}(\partial\sigma)^2\right]. \tag{4.9}$$

So the Gibbons–Hawking boundary terms take the form

$$\frac{1}{\kappa_5^2}\int d^4x a^4\sqrt{-g_4}\left[1 - \frac{1}{2a^2(\phi)}(\partial\phi)^2\right]K, \tag{4.10}$$

$$\frac{1}{\kappa_5^2}\int d^4x a^4\sqrt{-g_4}\left[1 - \frac{1}{2a^2(\sigma)}(\partial\sigma)^2\right]K. \tag{4.11}$$

The trace of the extrinsic curvature tensor can be calculated from

$$K = \frac{1}{\sqrt{-g_5}}\partial_\mu\left[\sqrt{-g_5}n^\mu\right]. \tag{4.12}$$

Neglecting higher order terms this gives

$$K = 4\frac{a'}{a}\left[1 - \frac{(\partial\phi)^2}{4a^2}\right]. \tag{4.13}$$

The terms for the second brane can be obtained analogously. Using the BPS conditions and keeping only the kinetic terms, we get for the Gibbons–Hawking boundary terms

$$+ \quad \frac{3}{4\kappa_5^2}\int d^4x\sqrt{-g_4}a^2(\phi)U_B(\phi)(\partial\phi)^2, \tag{4.14}$$

$$- \quad \frac{3}{4\kappa_5^2}\int d^4x\sqrt{-g_4}a^2(\sigma)U_B(\sigma)(\partial\sigma)^2. \tag{4.15}$$

Collecting all terms we find

$$S_{\mathrm{MSA}} = \int d^4x\sqrt{-g_4}\left[f(\phi,\sigma)\mathcal{R}^{(4)} + \frac{3}{4}a^2(\phi)\frac{U_B(\phi)}{\kappa_5^2}(\partial\phi)^2 - \frac{3}{4}a^2(\sigma)\frac{U_B}{\kappa_5^2}(\sigma)(\partial\sigma)^2\right]. \tag{4.16}$$

Note that the kinetic term of the field $\phi$ has the wrong sign. This is an artifact of the frame we use here. As we shall show below, it is possible to go to the Einstein frame with a simple conformal transformation, in which the sign in front of the kinetic term is correct for both fields.

The effective action is valid for any model based on supergravity-inspired five-dimensional models with two branes. In particular it is worth noticing that there is no potential for the moduli. The moduli describe flat directions reflecting the no-force condition on boundary branes for BPS-like systems.

The effective action for the two moduli $\phi$ and $\sigma$ has a nice interpretation in terms of supergravity; this is expected as we started from a two-brane system satisfying BPS conditions. Indeed we can write the Einstein-Hilbert term and the kinetic terms of the moduli as

$$\int d^4x\sqrt{-g_4}\left[f(\phi,\sigma)\mathcal{R}^{(4)}+\frac{1}{6}\partial_\Phi\partial_{\bar{\Phi}}f\partial_\mu\Phi\partial^\mu\bar{\Phi}+\frac{1}{6}\partial_\Sigma\partial_{\bar{\Sigma}}f\partial_\mu\Sigma\partial^\mu\bar{\Sigma}\right], \tag{4.17}$$

where

$$\phi=\frac{1}{2}(\Phi+\bar{\Phi}),\ \sigma=\frac{1}{2}(\Sigma+\bar{\Sigma}). \tag{4.18}$$

In terms of supergravity, the fields $\Phi$ and $\Sigma$ are the scalar parts of two chiral multiplets. One can read off the Kahler potential for these two moduli fields as

$$K=-3\ln f. \tag{4.19}$$

In the Randall–Sundrum case, we retrieve that

$$K=-3\ln(e^{-k(\Phi+\bar{\Phi})}-e^{-k(\Sigma+\bar{\Sigma})}); \tag{4.20}$$

notice that here we can rewrite the Kahler potential as

$$K=-3k(\Phi+\bar{\Phi})-3\ln(1-e^{-k(T+\bar{T})}), \tag{4.21}$$

where

$$T=\Sigma-\Phi \tag{4.22}$$

is the radion superfield. Moreover we immediately see that, in the Randall–Sundrum case, the field $\Phi$ can be eliminated by a Kahler transformation; this shows that one of the two moduli decouples, leaving only the radion as the relevant physical field. We will retrieve this result later when we analyze the equations of motion.

Coming back to the action above, we redefine the fields in the following way:

$$\tilde{\phi}^2 = \left(1-4k\alpha^2\phi\right)^{2\beta}, \tag{4.23}$$
$$\tilde{\sigma}^2 = \left(1-4k\alpha^2\sigma\right)^{2\beta}, \tag{4.24}$$

with

$$\beta=\frac{2\alpha^2+1}{4\alpha^2}; \tag{4.25}$$

then, the gravitational sector can be written as

$$S_{\rm MSA} = \frac{1}{2k\kappa_5^2(2\alpha^2+1)}\int d^4x\sqrt{-g_4}\left[\left(\tilde{\phi}^2-\tilde{\sigma}^2\right)\mathcal{R}^{(4)}+\frac{6}{2\alpha^2+1}\left((\partial\tilde{\phi})^2-(\partial\tilde{\sigma})^2\right)\right]. \quad (4.26)$$

This is an action of the form of a multi-scalar–tensor theory, in which one scalar field has the wrong sign in front of the kinetic term. Furthermore, in this frame there is a peculiar point where the factor in front of $\mathcal{R}$ can vanish, namely when $\tilde{\phi}=\tilde{\sigma}$, which corresponds to colliding branes. We will call the frame in which the action has the form of the equation above the bulk frame.

It is useful to go to the Einstein frame. To avoid mixed terms of the form $(\partial_\mu\tilde{\phi})(\partial^\mu\tilde{\sigma})$, we define two new fields[1]:

$$\tilde{\phi} = Q\cosh R, \quad (4.27)$$
$$\tilde{\sigma} = Q\sinh R, \quad (4.28)$$

and then perform a conformal transformation to effect the change of frame:

$$\tilde{g}_{\mu\nu} = Q^2 g_{\mu\nu}. \quad (4.29)$$

Then [93]

$$\sqrt{-g}Q^2\mathcal{R} = \sqrt{-\tilde{g}}\left(\tilde{\mathcal{R}}-\frac{6}{Q^2}(\tilde{\partial}Q)^2\right). \quad (4.30)$$

Collecting everything we get the action in the Einstein frame (where we now drop the tilde):

$$S_{\rm EF} = \frac{1}{2k\kappa_5^2(2\alpha^2+1)}\int d^4x\sqrt{-g}\left[\mathcal{R}-\frac{12\alpha^2}{1+2\alpha^2}\frac{(\partial Q)^2}{Q^2}-\frac{6}{2\alpha^2+1}(\partial R)^2\right]. \quad (4.31)$$

Clearly, in this frame both fields have the correct sign in front of the kinetic terms. Furthermore, we can identify the gravitational constant:

$$16\pi G = 2k\kappa_5^2(1+2\alpha^2). \quad (4.32)$$

Note that for $\alpha\to 0$ (i.e. the Randall–Sundrum case) the $Q$ field decouples. In this case, the field $R$ plays the rôle of the radion: it measures the distance between the branes.

[1]Do not confuse the Ricci scalar $\mathcal{R}$ with the new field $R$.

### 4.2.3 Moduli space approximation: the matter sector

In the following we introduce matter as well as supersymmetry breaking potentials $V(Q,R)$ and $W(Q,R)$ on each branes. We begin with the potentials: to first order in the moduli space approximation we get

$$\int d^4x\sqrt{-g_4}\left[a^4(\phi)V(\phi)\right] \tag{4.33}$$

with $a^4(\phi)=\tilde{\phi}^{4/(1+2\alpha^2)}$. The expression for a potential $W$ on the second brane is similar, but with $a(\phi)$ replaced by $a(\sigma)$. In the Einstein frame we have (dropping the tilde from the metric):

$$\int d^4x\sqrt{-g}Q^{-8\alpha^2/(1+2\alpha^2)}(\cosh R)^{4/(1+2\alpha^2)}V(Q,R)\equiv\int d^4x\sqrt{-g}V_{\text{eff}}(Q,R), \tag{4.34}$$

where we have defined

$$V_{\text{eff}}(Q,R)=Q^{-8\alpha^2/(1+2\alpha^2)}(\cosh R)^{4/(1+2\alpha^2)}V(Q,R). \tag{4.35}$$

The expression for $W(Q,R)$ in the Einstein frame is

$$\int d^4x\sqrt{-g}Q^{-8\alpha^2/(1+2\alpha^2)}(\sinh R)^{4/(1+2\alpha^2)}W(Q,R)\equiv\int d^4x\sqrt{-g}W_{\text{eff}}(Q,R), \tag{4.36}$$

where

$$W_{\text{eff}}(Q,R)=Q^{-8\alpha^2/(1+2\alpha^2)}(\sinh R)^{4/(1+2\alpha^2)}W(Q,R). \tag{4.37}$$

For matter, the action has the form

$$S_m^{(1)}=S_m^{(1)}(\Psi_1,g_{\mu\nu}^{B(1)})\quad\text{and}\quad S_m^{(2)}=S_m^{(2)}(\Psi_2,g_{\mu\nu}^{B(2)}), \tag{4.38}$$

where $g^B$ denotes the induced metric on each brane and $\Psi_i$ the matter fields on each branes. Note that we do not couple the matter fields $\Psi_i$ to the bulk scalar field, and thus not to the fields $Q$ and $R$. In changing frames we get

$$S_m^{(1)}=S_m^{(1)}(\Psi_1,A^2(Q,R)g_{\mu\nu})\quad\text{and}\quad S_m^{(2)}=S_m^{(2)}(\Psi_2,B^2(Q,R)g_{\mu\nu}), \tag{4.39}$$

In this expression we have used the fact that, in going to the Einstein frame, the induced metrics on each branes transform with a different conformal factor, which we denote with $A$ and $B$. We have neglected the derivative terms in the moduli fields when considering the coupling to matter on the brane. They lead to higher order operators which can be easily incorporated. The energy–momentum tensor in the Einstein frame is defined as

$$T^{(1)}_{\mu\nu} = 2\frac{1}{\sqrt{-g}}\frac{\delta S^{(1)}_m(\Psi, A^2(Q,R)g)}{\delta g^{\mu\nu}} \tag{4.40}$$

with an analogous definition for the energy–momentum tensor for matter on the second brane.

In the Einstein frame, the total action is therefore,

$$\begin{aligned} S_{\mathrm{EF}} &= \frac{1}{16\pi G}\int d^4x\sqrt{-g}\left[\mathcal{R} - \frac{12\alpha^2}{1+2\alpha^2}\frac{(\partial Q)^2}{Q^2} - \frac{6}{2\alpha^2+1}(\partial R)^2\right] \\ &\quad - \int d^4x\sqrt{-g}(V_{\mathrm{eff}}(Q,R) + W_{\mathrm{eff}}(Q,R)) \\ &\quad + S^{(1)}_m(\Psi_1, A^2(Q,R)g_{\mu\nu}) + S^{(2)}_m(\Psi_2, B^2(Q,R)g_{\mu\nu}). \end{aligned} \tag{4.41}$$

The theory derived has a form similar to the one discussed in [94, 95], although we have here two scalar degrees of freedom in general, and, in addition, these scalar fields couple differently to the two matter types on each brane.

### 4.2.4 The field equations in the Einstein frame

From the action derived above we can now derive the field equations for the metric and the two scalar degrees of freedom in the Einstein frame. They are

$$\begin{aligned} G_{\mu\nu} &= 8\pi G\left(T^{(1)}_{\mu\nu} + T^{(2)}_{\mu\nu} - g_{\mu\nu}V_{\mathrm{eff}} - g_{\mu\nu}W_{\mathrm{eff}}\right) \\ &\quad + \frac{12\alpha^2}{1+2\alpha^2}\frac{1}{Q^2}\left[(\partial_\mu Q)(\partial_\nu Q) - \frac{1}{2}g_{\mu\nu}(\partial Q)^2\right] \\ &\quad + \frac{6}{1+2\alpha^2}\left[(\partial_\mu R)(\partial_\nu R) - \frac{1}{2}g_{\mu\nu}(\partial R)^2\right] \end{aligned} \tag{4.42}$$

$$\Box R = 8\pi G\frac{1+2\alpha^2}{6}\left[\frac{\partial V_{\mathrm{eff}}}{\partial R} + \frac{\partial W_{\mathrm{eff}}}{\partial R} - \alpha^{(1)}_R T^{(1)} - \alpha^{(2)}_R T^{(2)}\right] \tag{4.43}$$

$$\frac{\Box Q}{Q^2} - \frac{(\partial Q)^2}{Q^3} = 8\pi G\frac{1+2\alpha^2}{12\alpha^2}\left[\frac{\partial V_{\mathrm{eff}}}{\partial Q} + \frac{\partial W_{\mathrm{eff}}}{\partial Q} - \alpha^{(1)}_Q T^{(1)} - \alpha^{(2)}_Q T^{(2)}\right]. \tag{4.44}$$

In these expressions $T^{(i)}$ is the trace of the energy–momentum tensor for each brane's matter; the coupling functions $\alpha_Q^{(i)}$ and $\alpha_R^{(i)}$ are defined as

$$\alpha_Q^{(1)} = \frac{\partial \ln A}{\partial Q}, \quad \alpha_Q^{(2)} = \frac{\partial \ln B}{\partial Q}; \tag{4.45}$$

$$\alpha_R^{(1)} = \frac{\partial \ln A}{\partial R}, \quad \alpha_R^{(2)} = \frac{\partial \ln B}{\partial R}. \tag{4.46}$$

We will give the expressions for these quantities in the next section and discuss solutions to the field equations in a cosmological setting in section 4.4. Due to the coupling of the moduli to the branes, cosmological matter is not conserved but satisfies

$$D_\mu T_i^{\mu\nu} = \alpha_Q^i(\partial^\nu Q)T_i + \alpha_R^i(\partial^\mu R)T_i \tag{4.47}$$

for each type of matter $i = 1, 2$. In deriving this equation we have assumed that the matter fields obey the equation of motion. Notice that matter non–conservation is directly linked to the spacetime variations of the moduli fields.

## 4.3 Couplings to matter and strong field constraints

In this section we will be interested in the coupling of matter living on both branes to the bulk. In particular we will pay particular attention to the constraints imposed by strong field limits. This, in turn, leads to stringent constraints on the parameter $\alpha$ and the allowed values of the field $R$.

Let us first notice that matter on the branes couples to the induced metric. The form of the induced metric implies that we have to deal with a bi-metric theory; this is a general result for moving branes. In the following we will only be interested in the non-derivative couplings between the two moduli and the matter fields; we are dealing with a low energy expansion and derivative interactions lead to higher order operators. If needs be, these derivative interactions can easily incorporated in the following.

First of all, couplings to the two branes result from a Lagrangian

$$\int \sqrt{-g_B}\mathcal{L}_m(\phi_m, g_B), \tag{4.48}$$

where $\phi_m$ can either be a scalar, fermion or vector boson field. We will study each case separately. Let us start with a scalar field, i.e. one where the Lagrangian is given by

$$\mathcal{L}_m = \frac{1}{2} g_B^{\mu\nu} \partial_\mu \phi_B \partial_\nu \phi_B - V(\phi_B). \tag{4.49}$$

We first write the boundary action in terms of the Einstein frame metric $\tilde{g} = \Omega^{-2} g$ leading to

$$\int \sqrt{-\tilde{g}} \left( a^2(\phi) \Omega^2 \tilde{g}^{\mu\nu} \partial_\mu \phi_B \partial_\nu \phi_B - a^4(\phi) \Omega^4 V(\phi_B) \right), \tag{4.50}$$

where $\Omega^2 = 1/f(\phi, \sigma)$. Now we can redefine the scalar field $\tilde{\phi} = a(\phi)\Omega\phi_B$ in such a way that the action becomes

$$\int \sqrt{-\tilde{g}} \left( \tilde{g}^{\mu\nu} \partial_\mu \tilde{\phi} \partial_\nu \tilde{\phi} - a^4(\phi) \Omega^4 V \left( \frac{\tilde{\phi}}{a(\phi)\Omega} \right) \right), \tag{4.51}$$

up to derivative interactions. Let us apply this to a simple renormalizeable potential

$$V = \frac{1}{2} m^2 \phi_B^2 + \lambda \phi^4. \tag{4.52}$$

In the Einstein frame, the couplings become

$$\tilde{m} = a(\phi)\Omega m, \ \ \tilde{\lambda} = \lambda. \tag{4.53}$$

Clearly, in this frame the mass of the scalar field becomes time-dependent.

We can apply the same technique to vector bosons with action

$$S_m = -\frac{1}{4g^2} \int \sqrt{-g_B} g_B^{\mu\rho} g_B^{\nu\lambda} F_{\mu\rho} F_{\nu\lambda} \tag{4.54}$$

We find that in the Einstein frame

$$g_E = g, \tag{4.55}$$

as expected vector bosons are conformally coupled, and therefore the gauge coupling constant are time-independent.

Finally let us deal with Dirac fermions:

$$S_m = \int \sqrt{-g_B} (i\bar{\psi}\gamma_B^\mu D_\mu \psi - m\bar{\psi}\psi), \tag{4.56}$$

where $\gamma_B^\mu$ are the gamma matrices for the induced metric. Using the results derived in [96], we can rewrite the action as

$$S_m = \int \sqrt{-\tilde{g}} \left( \bar{\tilde{\psi}} \tilde{\gamma}^\mu D_\mu \tilde{\psi} - m a(\phi) \Omega \bar{\tilde{\psi}} \tilde{\psi} \right), \tag{4.57}$$

where we have used the conformality of the coupling of massless Weyl fermions and defined $\tilde{\psi} = (a(\phi)\Omega)^{3/2}\psi$. Again we find that fermion masses become time-dependent

$$\tilde{m} = a(\phi)\Omega m; \tag{4.58}$$

notice that the time dependence of the fermion and scalar masses is the same. This is not true when comparing different particle species on the positive tension brane with species on the negative tension brane. Particles on the negative tension brane are, however, candidates for dark matter (they couple to the standard model particles via gravity only), and constraints imposed on models of dark matter by Equivalence Principle violations are less restrictive.

In conclusion, we see that, in the Einstein frame, the only time-dependent couplings in the matter Lagrangian are the masses. Indeed, in a general frame we have the following invariant relating Newton's constant to masses

$$I = Gm^2 = \tilde{G}\tilde{m}^2. \tag{4.59}$$

In particular we find that in the frame where masses are time-independent the Newton constant becomes time-dependent. As such $I$ gives the true measure of time variations in the braneworld models that we consider.

The fact that the coupling constants are frame–independent (see equation 4.55) and therefore spacetime-independent means that, in the theory we consider, we would not expect a time-varying fine-structure constant, as reported in [85, 86]. In order to explain a time-varying coupling constant, vector bosons would need to be coupled directly to the bulk scalar field and thus to $Q$ and $R$. We do not consider this possibility in this chapter.

Let us now consider the constraints imposed by the strong-field limits. For this it is convenient to write the moduli Lagrangian in the form of a non-linear sigma model with kinetic terms

$$\gamma_{ij}\partial\phi^i\partial\phi^j, \tag{4.60}$$

where $i = 1, 2$ labels the moduli $\phi^1 = Q$ and $\phi^2 = R$. The sigma model couplings here are

$$\gamma_{QQ} = \frac{12\alpha^2}{1+2\alpha^2}\frac{1}{Q^2},\ \gamma_{RR} = \frac{6}{1+2\alpha^2}. \tag{4.61}$$

Notice the potential danger of the $\alpha \to 0$ limit, the RS model, where the coupling to $Q$ becomes very small. In an ordinary Brans–Dicke theory with a single field, this would correspond to a vanishing Brans–Dicke parameter which is ruled out experimentally. Here we shall see that the coupling to matter is such that this is not the case. Indeed we can write the action expressing the coupling to ordinary matter on our brane as

$$S_m = S_m(\phi_m, A^2\tilde{g}),\ A = a(\phi)\Omega, \tag{4.62}$$

where we have neglected the derivative interaction and expressed[2] $g_B = A\tilde{g}$. Notice that $A$ enters in both the coupling of matter to the brane and the time variation of masses. As such it represents the actual time-dependence of couplings in our models. Let us introduce the parameters

$$\alpha_Q = \partial_Q \ln A,\ \alpha_R = \partial_R \ln A. \tag{4.63}$$

We find that ($\lambda = 4/(1+2\alpha^2)$)

$$A = Q^{-\frac{\alpha^2\lambda}{2}}(\cosh R)^{\frac{\lambda}{4}}, \tag{4.64}$$

leading to

$$\alpha_Q = -\frac{\alpha^2\lambda}{2}\frac{1}{Q}, \alpha_R = \frac{\lambda\tanh R}{4}. \tag{4.65}$$

Observations constrain the parameter

$$\theta = \gamma^{ij}\alpha_i\alpha_j \tag{4.66}$$

to be less than $10^{-3}$ [97]. We obtain therefore a bound on

$$\theta = \frac{4}{3}\frac{\alpha^2}{1+2\alpha^2} + \frac{\tanh^2 R}{6(1+2\alpha^2)}. \tag{4.67}$$

[2]The parameter $B$ which defines the coupling of matter to the second brane is similarly defined by $B = a(\sigma)\Omega$.

This bound implies that

$$\alpha \lesssim 10^{-2},\ \ R \lesssim 0.2, \tag{4.68}$$

which already rules out the supergravity model based on $\alpha^2 = 1/12$ [42]. The smallness of $\alpha$ indicates a strongly warped bulk geometry such as an Anti–de Sitter spacetime. In the case $\alpha = 0$, we can easily interpret the bound on $R$. Indeed in that case

$$\tanh R = e^{-k(\sigma-\phi)}, \tag{4.69}$$

i.e. this is nothing but the exponential of the radion field measuring the distance between the branes, and so we retrieve the well-known fact that gravity experiments require the branes to be sufficiently far apart. When $\alpha \neq 0$ but small, one way of obtaining a small value of $R$ is for the hidden brane to become close to the would-be singularity where $a(\sigma) = 0$. In the following we will analyze the cosmological behaviour of the present model and in particular the robustness of the condition $R \ll 1$ to cosmological evolution.

## 4.4 Cosmological evolution of the two brane system

As we have seen from the last section, the field $R$ has to be small today in order for the theory to be in agreement with observations. This required smallness of $R$ could result from one of the following possible features of our model: firstly, the minimum of $V_{\text{eff}}$ or $W_{\text{eff}}$ could be at small values of $R$, and consequently $R$ would have been driven towards this minimum in the very early universe; the form of the potential has to be derived from an underlying theory, whose form is unknown. A much more interesting alternative is that $R$ could be driven towards small values during the late cosmological evolution, i.e. after nucleosynthesis, by an attractor mechanism.

In scalar–tensor theories such a mechanism is well known (see e.g. [75, 83, 84]) and the question we address in this section is whether such an attractor mechanism exists for the brane world models we have discussed so far. Clearly, in our model there are two moduli fields, $Q$ and $R$, and even if $R$ is rapidly driven towards small values, there is the danger that the dynamics of the $Q$ field have no attractor behaviour. This could jeopardize the cosmology of the model we consider. Furthermore, even if such an attractor mechanism exists, it is not *a priori* clear whether it is efficient enough.

To address these important issues, we now discuss cosmological solutions to equations (4.42), (4.43) and (4.44). In this case the field equations are as follows ($\alpha \neq 0$): the

Friedman equation reads

$$H^2 = \frac{8\pi G}{3}\left(\rho_1 + \rho_2 + V_{\text{eff}} + W_{\text{eff}}\right) + \frac{2\alpha^2}{1+2\alpha^2}\dot{\phi}^2 + \frac{1}{1+2\alpha^2}\dot{R}^2. \tag{4.70}$$

where we have defined $Q = \exp\phi$. The second Einstein equation is

$$\begin{aligned} \dot{H} + H^2 &= -\frac{4\pi G}{3}\left(\rho_1 + 3p_1 + \rho_2 + 3p_2 - 2V_{\text{eff}} - 2W_{\text{eff}}\right) \\ &\quad - \frac{4\alpha^2}{1+2\alpha^2}\dot{\phi}^2 - \frac{2}{1+2\alpha^2}\dot{R}^2 \end{aligned} \tag{4.71}$$

The field equations for $R$ and $\phi$ read

$$\begin{aligned} &\ddot{R} + 3H\dot{R} = \\ &\quad -8\pi G\frac{1+2\alpha^2}{6}\left[\frac{\partial V_{\text{eff}}}{\partial R} + \frac{\partial W_{\text{eff}}}{\partial R} + \alpha_R^{(1)}(\rho_1 - 3p_1) + \alpha_R^{(2)}(\rho_2 - 3p_2)\right] \end{aligned} \tag{4.72}$$

and

$$\begin{aligned} &\ddot{\phi} + 3H\dot{\phi} = \\ &\quad -8\pi G\frac{1+2\alpha^2}{12\alpha^2}\left[\frac{\partial V_{\text{eff}}}{\partial \phi} + \frac{\partial W_{\text{eff}}}{\partial \phi} + \alpha_\phi^{(1)}(\rho_1 - 3p_1) + \alpha_\phi^{(2)}(\rho_2 - 3p_2)\right]. \end{aligned} \tag{4.73}$$

For the model we consider here, we have

$$\alpha_\phi^{(1)} = -\frac{2\alpha^2}{1+2\alpha^2}, \quad \alpha_\phi^{(2)} = -\frac{2\alpha^2}{1+2\alpha^2}, \tag{4.74}$$

$$\alpha_R^{(1)} = \frac{\tanh R}{1+2\alpha^2}, \quad \alpha_R^{(2)} = \frac{(\tanh R)^{-1}}{1+2\alpha^2}. \tag{4.75}$$

We will study numerical solutions of the system in more detail below, but if we consider matter on the positive tension brane only we can draw some conclusions concerning the evolution of the fields $\phi$ and $R$:

We assume that throughout the radiation- and matter-dominated eras the potentials $V_{\text{eff}}$ and $W_{\text{eff}}$ are negligible, a similar condition to that imposed in quintessence models. Then, in the radiation-dominated era, the traces of the energy–momentum tensors vanish, implying that

$$\dot{R} = a^{-3}, \dot{\phi} = a^{-3} \tag{4.76}$$

in such a way that $R$ remains small if it is small initially. Moreover, there is no change to the time dependence of the scale factor.

In the matter-dominated era, the equations of motion read

$$\begin{aligned} H^2 &= \frac{8\pi G_N}{3}\rho_1 + \frac{2\alpha^2}{3(1+2\alpha^2)}\dot{\phi}^2 + \frac{1}{1+2\alpha^2}\dot{R}^2 \\ \ddot{R} + 3H\dot{R} &= -\frac{8\pi G_N}{6}\rho_1 R \approx -\frac{H^2 R}{2}, \\ \ddot{\phi} + 3H\dot{\phi} &= \frac{8\pi G_N}{6}\rho_1 \approx \frac{H^2}{2}, \end{aligned} \tag{4.77}$$

together with the conservation equation

$$\dot{\rho}_1 + 3H\rho_1 \approx -2\alpha^2 \rho_1 \dot{\phi}, \tag{4.78}$$

where in order to comply with the tests of the Equivalence Principle we assume that both $\alpha$ and $R_0$ are small. Assuming that the energy density of matter dominates the expansion rate, the solutions to these equations are given by

$$\rho_1 = \rho_0 \left(\frac{a}{a_0}\right)^{-3-2\alpha^2/3}, \ a = a_0 \left(\frac{t}{t_0}\right)^{2/3-4\alpha^2/27} \tag{4.79}$$

together with

$$\phi = \phi_0 + \frac{1}{3}\ln\frac{a}{a_0}, \ R = R_0\left(2\left(\frac{t_0}{t}\right)^{\frac{1}{3}} - \left(\frac{t_0}{t}\right)^{\frac{2}{3}}\right) + 3t_0\dot{R}_0\left(\left(\frac{t_0}{t}\right)^{\frac{1}{3}} - \left(\frac{t_0}{t}\right)^{\frac{2}{3}}\right). \tag{4.80}$$

as soon as $t \gg t_0$. Note that this solution is consistent with our assumptions on the expansion rate as long as $R$ is small at $t = t_0$. Notice further that $R$ converges towards zero, hence retrieving general relativity at late times and that the change of the expansion rate is of order $\alpha^2$ and therefore small. The solution above is in good agreement with the numerical solution described below. We therefore conclude that during the matter–dominated era $R$ is driven to zero, provided $R$ was small at the beginning of the matter era.

### 4.4.1 Numerical Results

We now describe numerical solutions of the cosmological equations. There are different interesting cases to study. Firstly, all matter types could live on the positive tension brane;

a more intriguing alternative might be that the dark matter lives on the negative tension brane, whereas radiation and baryons live on the positive tension brane. We will discuss these cases below.

**No potentials**

We begin the analysis with the assumption that the potentials $V$ and $W$ are identically zero (in other words, that the brane potentials are unbroken from their supersymmetric values); thus we follow the evolution of the fields during radiation and matter domination. Both matter and radiation live on the positive tension brane. The calculations are made with $\alpha = 0.01$.

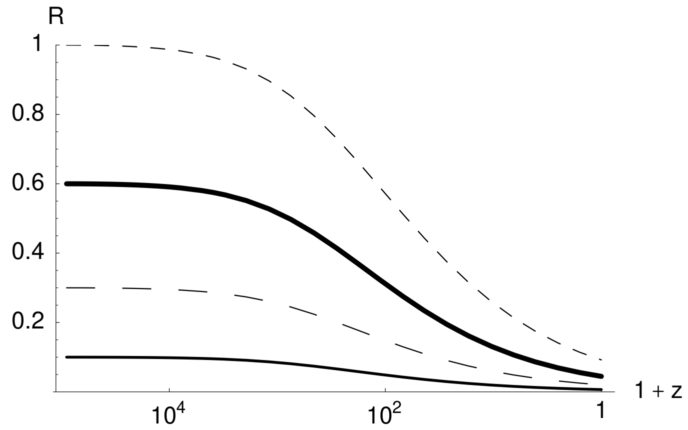


Figure 4.1: The evolution of $R$ with different initial conditions for the case of radiation and matter on the positive tension brane and no matter on the negative tension brane. We find that $R$ is driven towards zero.

The evolution of $R$ and $\phi$ are shown in figures 4.1 and 4.2 respectively. We can clearly see that during radiation domination both fields are frozen in, because the trace of the energy–momentum tensor is effectively zero. Soon after matter becomes important, both fields are forced to evolve due to the non–vanishing trace of the matter energy–momentum tensor. For the initial conditions we have chosen, the constraint $R_{\rm today} < 0.2$ can be fulfilled. However, if $R$ is initially large, it does not have enough time during matter domination to evolve to small enough values. Thus, this cosmological evolution implies that for consistency with observations today $R$ had to be small enough during radiation domination.

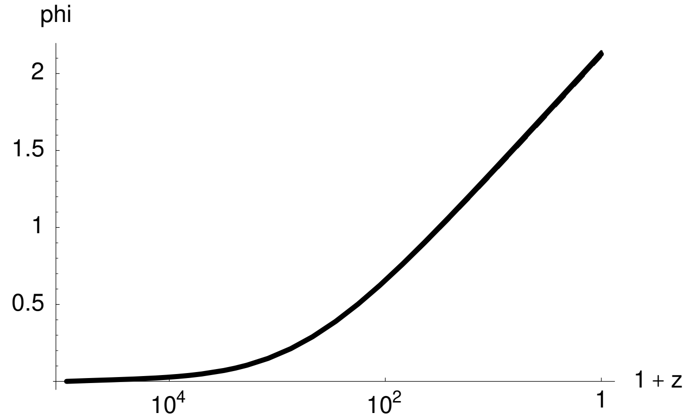


Figure 4.2: The evolution of $\phi$ for different initial conditions with the same cosmology as in figure 4.1.

If we put matter on the second brane as well, the evolution of $R$ is modified, as can be seen in figure 4.3 (see figure 4.4 for the evolution of $\phi$). For these cases, the matter on the second brane never dominates the expansion of the universe. However, due to the coupling function $\alpha_R^{(2)}$, the evolution of $R$ and $\phi$ are affected strongly by matter on the second brane. Indeed, as can clearly be seen, $R$ is driven faster towards small values even with only a small amount of matter on the second brane. The field $\phi$ stays constant longer after radiation domination if there is matter on the second brane.

We conclude that there is a cosmological attractor which drives $R$ towards small values and that the efficiency is enhanced if the energy density of matter on the second brane is not negligible initially.

### Including potentials

We now include potentials on the branes. We shall study the case where there is a potential on the positive tension brane only. We assume that the potential starts to dominate the energy density only recently in the cosmic history, because we are interested in the evolution of the moduli fields $R$ and $\phi$. In principle, both $\phi$ and $R$ are candidates to give cause to the dark energy. However, we do not address the coincidence problem, nor do we wish to provide a model for dark energy in this chapter (for a discussion about dark energy arising in particle physics models, see e.g. [46, 48, 98–104] and references therein). Instead, we use the simplest model for the potential: namely, we assume that $V$ has the form of an exponential potential. To be specific, we assume that supersymmetry is broken by tuning

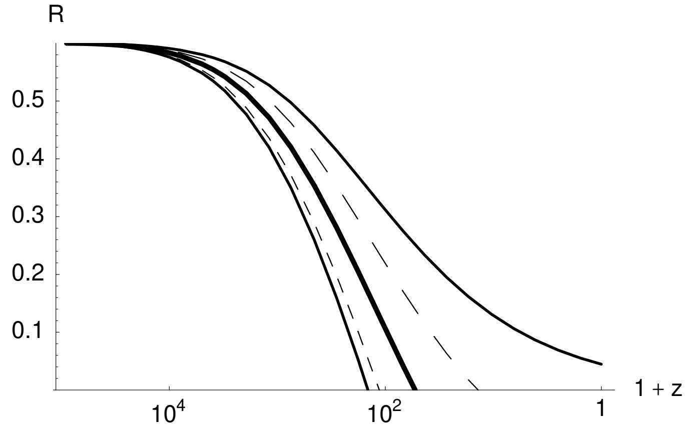


Figure 4.3: The evolution of $R$ with different initial conditions for the case of radiation and matter on the positive tension brane and pressureless matter on the negative tension brane. We find that $R$ is driven towards zero for all cases. Note, that if the ratio $\rho_2/\rho_1$ grows, $R$ evolves faster towards zero. The ratios of $\rho_2/\rho_1$ are given by 0, 0.11, 0.25, 0.42 and 0.5, for the curves from the right to the left.

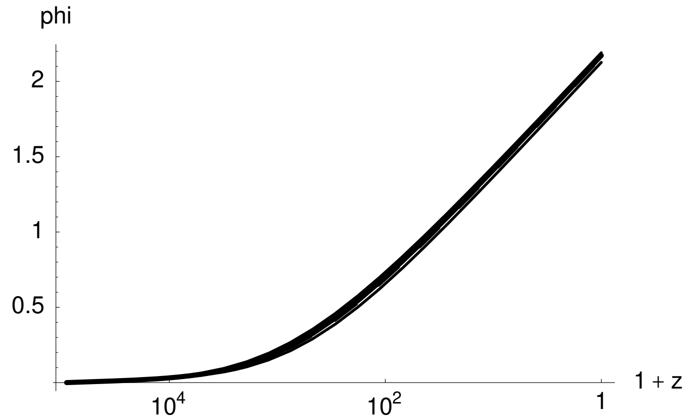


Figure 4.4: The evolution of $\phi$ for different initial conditions with the same cosmology as in figure 4.3.

$U_B$ away from the form (3.7) by setting

$$V = (T-1)4ke^{\alpha\psi}. \tag{4.81}$$

Here, $T \neq 1$ is a supersymmetry breaking parameter ($\psi$ is the bulk scalar field). Expressed in terms of $\phi$ and $R$ we have

$$V(\phi, R) = 4(T-1)ke^{-12\alpha^2\phi/(1+2\alpha^2)} (\cosh R)^{(4-4\alpha^2)/(1+2\alpha^2)} . \tag{4.82}$$

Notice that for $R$ close to zero, this is nothing but an exponential model with the field $\phi$ playing the role of a quintessence field. In the following we will set $4k(T-1)$ such that the universe starts to accelerate at a redshift around 1.

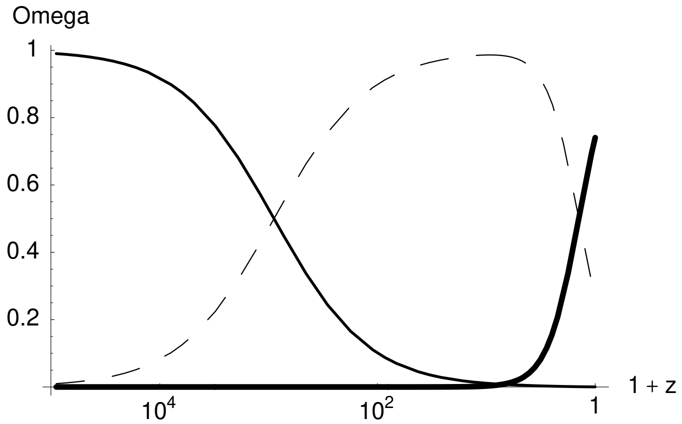


Figure 4.5: Evolution of the density parameter $\Omega_i$ as a function of redshift for radiation, matter and the scalar fields. When the potential of the moduli dominates, the universe is accelerating. Note that in order to explain the values for the energy density of dark energy, We have to fine–tune the parameters of the theory. For these plots we have set $\alpha = 0.01$. The dark matter lives on the positive tension brane; there is no matter on the negative tension brane.

The evolution of the cosmological parameters is shown in figure 4.5. After the usual matter dominated era, the universe becomes dominated by the potential energy of the fields and starts to accelerate.

The evolution for $R$ is shown in figure 4.6. We have chosen the same initial conditions for $R$ as in figure 4.1 and it can be seen that the evolution of $R$ is not much affected by the presence of a potential which dominates today. In figure 4.7 we have plotted the evolution of $\phi$. Note that as soon as the potential dominates the expansion, the evolution of $\phi$ is affected.

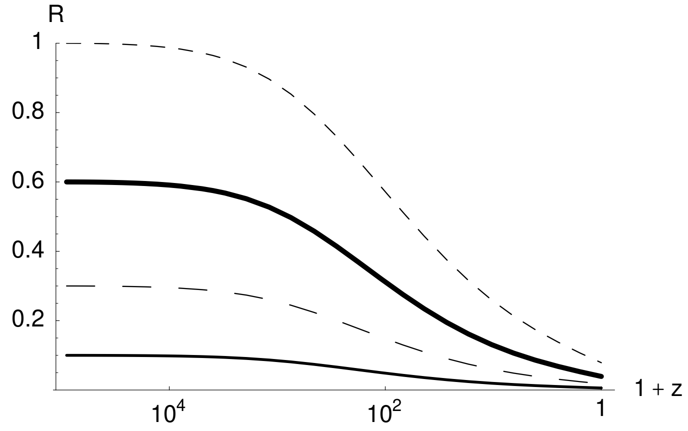


Figure 4.6: Evolution of the field $R$ as a function of redshift with different initial conditions. The constraint today is $R < 0.2$.

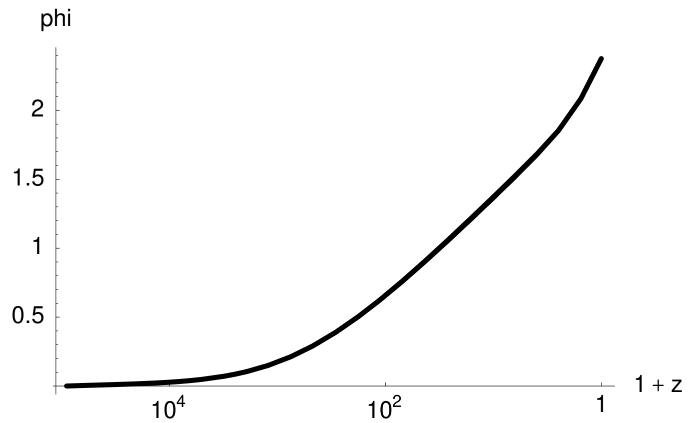


Figure 4.7: Evolution of the field $\phi$ as a function of redshift with different initial conditions. Note that when the potential energy starts to dominate (near a redshift of 1), $\phi$ changes its evolution over time.

### Time variation of masses or the Gravitational Constant

As explained in section 4.3, the quantity $I$, defined in equation (4.59), is an invariant under conformal transformations. This quantity specifies the variation of masses in the Einstein frame (or the gravitational constant in the frame where the masses on the positive tension brane are time-independent). The variation of the gravitational constant (and therefore of $I$) is constrained by nucleosynthesis (see e.g. [105, 106] for a recent discussion). We have plotted the evolution of $I$ for different initial conditions, one with initial conditions leading to an evolution in agreement with observations (figure 4.8), and one extreme case which is ruled out by nucleosynthesis constraints (figure 4.9). Therefore, the initial conditions for the fields $R$ and $\phi$ are not arbitrary, but constrained by nucleosynthesis. The details of the evolution of $I$ are strongly dependent on the matter contents of the branes.

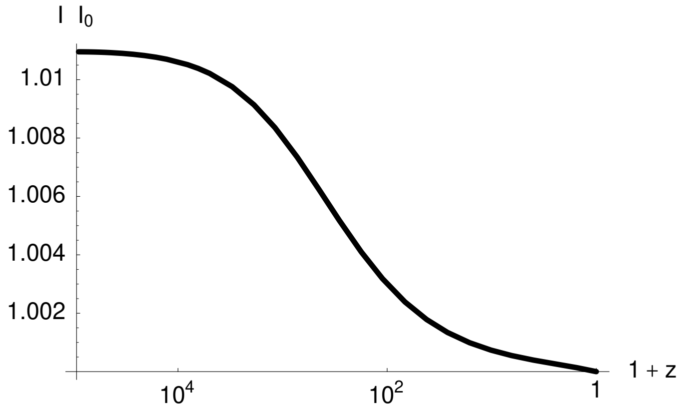


Figure 4.8: Evolution of $I/I_0$ ($I$ is defined in equation (4.59), where $I_0$ is its value today) for initial conditions which are allowed by nucleosynthesis. The value of the gravitational constant at nucleosynthesis was of order one percent larger than its value today.

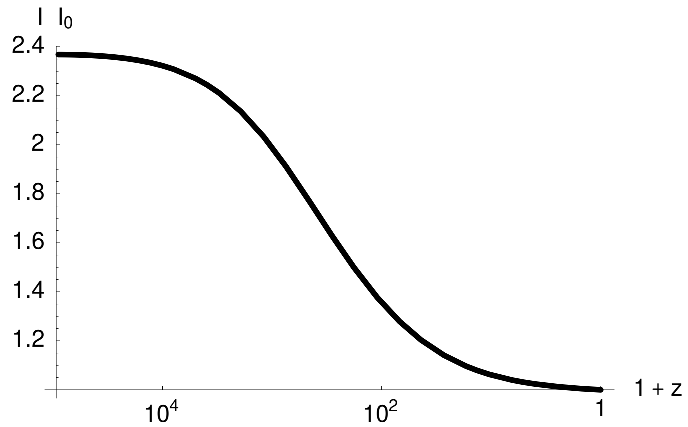


Figure 4.9: Evolution of $I/I_0$ for initial conditions which are forbidden by nucleosynthesis.

### 4.4.2 The Five-dimensional Picture

Having applied the four-dimensional effective theory to cosmology, we now turn our attention to the five-dimensional interpretation of the solutions above. Specifically, we consider the brane positions, which are related to $\phi$ and $R$ by equations (4.23), (4.24), (4.27) and (4.28); we plot the brane positions as a function of redshift in figure 4.10. It is clear from equation (4.28), that $R = 0$ corresponds to $\sigma = 1/4k\alpha^2$, i.e. the negative tension brane is attracted towards the singularity. Negative values of $R$ do not make sense in this description, when the transformations (4.23), (4.24), (4.27) and (4.28) are applied. Therefore, cosmological solutions based on the moduli space approximation in which $R$ is negative do not have a sensible five-dimensional interpretation.

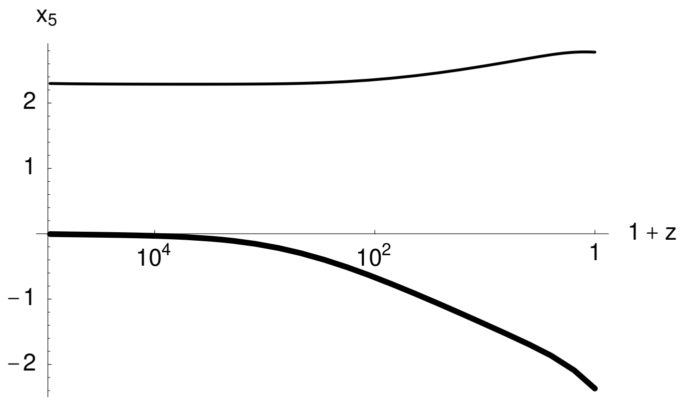


Figure 4.10: Evolution of the brane positions for the cosmology as in figure 4.5.

There are two obvious possible interpretations of this result:

- At the singularity (i.e. at $R = 0$) the negative tension brane will be destroyed. There is only one remaining scalar degree of freedom $\phi$. The late-time evolution is essentially that of a one brane system.
- The negative tension brane is repelled from the singularity. It is tempting to speculate that the repelling can be described by an effective potential in the effective four-dimensional description. This option will be briefly discussed below.

Thus, for a complete understanding of brane cosmology with a bulk scalar field and two branes, we would need a better understanding of the singularity, which would perhaps come from string theory considerations (for a discussion on singularities in string theory see e.g. [107, 108]). Nevertheless, we would like to emphasize that the net effect remains the same: $R$ is initially attracted towards small values.

### 4.4.3 Avoiding the Singularity?

Given that during the matter dominated epoch the negative tension brane is attracted towards a singularity, we will now investigate the response of the system with the adoption of the second option mentioned above; i.e. we add a potential which drives the branes away from the singularity. What are the conditions for such a potential? First, whatever type of matter we have on the branes, near the singular point, i.e. $Q = 0$ ($\phi = -\infty$) and/or $R = 0$, the potential term in the Klein–Gordon equations must dominate. This can be achieved by an inverse–power law potential. A second ingredient is that for consistency with the limit $\alpha \to 0$, the derivative of the potential must be proportional to $\alpha^2$ or some higher power (see equation 4.44). A simple example of a potential which fulfills these requirements is

$$V_{\rm add} = V_0(Q^{\alpha^2} R)^{-\gamma}. \tag{4.83}$$

However, once the negative tension brane is repelled from the singularity, the field $R$ grows again and is at the present epoch, generically, too large to be consistent with observations. Therefore, adding a potential which repels the branes from the singularity jeopardizes the valuable properties of the attractor mechanism during the matter dominated epoch. This can be easily understood: the attractor mechanism is due to the coupling functions $\alpha_R^{(1)}$ and $\alpha_R^{(2)}$ appearing in the Klein–Gordon equation (4.72). If at some point during the matter dominated epoch these terms become negligible compared to the potential term, the field $R$ will be driven by the gradient of the potential. For the potential above, this will be towards larger values of $R$. Then, at some point the potential term in the Klein–Gordon equation becomes negligible again compared to the matter–coupling terms, which drive $R$ towards smaller values until the potential term dominates again. During this interplay between the terms in the Klein–Gordon equation, $R$ will be driven towards larger and larger values because the density of matter drops and it takes more and more time for the potential term to be negligible. The expansion of the universe is never dominated by the potential energy of the moduli fields for the potential (4.83).

What happens in the dark energy dominated régime? This clearly depends on the nature of the dark energy. If the fields $\phi$ and $R$ are responsible for dark energy, then we need to modify the potential at large $R$, as otherwise $R$ will be too large to be consistent with observations and, as explained above, the potential (4.83), for example, will not lead to an accelerating universe. An example which delivers an accelerating universe would be the potential (4.82) added to (4.83). However, this corresponds to the situation where the total potential has a minimum at $R \ll 1$, which has to be fine–tuned. A cyclic universe can be modelled by the inclusion of a potential which is negative in value for some range of the moduli fields [92]. If instead the dark energy has a different origin, and is a field which is confined on a brane, then there is an important interplay between the potential term and the coupling term in (4.72).

## 4.5 Conclusions

In this chapter we have investigated the cosmological evolution of brane world moduli for a general class of brane world models with two boundary branes and a bulk scalar field. The theory we have used contains the Randall–Sundrum model as a special case. The parameter $\alpha$ regulates how strongly the bulk geometry is warped; small values of $\alpha$ correspond to highly warped geometries, whereas large values of $\alpha$ correspond to only slightly warped geometries.

We have obtained the four-dimensional effective theory from the five-dimensional theory using the moduli space approximation. As we are interested in late-time cosmology, namely from nucleosynthesis on, the moduli space approximation should be accurate enough. We have discussed observational constraints and found that the parameter $\alpha$ must be small, pointing towards a warped bulk geometry. Furthermore, the field $R$ must be small enough today, meaning that the distances between the branes must be large enough.

In the Einstein frame, the masses of particles vary, because the two scalar fields $\phi$ and $R$ couple to the matter on both branes. Alternatively, it is possible to consider the frame in which the masses of particles living on the positive tension brane are constant; in that case, not only are the masses of particles confined on the negative tension brane time-varying, but also the gravitational constant is not constant. These conclusions are generic for the kind of theories we consider. The constraint (4.68) ensures that the time-variation is consistent with current observations. (There are constraints on the amplitude of $R$ and $\phi$ in the early universe from nucleosynthesis; we do not discuss this issue here.)

As long as matter is not directly coupled to the bulk scalar field, and therefore to $\phi$ and $R$, the theory predicts that coupling constants such as the fine-structure constant are not spacetime-dependent. Thus, if the observations made in [85, 86] hold, more complicated models of braneworlds would have to be investigated. For instance, to explain the variation of the fine-structure constant we could invoke a coupling of the form

$$S_m = -\frac{1}{4g^2}\int \sqrt{-g_B} f(R,\phi) g_B^{\mu\rho} g_B^{\nu\eta} F_{\mu\rho} F_{\nu\eta}. \tag{4.84}$$

Such a coupling appears naturally in heterotic M–theory, as demonstrated for example in [26, 27]. In this theory the bulk scalar field has an geometrical interpretation: it is a measure of the deformation of a Calabi–Yau threefold. Generally, we would expect that the function $f$ is a function of the parameter $\alpha$ and that for $\alpha \to 0$ we would have $f \to 1$, because for $\alpha = 0$ the bulk scalar field decouples from the dynamics. The attractor behaviour found in the last section implies that any time variation of the gauge couplings at redshifts between 0 and 5 is mainly due to the evolution of $\phi$. The amount of variation depends on the function $f$ above.

Finally, we have discussed the cosmological evolution of the moduli fields. We focused in particular on the question of whether $R$ is driven towards small values during the cosmological evolution (which it must be in order to be consistent with observations today). Our findings indicate that there are cosmological attractors for the field $R$, similar to the attractor found in scalar–tensor theories [75, 83, 84]. We have also found that the efficiency of the attractor strongly depends on the matter content on the negative tension brane. In the five-dimensional picture, the attractor solution drives the negative tension brane towards a bulk singularity. When $R = 0$, the negative tension brane hits the singularity. Negative values of $R$ correspond to the situation where the singularity is between the branes. As the four-dimensional solution suggests that $R$ crosses the origin, we must take some care when interpreting this behaviour. Indeed, a proper understanding of the singularity is absolutely necessary in order to fully understand the cosmology of the two brane system. In the case where the brane is repelled by the singularity, we have argued that the details of the evolution of the two brane system can be significantly altered.

To conclude, the attractor behaviour we have identified might be related to the stabilization of the moduli fields in brane world scenarios. When the moduli fields are not stabilized, an evolution of masses or the gravitational constant (depending on the frame) is generally predicted, whereas an evolution of the fine-structure constant is not generically predicted. Only if vector bosons are directly coupled to the bulk scalar field would we expect coupling constants to vary. This is the case in models based on string theory and therefore we would necessarily predict a time variation of coupling constants as long as the moduli fields are not stabilized at a minimum of some potential.

We would like to emphasize again that the class of brane world models we have considered in this chapter predict the coupling functions (4.74) and (4.75). These functions control the evolution of the fields $\phi$ and $R$ and the coupling to the different matter species.

Having studied the cosmological evolution of moduli fields, we are now in a position to confront these models with observation. As we discussed in chapter 1, the observations of the Cosmic Microwave background radiation provide excellent tests for cosmological theories, probing earlier times in the Universe than we are able to observe by any other means. We shall present in chapter 5 the results of considering cosmological models of the form discussed here for the observations that we would expect to make of the Cosmic Microwave background.

# Chapter 5

# The CMBR in braneworlds

## 5.1 Introduction

In the previous chapter, we studied the cosmological (low-energy) evolution of a general class of braneworld models, finding that there are constraints on the parameters of the theory from solar system tests of General Relativity. We found that, for the theory not to make predictions in conflict with the results of experiments thus far known, the bulk geometry (as measured by the background parameter $\alpha$) must be strongly warped, while the distance between the branes (measured in the effective field theory by the field $R$) must be large. Though the warping parameter $\alpha$ is a fixed parameter of the underlying theory of the Universe, the field $R$ is a dynamical field, and Solar System and other local tests of gravity probe only its value today; we have found that the system exhibits a cosmological attractor whereby the field $R$ is rapidly driven towards small values (such that the distance between the branes becomes large).

There is therefore still a good deal of uncertainty surrounding the value of the $R$ field at early times in the Universe's evolution: while Solar System tests constrain the value of $R$ to be small today, there is no such local probe of the value of $R$ at early times. We are therefore reliant on indirect evidence, and two sensitive and powerful probes of the early Universe: primordial nucleosynthesis and the Cosmic Microwave Background Radiation. We saw in chapter 4 that primordial nucleosynthesis constrains the variation of fields between the time of nucleosynthesis and the present epoch; in this chapter, we shall investigate the effects that this braneworld theory predicts on the spectrum of Cosmic Microwave Background anisotropies. By comparing the theory's predictions with the observed results, we can derive bounds for values of the dynamical field $R$ at early times.

We compare the predictions of the cosmic microwave anisotropies given by our model to those of the concordance $\Lambda$CDM model, on the assumption that there is no potential energy for the scalar fields, so that the energy density of the scalar field is always much smaller than radiation or matter energy density. In the models used in this chapter, the reported acceleration of the universe at low redshift is always caused by a cosmological constant. This ensures that the distance to the last scattering surface and the time of matter–radiation equality is only marginally affected by the presence of the scalar fields. In order to distinguish between the traces of the different fields we study them individually.

The chapter is organised as follows: in section 5.2 we briefly review the five-dimensional setup of a brane world theory and discuss the effective theory in four dimensions. In section 5.3 we set out the action to be discussed in this chapter and derive the field equations, and also study the cosmological background evolution of the fields. In section 5.4 we derive the perturbation equations and discuss the influence of the individual fields on CMB anisotropies and the matter power spectrum, and we conclude in section 5.5.

## 5.2 The effective field theory at low energies

We shall be examining the theory developed in chapter 4; here we summarize the derivation of the effective field theory at low energies of the higher-dimensional brane world theory and discuss its salient points. Our braneworld setup is strongly motivated by recent developments in string theory and provides a useful starting point for more complicated models [109]. Of cosmological interest, but beyond the scope of this chapter to investigate fully, is the possibility of matter confined to the second, hidden, brane being a potential dark matter candidate, as it undergoes only gravitational interaction with ordinary matter.

The effective field theory at low energies (i.e. at energies much less than the brane tension) can be written as a scalar–tensor theory with two scalar fields. The action of the theory was derived in chapter 4 and reads for the gravitational sector

$$S_{\mathrm{EF}} = \frac{1}{16\pi G_N}\int d^4x\sqrt{-g}\left[\mathcal{R} - \frac{12\alpha^2}{1+2\alpha^2}(\partial\varphi)^2 - \frac{6}{2\alpha^2+1}(\partial R)^2 - V(\varphi,R)\right]. \quad (5.1)$$

We remind the reader that $\alpha$ is a parameter of the higher-dimensional theory, which will be left free, though note that models of particle physics, in general, will make predictions about its value [42]. In the Einstein frame, each individual matter form on the branes usually couples to the fields $\varphi$ and $R$, so that the matter action has the general form

$$S_{\mathrm{matter}} = S_{\mathrm{matter},1}(\psi_1, A(\varphi,R)^2 g_{\mu\nu}) + S_{\mathrm{matter},2}(\psi_2, B(\varphi,R)^2 g_{\mu\nu}), \quad (5.2)$$

where $\psi_1$ denotes the matter form on brane 1 and $\psi_2$ the matter form on brane 2. The functions $A$ and $B$ in general depend on both fields and are not equal.

The full interpretation of $\varphi$ and $R$ is covered in chapters 3 and 4, but the fact that there must be two scalar degrees of freedom at low energies can be understood as follows: first, the bulk scalar field can propagate along the brane directions, because it depends on all spacetime coordinates. The other degree of freedom which appears in the low energy effective action is related to the distance between the branes, which is a scalar function of the four spacetime coordinates. We note furthermore that the case where $\alpha$ is zero (corresponding to the second, field-dependent coupling we consider below) subsumes the Randall–Sundrum two brane model, in which there is no bulk scalar field.

The matter couplings are determined by the functions $A$ and $B$, or, to be more precise, by their derivatives with respect to $\varphi$ and $R$. For the brane world model we consider, the coupling functions are given by (see chapter 4 for details)

$$\beta_\varphi^{(1)} \equiv \frac{\partial \ln A}{\partial \varphi} = -\frac{2\alpha^2}{1+2\alpha^2}, \quad \beta_\varphi^{(2)} \equiv \frac{\partial \ln B}{\partial \varphi} = -\frac{2\alpha^2}{1+2\alpha^2}, \tag{5.3}$$

$$\beta_R^{(1)} \equiv \frac{\partial \ln A}{\partial R} = \frac{\tanh R}{1+2\alpha^2}, \quad \beta_R^{(2)} \equiv \frac{\partial \ln B}{\partial R} = \frac{(\tanh R)^{-1}}{1+2\alpha^2}. \tag{5.4}$$

The functions $\beta$ depend on the details of the higher dimensional theory, as they provide all information about the nature of the higher-dimensional space (such as its geometry or curvature) relevant at low-energy. Throughout this chapter we shall consider coupling functions of the form above.

Although we used the moduli space approximation to obtain the low-energy effective theory in chapter 4, there are different routes to that end. Strictly speaking, the action (5.1) is only valid if the Kaluza–Klein excitations, corresponding to massive particles in four dimensions, are negligible. For example, massive partners of the gravitational zero mode, described by $g_{\mu\nu}$, are neglected. However, another method to derive the low-energy effective action was used in [69, 78, 110–112], which is based on solving the five-dimensional Einstein equation to linear order, and then projecting onto the brane on which the standard model particles are confined. The theory is then written in the Jordan frame. This method is widely used in works on brane cosmology and has the advantage in that it provides a geometrical framework for the full five-dimensional problem[1]. We note that the two methods lead to the same low-energy effective theory: after a transformation to the Einstein frame, the action obtained by the projective approach is equivalent to the action (5.1).

In practical terms, the use of the moduli space approximation limits the backwards extrapolation in time; for the use of the moduli space approximation to be valid, we require that the Hubble scale be much greater than the scale under consideration. So, $H(z) \approx (1+z)^2 H_0$ must be much less than $k^{-1}$, the size of the extra dimension, so we can see for instance that millimetre (about $10^{13}\text{GeV}^{-1}$) scales can be dealt with using this approximation to redshifts of about $10^{15}$ (while numerical integration, of which more discussion in section 5.4, typically starts at redshifts of $10^9$). As already stated, in deriving the action above, we assume that Kaluza–Klein excitations are negligible at these redshifts. For example, the bulk scalar field in this approximation does not depend on the extra

[1] In Ref. [113] this formalism was used to calculate the CMB anisotropies in the one–brane scenario of Randall and Sundrum [39].

dimension. We further assume that such excitations are not produced at the epochs in which we are interested. This should be valid, because any such excitation corresponds to a heavy particle.

Clearly this theory, described by the action in equation (5.1), is different from GR, and therefore gravitational experiments constrain parameters of the theory. As shown in chapter 4, for the theory to agree with experiments on earth and observations in the solar system, the parameter $\alpha$ has to be rather small ($\alpha \leq 10^{-2}$), and present values of the field $R$ should likewise be small ($R \leq 10^{-2}$). However, whereas the parameter $\alpha$ has to be chosen small from the beginning, the field $R$ is dynamical and so one has to choose its initial condition such that it is small today.

Given this observation and our work in chapter 4, where it was shown that $R$ is driven toward small values in a stable fashion, to characterize the possible behaviour exhibited by the system we need to examine possible constraints on $R$ at different points in time. Apart from local experiments, the theory is constrained by cosmological considerations. Firstly, nucleosynthesis bounds have to be respected, putting constraints on both $\alpha$ and the initial value of the field $R$. It is beyond the scope of this chapter to constrain the theory by nucleosynthesis, as a detailed analysis with the two fields involved would have to be performed, though we shall discuss this further. The second important cosmological constraint on the fields is enforced by CMB anisotropies and large scale structure considerations. We will in this chapter develop an understanding of the how the CMB is influenced by the fields.

Before we discuss perturbations in models of the form above, we comment on the frame to be used. The issue of the frame and its physical relevance is not new, and has been hotly discussed in the literature (see e.g. [114]). The reason for choosing the Einstein frame instead of the Jordan frame is that, written in the Jordan frame, one the of the scalar fields has a negative kinetic energy (see chapter 4; the metric in the Jordan frame is the induced metric of the first brane, where the standard model particles live). However, this is not a signal of an instability in the system, because in the Einstein frame the kinetic term is positive. The fact that the energy density of the scalar field is not positive definite in the Jordan frame is not unique to field theories derived from brane worlds but appears often in scalar–tensor theories. Several authors have used this as an argument for using the Einstein frame (which is unique) as the physical frame, and we follow this argument here. We would like to point out, however, that in the case of the field with non-constant coupling, the coupling to matter of this field is very small at the present epoch, so that the theory is indistinguishable from General Relativity by local observations made today.

## 5.3 Cosmology and Moduli Fields

As discussed in the last section, there are usually several scalar fields in the low-energy effective action, each of which couples to matter. The goal of this chapter is to understand the effects of the individual fields on the evolution of perturbations. We shall henceforth discuss them separately, dealing with only one scalar field at a time. We shall see in the next section that there are differences in the predicted CMB power spectrum due to the fact that the field coupling function is in one case constant whereas in the other case depends on the field. We shall study two cases individually: the matter coupling will either be of the form (5.3) or (5.4).

The model we consider in this chapter is described by the following action:

$$\begin{aligned} S &= \int d^4x\sqrt{-g}\left[\frac{\mathcal{R}}{2\kappa^2} - g^{\mu\nu}(\partial_\mu\phi)(\partial_\nu\phi) - V(\phi)\right] \\ &\quad + S_V(\psi_V, A(\phi)^2 g_{\mu\nu}) + S_{IV}(\psi_{IV}, B(\phi)^2 g_{\mu\nu}) \end{aligned} \tag{5.5}$$

In the context of brane worlds, the index $V$ stands here for matter on brane 1, whereas $IV$ stands for matter on brane 2. The functions $\psi_V$ and $\psi_{IV}$ stand for the matter fields on each individual brane. The field $\phi$ in equation (5.5) takes the role of either $\varphi$ or $R$ in the last section. In the following we shall work with reduced Planck units $\kappa \equiv 1$.

From the action above, one can derive the following field equations:

$$G_{\mu\nu} = \left(T^{(V)}_{\mu\nu} + T^{(IV)}_{\mu\nu} + \phi_{,\mu}\phi_{,\nu} - \frac{1}{2}g_{\mu\nu}(\partial\phi)^2 + V(\phi)\right) \tag{5.6}$$

$$\Box\phi = -\beta_V T^V - \beta_{IV} T^{IV} \tag{5.7}$$

$$T^{(i)\nu;\mu}_{\mu} = \beta_{(i)} T^{(i)} \phi^{,\nu}, \qquad \text{with } i = (V, IV). \tag{5.8}$$

In these equations, $T$ stands for the trace of the energy–momentum tensor for each individual matter. The functions $\beta$ are given by

$$\beta_1 = \frac{\partial \ln A}{\partial\phi}, \quad \beta_2 = \frac{\partial \ln B}{\partial\phi}. \tag{5.9}$$

In the first case under consideration, the functions $\beta$ do not depend on the scalar field (as is the case with the field $\varphi$ in section 5.2) and choose $\beta$ to be the form[2]

$$\text{Case I}: \quad A = B \propto \exp(-2\alpha'^2\phi/(1+2\alpha'^2)) \Rightarrow \quad \beta_1 = -\frac{2\alpha'^2}{1+2\alpha'^2} = \beta_2. \tag{5.10}$$

We have retained the main features of the brane model, i.e. $\beta_{1,2}$ is negative and bounded. In the second case (corresponding to the field $R$ in the last section), the functions $\beta$ depend on the field and we have

$$\text{Case II}: \quad A \propto \cosh(\phi), \ \ B \propto \sinh(\phi) \Rightarrow \quad \beta_1 = \tanh(\phi) = 1/\beta_2. \tag{5.11}$$

As before we have kept the same functional dependence as in the brane models.

For a homogeneous and isotropic universe with flat spatial sections, the line element reads

$$ds^2 = a^2(\tau)\left(-d\tau^2 + \delta_{ij}dx^i dx^j\right). \tag{5.12}$$

The field equations read

$$H^2 = \frac{1}{3}a^2\left(\rho_V + \rho_{IV} + \frac{1}{2a^2}\dot\phi^2 + V(\phi)\right), \tag{5.13}$$

$$\ddot\phi + 2H\dot\phi + a^2\frac{\partial V}{\partial\phi} = -\beta_V(\rho_V - 3p_V)a^2 - \beta_{IV}(\rho_{IV} - 3p_{IV})a^2 \tag{5.14}$$

$$\dot\rho_{(i)} + 3H(\rho_{(i)} + p_{(i)}) = \beta_{(i)}\left(\rho_{(i)} - 3p_{(i)}\right)\dot\phi. \tag{5.15}$$

In these equations, the dot represents a derivative with respect to the conformal time $\tau$ and $H = \dot a/a$. Note that in equations (5.7) and (5.14) we must sum over all matter forms. In this chapter we will assume that $T^{IV}_{\mu\nu} = 0$, which corresponds to the case with no matter on the second brane (see figures 4.2 and 4.1).

The theory above differs from General Relativity and is therefore constrained by observations. Firstly, local experiments (i.e. on earth and in the Solar System) constrain the post–Newtonian parameters $\gamma_{\rm PN}$ and $\beta_{\rm PN}$ given by

$$\gamma_{\rm PN} - 1 \ \ = \ \ -2\frac{\beta^2_{\rm A/B}}{1+\beta^2_{\rm A/B}}, \tag{5.16}$$

[2]Note that $\alpha'$ in this expression is different from $\alpha$ in chapter 4, because of a field redefinition. We will henceforth drop the prime, treating $\alpha$ as a parameter of the theory, and derive constraints in terms of this parameter later in this section.

$$\beta_{\rm PN} - 1 \;=\; \frac{1}{2}\frac{\beta^2_{\rm A/B}}{(1+\beta^2_{\rm A/B})^2}\frac{d\beta_{\rm A/B}}{d\phi}, \tag{5.17}$$

where $\beta_{\rm A/B}$ stand for the functions $\beta_1$ for the cases I or II, respectively. Current constraints give [115]

$$|\gamma_{\rm PN} - 1| \leq 2\cdot 10^{-3}, \quad |\beta_{\rm PN} - 1| \leq 6\cdot 10^{-4}. \tag{5.18}$$

Nucleosynthesis constraints limit the effective number of degrees of freedom for relativistic particles at this epoch. In general the constraints have to be worked out in detail, but there is a simple way to get a rough limit on the theory from nucleosynthesis. Because the energy conservation equation (5.15) implies that $\rho_{\rm M}a^3 \neq$ constant in general, the expansion rate at nucleosynthesis is different from its value in General Relativity. This leads to [116]

$$0.8 \leq \left(\frac{A(\phi_{\rm nuc})}{A(\phi_0)}\right)^2 \leq 1.2. \tag{5.19}$$

Although we have derived the general equations, from now on we shall set $V(\phi) = \Lambda$, for ease of comparison between the results we obtain for the perturbations and those in the $\Lambda$CDM model. Before we turn our attention to cosmological perturbations and their evolution, however, we briefly study the evolution of the background in the matter dominated era for cases I and II (above) separately.

**Background evolution for constant $\beta$**

The model in this case has similarities to the model discussed in [117], although we do not have an exponential potential for the field. In the radiation dominated epoch, the field is almost constant, because the terms on the left–hand side on the Klein–Gordon equation (5.14) dominate. The constraints (5.18) on the post–Newtonian parameter lead to $\alpha \leq 0.1$. We can easily find the solutions to the background equations in the matter dominated epoch:

$$\begin{aligned} a(\tau) &= \left(\frac{\tau}{\tau_0}\right)^x, \text{ with } \quad x = 2 - 8\alpha^4 \\ \phi &= \phi_0 + 4\alpha^2 \ln\left(\frac{\tau}{\tau_0}\right). \end{aligned} \tag{5.20}$$

Therefore, the universe expands a little more slowly than expected, although the correction is very small. An important point has to be made here, namely that the matter density

$\rho_{\text{matter}}$ does not scale proportionally to $a^{-3}$, but rather like

$$\rho_{\text{matter}} \propto a^{-3} \exp\left(\int \beta d\phi\right). \tag{5.21}$$

For the theory under consideration here, this implies that for a given matter density today, the matter density in the past was greater than it would have been under standard cosmology.

**Background evolution for non-constant $\beta$**

The low-energy effective theory now corresponds to the first model by Randall and Sundrum [38]. As we shall see, there is an attractor mechanism at work which drives the field towards small values, thereby generating small couplings between $\phi$ and matter, as it is dictated by observations on Earth and in the Solar System.

The equations are difficult to handle analytically. Assuming that $\phi$ is small and slowly varying at the onset of matter domination, one can find that

$$a(\tau) = \left(\frac{\tau}{\tau_0}\right)^2, \tag{5.22}$$

and that $\rho_{\text{matter}} \propto a^{-3}$. The field $\phi(\tau)$ now obeys

$$\phi(\tau) = \mathcal{C}\frac{\cos\left(\sqrt{\frac{39}{4}}\ln\left(\tau/\tau_0\right)\right)}{(\tau/\tau_0)^{3/2}} + \mathcal{D}\frac{\sin\left(\sqrt{\frac{39}{4}}\ln\left(\tau/\tau_0\right)\right)}{(\tau/\tau_0)^{3/2}}, \tag{5.23}$$

where $\mathcal{C}$ and $\mathcal{D}$ are constants of integration. Thus, apart from oscillating behaviour, the field $\phi$ in this case decays during matter domination.

Although the solutions above are based on a crude approximation, this qualitative behaviour is found even if the field value was initially larger (confirmation may be seen in 4). For large values of $\phi$, however, equation (5.21) is a better approximation.

Thus, although it is easy to fulfill the constraints (5.18) due to the cosmological attractor, the nucleosynthesis constraints give a limit on $\phi(\tau = \tau_{\text{nucl}}) \leq 0.4$.

## 5.4 Cosmological Perturbations and Moduli Fields

In the following we discuss the evolution of perturbations in the presence of moduli fields. This section is organized as follows: first we will set out the perturbation equations. Then we will solve them (approximately) in the matter dominated era, in order to gain some understanding of the effects of the coupling between the field and matter. Finally we discuss the solutions of the numerical computation of the spectrum of anisotropies in the CMB and the matter power spectrum.

### 5.4.1 The Perturbation Equations in the Synchronous Gauge

We work in the synchronous gauge (using the notation of [118]); i.e. the perturbed line element has the form

$$ds^2 = a^2(\tau)\left(-d\tau^2 + (\delta_{ij} + h_{ij})dx^i dx^j\right). \tag{5.24}$$

After Fourier transformation, the perturbed Einstein equations read:

$$2k^2\eta - \frac{\dot{a}}{a}\dot{h} = a^2\delta T^0_{\ 0} \tag{5.25}$$

$$\ddot{h} + 2\frac{\dot{a}}{a}\dot{h} - 2k^2\eta = -a^2\delta T^i_{\ i}, \tag{5.26}$$

where $h$ and $\eta$ are defined by ($\hat{\mathbf{k}}$ is the unit vector in direction of $\mathbf{k}$)

$$h_{ij} = \int d^3k e^{i\mathbf{k}\cdot\mathbf{x}}\left[\hat{\mathbf{k}}_i\cdot\hat{\mathbf{k}}_j h(\mathbf{k},\tau) + \left(\hat{\mathbf{k}}_i\cdot\hat{\mathbf{k}}_j - \frac{1}{3}\delta_{ij}\right)6\eta(\mathbf{k},\tau)\right] \tag{5.27}$$

From the energy–momentum conservation equation we obtain a set of two equations for the evolution of the density contrast and the divergence of the velocity field. Defining

$$(\rho + p)\theta = ik^j\delta T^0_{\ j} \tag{5.28}$$

$$(\rho + p)\sigma = -\left(\hat{k}_i\cdot\hat{k}_j - \frac{1}{3}\delta_{ij}\right)\left(T^{ij} - \delta^{ij}T^k_{\ k}/3\right) \tag{5.29}$$

and writing $p_i = w_{(i)}\rho_{(i)}$, $c^2_{s(i)} = \partial p_{(i)}/\partial\rho_{(i)}$ and $\theta = ik^i v_i$, we find from the evolution equation for the density contrast $\delta_{(i)} = \delta\rho_{(i)}/\rho_{(i)}$

$$\begin{aligned}\dot{\delta}_{(i)} &= -\left(1+w_{(i)}\right)\left[\theta_{(i)}+\frac{\dot{h}}{2}\right]-3\frac{\dot{a}}{a}\left(c^2_{s(i)}-w_{(i)}\right)\delta_{(i)} \\ &+ \frac{\partial\beta_i}{\partial\phi}\left(1-3w_{(i)}\right)\dot{\phi}\delta\phi+\beta_i\left(1-3w_{(i)}\right)(\dot{\delta\phi})-3\dot{\phi}\beta_i\left(c^2_{s(i)}-w_{(i)}\right)\delta_{(i)}. \qquad (5.30)\end{aligned}$$

The divergence of the velocity field $\theta_{(i)} = v^{(i)j}{}_{,j}$ of each individual fluid evolves according to

$$\begin{aligned}\dot{\theta}_{(i)} &= -\frac{\dot{a}}{a}\left(1-3w_{(i)}\right)\theta_{(i)}-\frac{\dot{w}_{(i)}}{1+w_{(i)}}\theta_{(i)}+\frac{c^2_{s(i)}}{1+w_{(i)}}k^2\delta-k^2\sigma_{(i)} \\ &+ \beta_i\frac{1-3w_{(i)}}{1+w_{(i)}}k^2\delta\phi-\beta_i(1-3w_{(i)})\dot{\phi}\theta_{(i)}. \qquad (5.31)\end{aligned}$$

It is important to note that these equations reduce to those of ordinary General Relativity, if the fluid under consideration has an radiation–like equation of state, i.e. if $w_{(i)} = 1/3$. This means that the equations governing the dynamics of photons and relativistic neutrinos are those found in General Relativity. Important changes occur in the equations for CDM and baryons:

### Cold Dark Matter

In this case, we have $w = 0 = c_s$ and vanishing anisotropic stress. Thus

$$\dot{\delta}_c = -\left[\theta_c+\frac{\dot{h}}{2}\right]+\frac{\partial\beta_c}{\partial\phi}\dot{\phi}\delta\phi+\beta_c(\dot{\delta\phi}) \qquad (5.32)$$

$$\dot{\theta}_c = -\frac{\dot{a}}{a}\theta_c+\beta_c k^2\delta\phi-\beta_c\dot{\phi}\theta_c \qquad (5.33)$$

### Baryons

In this case, we have $w = 0 = c_s$ and vanishing anisotropic stress (a very good approximation after neutrino decoupling [118]). As in [118], we do not neglect the quantity $c_s^2k^2\delta$, which becomes important on small length scales (large $k$). We also have to add the terms describing the momentum transfer between photons and baryons due to Thomson scattering. Therefore, we have

$$\dot{\delta}_b = -\left[\theta_b + \frac{\dot{h}}{2}\right] + \frac{\partial \beta_b}{\partial \phi}\dot{\phi}\delta\phi + \beta_b(\dot{\delta\phi}) \tag{5.34}$$

$$\dot{\theta}_b = -\frac{\dot{a}}{a}\theta_b + c_s^2 k^2 \delta_b + \frac{4\rho_\gamma}{3\rho_b} a n_e \sigma_T(\theta_\gamma - \theta_b) + \beta_b k^2 \delta\phi - \beta_b \dot{\phi}\theta_b \tag{5.35}$$

where $n_e$ is the number density of free electrons and $\sigma_T$ the Thomson cross section.

For completeness, we include the perturbation equations (unchanged from General Relativity) for photons and massless neutrinos [118]:

**Massless Neutrinos**

$$\dot{\delta}_\nu = -\frac{4}{3}\theta_\nu - \frac{2}{3}\dot{h} \tag{5.36}$$

$$\dot{\theta}_\nu = k^2\left(\frac{1}{4} - \sigma_\nu\right) \tag{5.37}$$

$$\dot{F}_{\nu 2} = 2\dot{\sigma}_\nu = \frac{8}{15}\theta_\nu - \frac{3}{5}kF_{\nu 3} + \frac{4}{15}\dot{h} + \frac{8}{5}\dot{\eta} \tag{5.38}$$

$$\dot{F}_{\nu l} = \frac{k}{2l+1}\left[lF_{\nu(l-1)} - (l+1)F_{\nu(l+1)}\right] \tag{5.39}$$

**Photons**

$$\dot{\delta}_\gamma = -\frac{4}{3}\theta_\gamma - \frac{2}{3}\dot{h} \tag{5.40}$$

$$\dot{\theta}_\gamma = k^2\left(\frac{1}{4}\delta_\gamma - \sigma_\gamma\right) + a n_e \sigma_T(\theta_b - \theta_\gamma) \tag{5.41}$$

$$\begin{aligned}\dot{F}_{\gamma 2} = 2\dot{\sigma}_\gamma \quad &= \quad \frac{8}{15}\theta_\gamma - \frac{3}{5}kF_{\gamma 3} + \frac{4}{15}\dot{h} + \frac{8}{5}\dot{\eta} \\ &\quad - \frac{9}{5}a n_e \sigma_T \sigma_\gamma + \frac{1}{10} a n_e \sigma_T (G_{\gamma 0} + G_{\gamma 2})\end{aligned} \tag{5.42}$$

$$\dot{F}_{\gamma l} = \frac{k}{2l+1}\left[lF_{\gamma(l-1)} - (l+1)F_{\gamma(l+1)}\right] - a n_e \sigma_T F_{\gamma l} \tag{5.43}$$

$$\dot{G}_{\gamma l} \quad = \quad \frac{k}{2l+1}\left[lG_{\gamma(l-1)} - (l+1)G_{\gamma(l+1)}\right]$$

$$+ a n_e \sigma_T \left[ -G_{\gamma l} + \frac{1}{2} \left( F_{\gamma 2} + G_{\gamma 0} + G_{\gamma 2} \right) \left( \delta_{l0} + \frac{\delta_{l2}}{5} \right) \right] \tag{5.44}$$

The only new terms compared to General Relativity are the ones proportional to $\beta$ and its derivative. Note that we have had to add an evolution equation for the divergence of the cold dark matter velocity field $\theta_c$: while we can still set $\theta_c = 0$ initially (in order to fix the synchronous gauge completely), in General Relativity, where there is no extra field, it stays at its initial value (usually taken as zero for convenience); however, fluctuations in $\phi$ are a source and therefore, in the theory we consider, it evolves according to the above equation.

Finally, the fluctuations in $\phi$ evolve according to

$$\begin{aligned} &(\ddot{\delta\phi}) + 2\frac{\dot{a}}{a}(\dot{\delta\phi}) + \left( k^2 + a^2 \frac{\partial^2 V}{\partial \phi^2} \right) \delta\phi + \frac{1}{2}\dot{h}\dot{\phi} = \\ &-a^2 \left( \beta_c \rho_c \delta_c + \beta_b \rho_b \delta_b + \frac{\partial \beta_b}{\partial \phi} \rho_b (\delta\phi) + \frac{\partial \beta_c}{\partial \phi} \rho_c (\delta\phi) \right) \end{aligned} \tag{5.45}$$

These equations are quite general in their applicability. Again, note that in the numerical calculations we took $V = \Lambda =$ constant.

### 5.4.2 Solutions in the Matter Dominated Era

Before we give the results for the CMB anisotropies and matter power spectrum, we try to gain some analytical insight from the perturbation equations in the matter dominated epoch on sub-horizon scales. We neglect radiation and the baryons, taking into account only CDM and the scalar field in this regime. Furthermore, we consider only the case for the field with constant coupling, which is tractable analytically.

Taking the derivative of equation (5.32) and making use of equations (5.25), (5.26), (5.33) and the Friedman equation, we get

$$\ddot{\delta}_c + H\dot{\delta}_c - \frac{3}{2}H^2\delta_c = 2\alpha^2 k^2 \delta\phi + 2\dot{\phi}(\dot{\delta\phi}) - 2\alpha^2 \left( H(\dot{\delta\phi}) + (\ddot{\delta\phi}) \right) - 2\alpha^2 \dot{\phi}\theta_c. \tag{5.46}$$

Using the perturbed Klein–Gordon equation, ignoring oscillations in $\delta\phi$ and inserting (5.32) we obtain

$$\ddot{\delta}_c + (H - 2\alpha^2\dot{\phi})\dot{\delta}_c - \frac{3}{2}H^2 \left( 1 + 8\alpha^4 \right) \delta_c = 0. \tag{5.47}$$

A similar equation was found in [119], where the effects of baryons were also considered. Assuming $a \propto \tau^x$, using the background solution equation (5.20) and making the Ansatz

$\delta_c \propto \tau^m$, we get up to $\mathcal{O}(\alpha^4)$

$$m = 2 + \frac{32}{5}\alpha^4 \tag{5.48}$$

for the growing mode. Due to the non–vanishing coupling, compared to the ΛCDM model, perturbations in CDM grow faster than the scale factor and the transfer function is on small scales biassed towards larger values. We have confirmed this numerically.

### 5.4.3 CMB Anisotropies and the Matter Power Spectrum

In the following we will discuss the spectrum of anisotropies in the CMB and the matter power spectrum. It is customary to expand the temperature anisotropy measured in a given direction $\mathbf{n}$ in spherical harmonics according to

$$\frac{\Delta T}{T}(\mathbf{n}) = \sum_{lm} a_{lm} Y_{lm}(\mathbf{n}). \tag{5.49}$$

We assume that the density fluctuations are Gaussian random variables, as predicted by the inflationary scenario. The statistics of the fluctuations are completely specified by the power spectrum $C_l$, defined as

$$\langle a_{lm} a^*_{l'm'} \rangle \equiv C_l \delta_{ll'} \delta_{mm'}. \tag{5.50}$$

Let us briefly summarize how the $C_l$s depend on the perturbation variables and how they are calculated (see [120], [121] and [122] for excellent detailed reviews on the physics of CMB anisotropies). To illustrate the essential steps involved in calculating the anisotropy power spectrum, we neglect the polarization states of the photons. However, when we present the results of the calculations, the polarization states have been taken into account.

At very early times the universe was radiation dominated and the temperature of the universe was so high, that photons and baryons formed a plasma. At these high temperatures, photons and baryons are tightly coupled. On scales less than the horizon the fluid undergoes acoustic oscillations due to the interplay of gravity, which tries to compress overdense regions, and the photon pressure, which, when high enough, acts against the force of gravity. When the temperature dropped below 4000 K, electrons and nuclei were able to combine to form atoms (mainly hydrogen and helium) and the mean free path of the photons became larger than the Hubble horizon. Around that time, the photons completely decoupled from matter. On their path, photons may experience energy loss due to time-changing gravitational fields (the so-called integrated Sachs–Wolfe effect, or ISW). Additionally, photons may interact with reionized gas (reionization might happen due to early star formation).

In order to follow the perturbations in the photons correctly, one must go beyond the fluid description and study the evolution of the photon distribution function $f_\gamma$ in phase space, i.e. solve the Boltzmann equation. In general, $f_\gamma$ is a function of the comoving position $\mathbf{x}$, the photon momentum $\mathbf{p}$ and conformal time $\tau$. To first order we write $f_\gamma = f_0 + \delta f_\gamma$, where $f_0$ is the unperturbed photon distribution. The brightness function $\Delta_T(\mathbf{x}, \mathbf{n}, \tau)$ is defined as

$$\delta f_\gamma(\mathbf{x}, \mathbf{p}, \tau) = \left( \frac{\bar{T}}{4} \frac{\partial f_0}{\partial \bar{T}} \right) \Delta_T(\mathbf{x}, \mathbf{n}, \tau), \tag{5.51}$$

where $\bar{T}$ is the unperturbed temperature of the photon gas (i.e. of the background) and $\mathbf{n}$ is a unit vector in the direction of the photon momentum $\mathbf{p}$. One can now formulate a perturbed version of the Boltzmann equation, describing the evolution of $\Delta_T$. However, it is more useful to perform a Fourier transform of $\Delta_T(\mathbf{x}, \mathbf{n}, \tau)$ and expand the Fourier coefficients $\Delta_T(\mathbf{k}, \mathbf{n}, \tau)$ in Legendre polynomials ($\hat{\mathbf{k}}$ is a unit vector in direction of $\mathbf{k}$):

$$\Delta_T(\mathbf{k}, \mathbf{n}, \tau) = \sum_{l=0}^{\infty} (-i)^l (2l+1) \Delta_{Tl}(k, \tau) P_l(\hat{\mathbf{k}} \cdot \mathbf{n}). \tag{5.52}$$

It can be shown that the density contrast in the photon energy density, $\delta_\gamma$, the divergence of the photon velocity field, $\theta_\gamma$ and the photon anisotropic stress, $\sigma_\gamma$, are related to $\Delta_{Tl}$ by

$$\delta_\gamma = \Delta_{T0}, \quad \theta_\gamma = \frac{3}{4} k \Delta_{T1}, \quad \sigma_\gamma = \frac{1}{2} \Delta_{T2}. \tag{5.53}$$

In terms of the moments $\Delta_{Tl}$, the Boltzmann equation becomes a hierarchy of equations. Using equation (5.53), the evolution equations are given by

$$\begin{aligned}
\dot{\delta}_\gamma &= -\frac{4}{3}\theta_\gamma - \frac{2}{3}\dot{h}, && (5.54)\\
\dot{\theta}_\gamma &= k^2 \left( \frac{1}{4}\delta_\gamma - \sigma_\gamma \right) a n_e \sigma_T \left( \theta_b - \theta_\gamma \right), && (5.55)\\
2\dot{\sigma}_\gamma &= \frac{8}{15}\theta_\gamma - \frac{3}{5} k \Delta_{T3} + \frac{4}{15}\dot{h} + \frac{8}{5}\dot{\eta} - \frac{9}{5} a n_e \sigma_T \sigma_\gamma, && (5.56)\\
\dot{\Delta}_{Tl} &= \frac{k}{2l+1} \left[ l \Delta_{T(l-1)} - (l+1)\Delta_{T(l+1)} \right] - a n_e \sigma_T \Delta_{Tl}, \qquad (l \geq 3). && (5.57)
\end{aligned}$$

Furthermore, it can be shown that the quantity $C_l$, defined in equation (5.50), is related to the brightness function $\Delta_{Tl}$ by

$$C_l = 4\pi \int \frac{dk}{k} \left|\Delta_{Tl}(k,\tau_0)\right|^2 . \tag{5.58}$$

It is straightforward to include polarization. Due to Thomson scattering, photons are linearly polarized in the plane perpendicular to $\mathbf{n}$. The collision terms in the Boltzmann equation depend on the polarization state. In order to follow the evolution in phase space, we define a total distribution function $f_\gamma$, which includes all polarization states and another distribution function, $g_\gamma$, which is defined as the difference of the distribution functions for the individual polarized photons. Defining the temperature brightness function $\Delta_T$ and the polarization brightness function $\Delta_P$ in the same way as in the above procedure, we can show that $\Delta_T$ obeys the equations (5.54)–(5.57), provided that, because the collision term in the Boltzmann equation depends on the polarization state, equation (5.56) is adjusted to

$$2\dot{\sigma}_\gamma = \frac{8}{15}\theta_\gamma - \frac{3}{5}k\Delta_{T3} + \frac{4}{15}\dot{h} + \frac{8}{5}\dot{\eta} - \frac{9}{5}an_e\sigma_T\sigma_\gamma + \frac{1}{10}an_e\sigma_T\left(\Delta_{P0} - \Delta_{P2}\right). \tag{5.59}$$

Additionally, we obtain a hierarchy for the functions $\Delta_{Pl}$:

$$\begin{aligned} \dot{\Delta}_{Pl} &= \frac{k}{2l+1}\left[l\Delta_{P(l-1)} - (l+1)\Delta_{P(l+1)}\right] \\ &\quad -an_e\sigma_T\left[\Delta_{Pl} + \frac{1}{2}\left(\Delta_{T2} + \Delta_{P0} + \Delta_{P2}\right)\left(\delta_{0l} + \frac{\delta_{2l}}{5}\right)\right], \end{aligned} \tag{5.60}$$

where $\delta_{il}$ in the last term is the Kronecker delta.

The CMB anisotropy power spectrum $C_l$ is still as given by equation (5.58). Thus, in order to calculate the CMB power spectrum $C_l$ (as well as the polarization power spectrum and the temperature/polarization cross correlation spectrum), a large set of differential equations must be solved: the equations for baryons, CDM and the scalar field presented in section 5.4.1 and the hierarchy above. In [123] solutions to the Boltzmann equation are found. Here we use an existing code [124] and make the appropriate changes to the evolution of background and perturbation variables to incorporate the above theory.

**Numerical Approach**

In order to calculate the CMB power spectrum, we make changes to an existing code [124], whose method is based on [19]. As described in section 5.4.1 we have to make changes in the equations for CDM and baryons and the modified Klein–Gordon equation for the scalar field must be included. We assume a scale–invariant initial power spectrum and adiabatic initial conditions. In the course of making these modifications, an error was found in the quintessence module of CAMB, which thankfully has not led [125] to erroneous results in the literature.

Since the background evolution is modified in the models we wish to consider (and there is no analytic solution as in [126]), we shall have to compute the background numerically as well as the perturbations. For the models under consideration here, this additional numerical calculation did not lead to a significant degradation in performance; however, should it prove problematic, it should be noted that the background calculation for given initial conditions is independent of the perturbations and is therefore precomputable. The revised program was compared against known special cases in our framework (such as a reduction to a pure General Relativity theory) to verify that there were no gross errors in the modifications.

### Constant Coupling

What are the expected effects of the non–vanishing coupling? There are two which come in when $\alpha$ differs from zero. Firstly, as mentioned in section 5.3, the dependence of the matter density (both for baryons and CDM) on the scale factor is no longer given by $\rho_{\rm matter} \propto a^{-3}$, but rather by equation (5.21). Therefore, relative to the $\Lambda$CDM model, the density of matter (and in particular of baryons) is larger at decoupling (we remind the reader that the models are normalized such that their matter density is equal at the present epoch). Hence, the amplitudes of the peaks are larger.

Additionally, there are changes to the sound speed $c_s^2 = \dot{p}_\gamma/(\dot{\rho}_{\rm b} + \dot{\rho}_\gamma)$. The sound speed decreases with increasing $\alpha$; this affects the peak separation, which is proportional [120] to

$$\delta l = \frac{\chi(\tau_0 - \tau_{\rm dec})}{D_s}, \tag{5.61}$$

where $\chi(\tau_0 - \tau_{\rm dec})$ is the angular diameter distance to the surface of last scattering and $D_s = \int^{\tau_{\rm dec}} c_s d\tau$ is the sound horizon. Aside from having an effect on $c_s$, the presence of the scalar field additionally alters the distance to the last scattering surface. Let us estimate the position of the first peak, given by $l_0 = \pi\chi(\tau_0 - \tau_{\rm dec})/D_s$. It is simple to calculate $\chi(\tau_0 - \tau_{\rm dec})$:

$$\chi(\tau_0 - \tau_{\rm dec}) = \int_{\tau_{\rm dec}}^{\tau_0} d\tau \approx \frac{2}{H_0}\frac{1}{1+C} \tag{5.62}$$

where $C = 2\alpha^4/(1-8\alpha^2)(1+2\alpha^2)$. Putting $c_s^2 \approx 1/3$ and neglecting the radiation dominated epoch, one finds

$$D_s \approx \frac{1}{3}\frac{1}{H_0}\frac{2}{1+C}a_{\rm dec}^{\frac{1}{2}+\frac{C}{2}}. \tag{5.63}$$

Therefore, the position of the peak is given by (note that we have $a(\tau_0) = 1$)

$$l_0 = \tilde{l}_0 a_{\rm dec}^{-C/2}, \tag{5.64}$$

where $\tilde{l}_0 \approx 200$ is the position of the peak for the flat model with no coupling. Therefore, the peak moves towards larger values (i.e. to the right in the spectrum).

To reach this conclusion we have assumed that $c_s \approx 1/3$, which is somewhat crude. Note, however, that if one takes the baryons into account the sound speed is smaller and hence, the sound horizon $D_s$ is smaller. Thus, $l_0$ is if anything somewhat larger than the value given in equation (5.64).

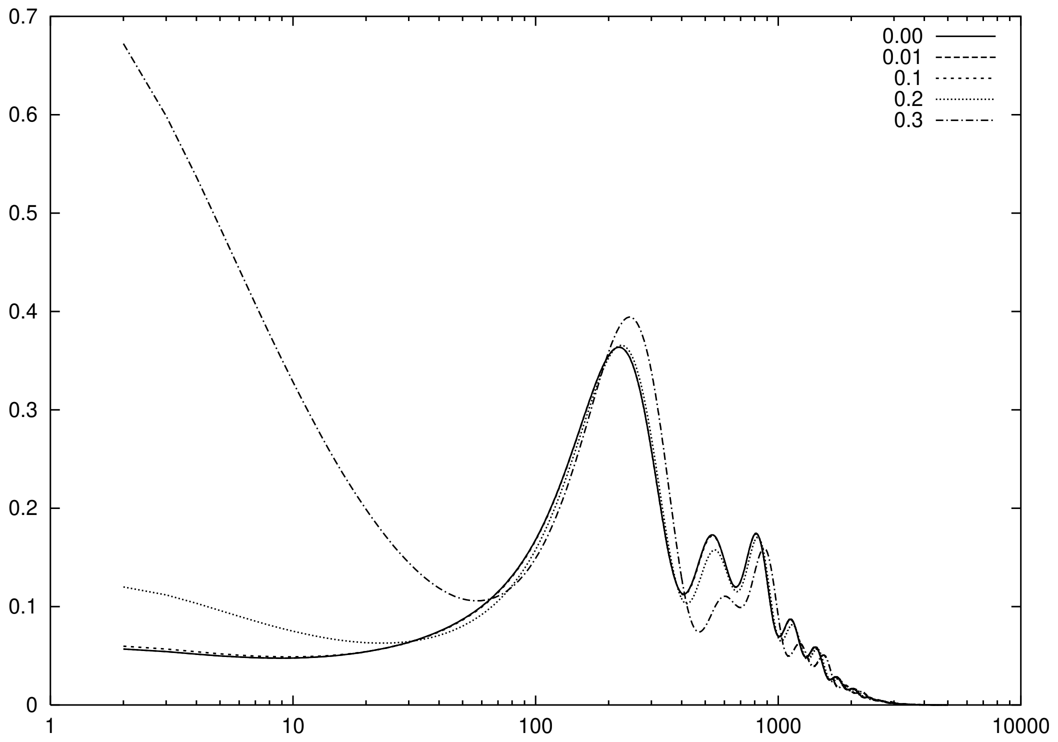


Figure 5.1: The temperature anisotropy power spectrum, $l(l+1)C_l/2\pi$, for the constant coupling case: the values in the legend are the values of $\alpha$.

The second important change when the coupling is non–vanishing is that there is a larger contribution from the integrated Sachs–Wolfe effect. Note that for some time into the matter dominated era, the gravitational potential continues to change with time, because the matter density contrast no longer grows like $\delta(\tau) \propto a(\tau)$. The evolution of perturbations in models similar to the one discussed in this section was considered in depth in [127]. As the time–evolution of the scale factor is altered in the presence of the scalar field, the duration of the recombination era is affected, too.

In figure 5.1 we plot the results for the temperature anisotropy power spectra. We assume an initial power spectrum with equal power on all scales. It can clearly be seen that the both the amplitude and the separation of the peaks are affected by increasing the coupling constant. Also, on large scales (low $l$) one can see the additional power due to the integrated Sachs–Wolfe effect.

In order to compare the theory to observations, we normalize the curves appropriately. Usually this is done at large angular scales, using the COBE data as reference. The curves normalized to COBE are plotted in figure 5.2. Clearly, the normalized curves show less power on small scales because of the enhanced integrated Sachs–Wolfe effect in models with non–vanishing coupling. On larger scales (small multipole number $l$) one clearly sees a boost of power. Additionally, the normalized matter power spectra for models with non–vanishing coupling are below the $\Lambda$CDM curve.

For completeness we plot the E–type polarization spectra and the cross correlation between temperature and E–type polarization in figure 5.3. One can clearly see that in both spectra on small scales the power is suppressed when $\alpha$ is increased.

In figure 5.4 we plot the anisotropy spectra for the $\Lambda$CDM model and the model with the maximal value of $\alpha$ allowed by local experiments ($\alpha = 0.1$). One can see that the COBE normalized curves differ from each other by a few percent on small angular scales.

**Non-constant Coupling**

In this case, where the field $\phi$ corresponds to the $R$ field in equation 5.1, the coupling function now decays. But also here, the baryon density is larger at decoupling compared to the $\Lambda$CDM, which leaves a similar effect on the peak position and amplitudes as in the case of constant coupling.

However, well inside the matter dominated epoch, the coupling becomes very small, so that the density contrast grows essentially like $a(\tau)$ from that time on. Therefore, the ISW effect is not as pronounced as in the case of constant coupling. Only if $\phi$ was initially very large will the field have not evolved to small values by today; consequently, for the

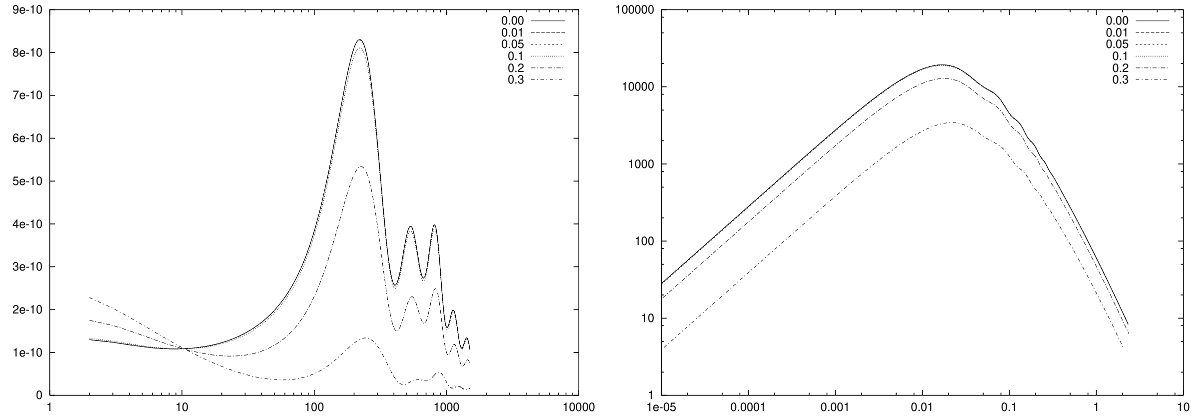


Figure 5.2: COBE-normalized temperature anisotropy $l(l+1)C_l/2\pi$ (left panel) and matter power spectrum (right panel) for the case of constant coupling. On small scales the COBE–normalized spectra are below the predictions for vanishing coupling due to the enhanced ISW.

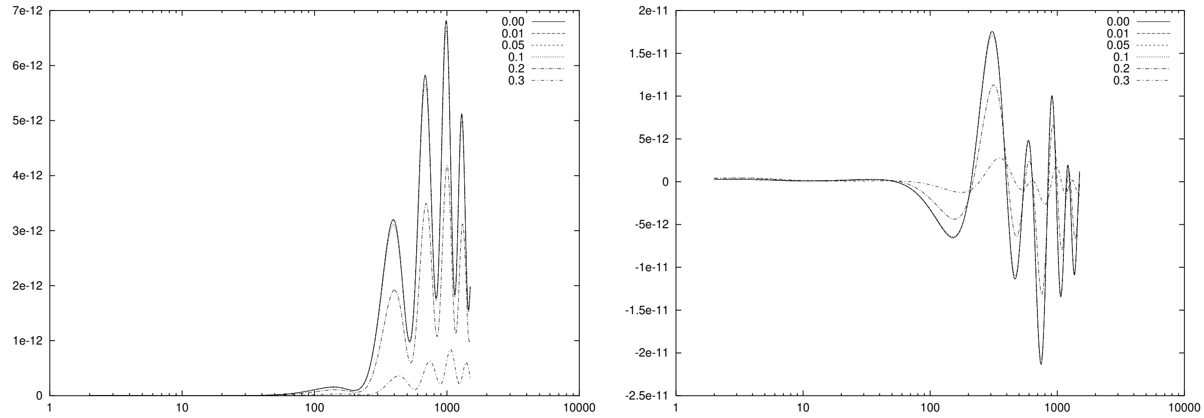


Figure 5.3: COBE-normalized E-mode polarization anisotropy (left panel) and TE cross-correlation (right panel) for the case of constant coupling.

field-dependent coupling case, only for large initial field values will the impact on the ISW effect become more apparent (see figure 5.5).

The normalized anisotropy and matter power spectra are shown in figure 5.6, and the normalized E-mode polarization anisotropy and the TE–cross–correlation in figure 5.7. Increasing the initial value of the field implies that the power in both the E–polarization spectrum and the cross correlation spectrum between temperature and E–polarization is suppressed on small scales.

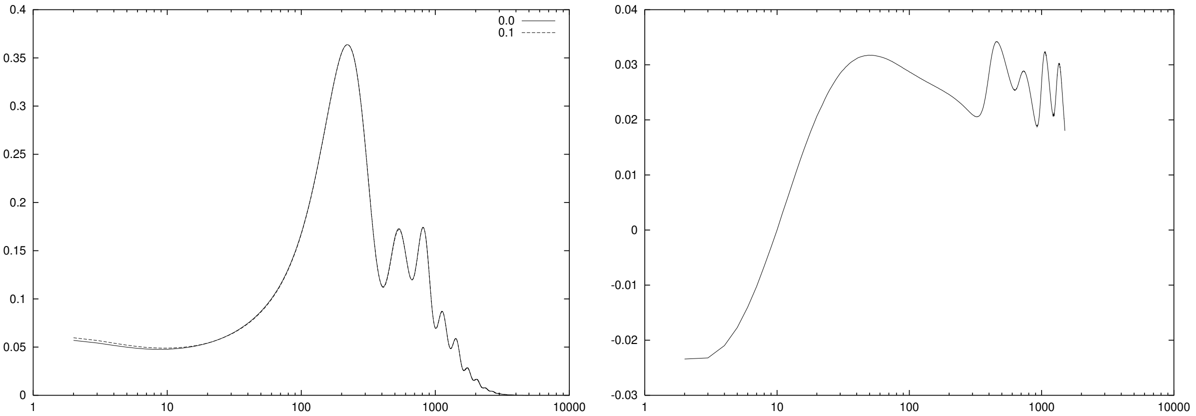


Figure 5.4: CMB anisotropy spectra (left panel) for the constant-coupling case, with $\alpha$ taking the extreme value permitted by local experiments, with a reference curve from the $\Lambda$CDM model; the right panel shows the relative discrepancy. Although the differences are around 3 percent at high multipoles, a different choice of normalization – normalizing to COBE at $l = 800$, say – would move all the observed discrepancies into the low–multipole region, where cosmic variance dominates.

The initial field values in figures (5.5) and (5.6) have been used without taking into account constraints from nucleosynthesis (5.19), which implies that $\phi_{\rm nuc} < 0.4$. We remind the reader again, that the field is driven towards zero during the matter dominated epoch and the field value today is much smaller. In figure 5.8 we plot the cases for $\phi_{\rm init} = 0.4$ and the $\Lambda$CDM curve. We can see that there are differences in the predictions for the temperature anisotropy as large as 6 percent at small angular scales and 3 percent on degree scale. This is potentially distinguishable with WMAP and the Planck Surveyor.

We would like to point out that constraints on $\phi$ become stronger once the CMB is included. In all cases plotted in the figures, the field fulfills the constraints today; but, a large field value in the early universe modifies the predictions for the temperature and polarization power spectra (as well as the matter power spectra). Hence, the CMB provides vital complementary information to the local experiments.

## 5.5 Conclusions

In this chapter we have investigated the implications of time-varying extra dimensions for CMB anisotropies and large scale structure formation. In theories with extra dimensions, certain scalar fields – so called 'moduli fields' – appear in the low energy effective theory,

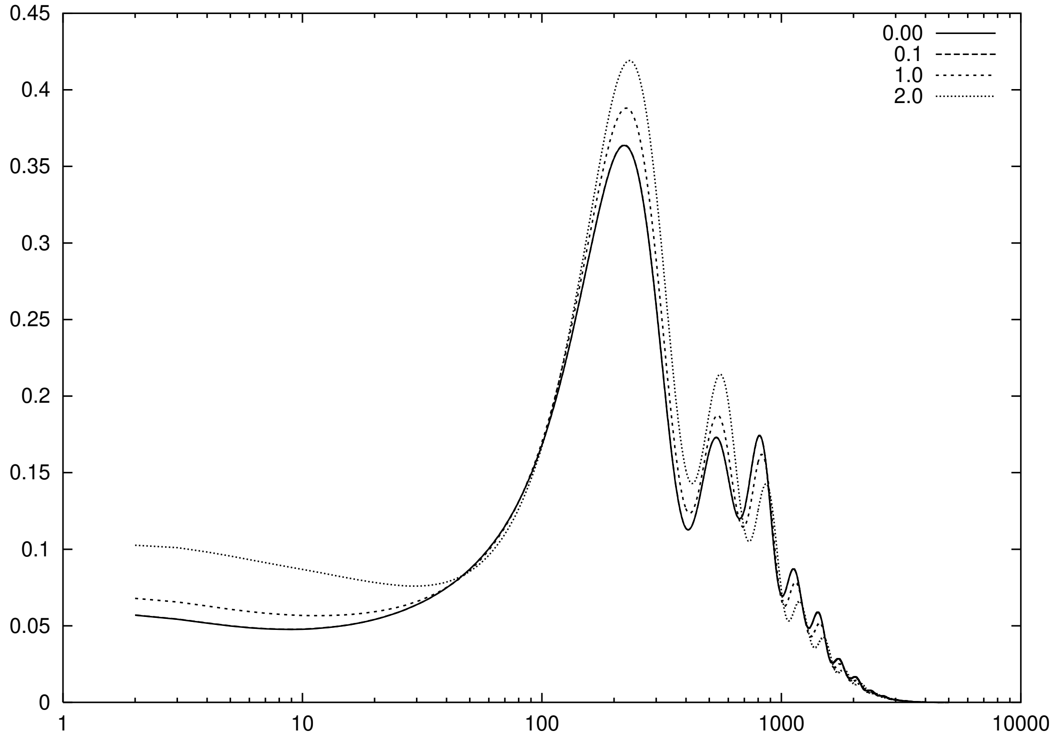


Figure 5.5: The temperature anisotropy power spectrum, $l(l+1)C_l/2\pi$, for the field-dependent coupling case: the values in the legend are for the initial values of the scalar field $\phi$.

coupling directly to matter fields. We have investigated in particular the couplings which appear in a five-dimensional model based on the brane world idea. The model contains two branes which are the boundaries of the higher-dimensional spacetime, with, in general, four-dimensional matter fields confined on these branes. Additionally, we allowed for a scalar field propagating in the extra-dimensional spacetime. At low energies the dynamics of this system is described by a bi–scalar–tensor theory. The first scalar fields has a constant (i.e. field- and coordinate-independent) coupling to the matter fields, whereas in the case of the second field the coupling function is field dependent.

We have investigated the effects of the individual fields on the CMB anisotropies, the cross–correlation between temperature and polarization of the CMB and the matter power spectrum. Due to the coupling, both the amplitude and the positions of the peaks are affected. The spectra normalized to COBE lie below the spectra of the reference $\Lambda$CDM model on small scales.

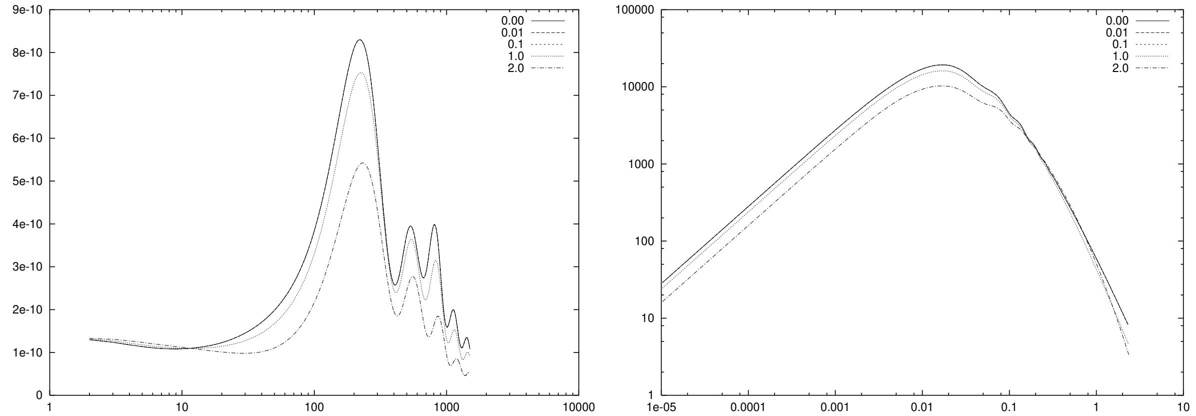


Figure 5.6: COBE-normalized temperature anisotropy $l(l+1)C_l/2\pi$ (left panel) and matter power spectrum (right panel) for the case of field-dependent coupling. As in figure 5.2, on small scales the COBE-normalized spectra are below the predictions for vanishing coupling.

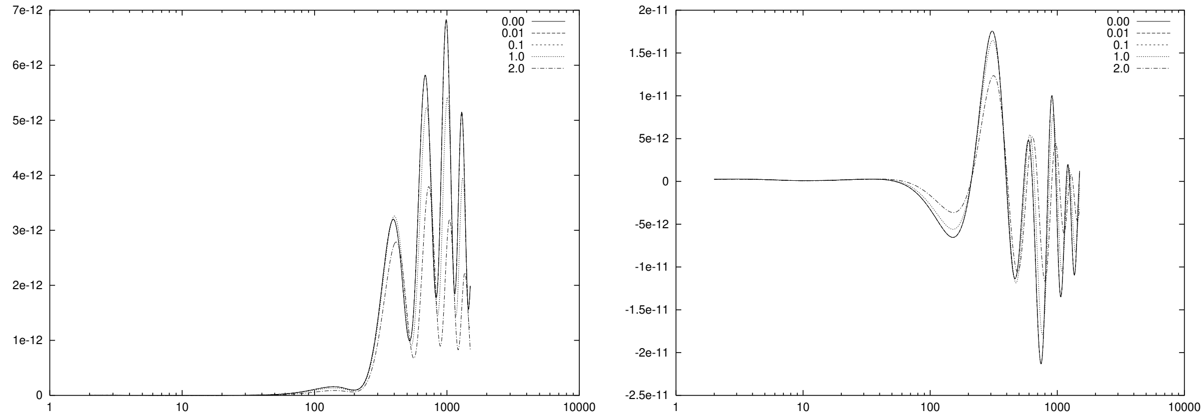


Figure 5.7: COBE-normalized E-mode polarization anisotropy (left panel) and TE cross-correlation (right panel) for the case of field-dependent coupling.

The results presented in section 5.4 imply that, for the brane world model presented in section 5.2, each field potentially has a measurable effect on the CMB. If it turns out that the second field needs to be already quite small during the radiation dominated epoch, then some mechanism has to drive it to these small values in the very early universe. This can happen, for example, if there is some matter on the second brane, in which case the field $R$ is driven even faster to zero, so that it might be small at decoupling. Note, however, that in this case the evolution of perturbations would be affected in the radiation dominated epoch.

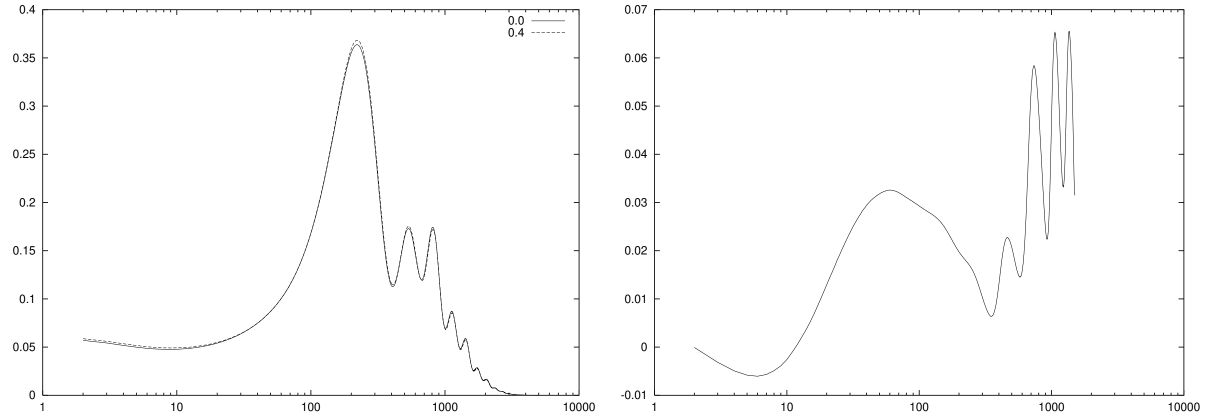


Figure 5.8: CMB anisotropy spectra (left panel) for the case of an initial value ($\phi_{\rm ini} = 0.4$) allowed by nucleosynthesis. The right-hand panel shows the relative error between the $\Lambda$CDM and the model with $\phi_{\rm ini} = 0.4$. For $l \approx 100$ the difference between the models is as large as 3 percent and gets larger at higher $l$ (smaller angular scales).

Clearly, the CMB anisotropies as well as the polarization provide complementary information about time–evolution of the extra dimensions. Together with other tests, such as gravity experiments in the solar system and/or on earth and tests of time–varying gauge couplings and primordial nucleosynthesis, these cosmological considerations strongly constrain any model involving extra dimensions. For example in the case of the model considered here, the field with constant coupling is already constrained by local experiments such that its effects on the CMB are negligible. For the second field, however, we have seen that although its effect is constrained to be minimal today, it can have a significant impact on the CMB anisotropies.

There is another important point not addressed in this chapter: we have not discussed the time evolution of Kaluza–Klein excitations and their influence on the CMB. It is possible that they are still present in the radiation dominated epoch, thereby affecting the evolution of perturbations at least initially: their presence could imply, for example, that the initial perturbations are not purely adiabatic. The details would depend on the mechanism which produces the primordial fluctuations, such as inflation or the cyclic model: see e.g. [92] and [128]. To address this important issue one has to go beyond the moduli space approximation (and in fact beyond the lowest order in the method used in [78], [110] and [112]).

We have investigated the effects of moduli fields on the CMB motivated from a certain class of brane world theories. There are other brane world models, in which the theory at low energies cannot be described by an action of the form (5.1). For example, in the models of [129–131], gravity becomes five-dimensional at large distances. We expect that some of the conclusions drawn in this chapter do not hold for such models. Nevertheless, the CMB gives useful constraints on these models, too [132].

We remind the reader that the above analysis was based on an effective four-dimensional theory of gravity obtained through the use of the Moduli Space Approximation in chapter 4, and is therefore only valid when the moduli of the higher-dimensional theory are suited to this approximation; that is, are sufficiently slowly-varying. We would expect this to be the case for times well after the epoch of nucleosynthesis. In [113], a different region of the approximation space was studied, examining the five-dimensional world directly by solving directly for the higher-dimensional Weyl $E_{\mu\nu}$ term, but with an imposed stabilised radion; we must therefore be careful when comparing results both to other theories and with observation.

# Chapter 6

# Further work and Conclusions

## 6.1 Conclusions

In this dissertation, we have considered the cosmological evolution of extra-dimensional models, focusing in particular on models related to the Randall–Sundrum scenarios. We have discussed how the derivation and use of cosmological predictions in these models can lead to insight into their validity and utility as applied to our apparently four-dimensional Universe; we have investigated alterations to currently known phenomena, and considered the possibility of entirely new cosmological effects fundamentally due to the extra-dimensionality of the model.

We have examined an interesting proposal for an intrinsically five-dimensional effect with potentially important repercussions for cosmology in chapter 2. We investigated the behaviour of null geodesics taking shortcuts through the bulk in a variety of brane world models, and the extent of apparent acausality as seen by an observer confined to the four-dimensional brane. In the case of the cosmological extension of the single brane model, we have found that the ratio of the effective speed of five-dimensional signals to that of light was not larger than two.

In all models, both those with one brane and those with two, we demonstrated that, although a four-dimensional observer could see apparent causality violations of significant extent, the impact on the cosmological horizon problem is minimal. However, the shortcuts could have an effect on the particle horizon, and might also provide a way of testing experimentally for higher dimensions in future gravitational wave detectors.

In chapter 3, we discussed the dynamics of a braneworld model with a bulk scalar field. We investigated the coupling of the distance between the branes to the bulk scalar, and found that in a static supergravity background we obtain an effective theory of gravity that resembles a Brans–Dicke scalar–tensor theory. We discussed the presence of an attractor of the theory towards four-dimensional General Relativity, and found that many initial configurations of the braneworld model allow the attractor to work.

With Standard Model fields on both branes in this scenario, we found that the matter types coupled to gravity differently, leading to Equivalence Principle violations. This provided a potential dark matter candidate, as the applicability of the Equivalence Principle to dark matter is less constrained by experiment than to ordinary matter; and also other potential effects for cosmology.

We considered these cosmological implications in more depth in chapter 4. We consider the constraints on the model parameters and the fields if we are to recover four-dimensional General Relativity at times corresponding to the present, finding a distinct constraint towards strong warping of the background spacetime, and further that the branes must be far apart at the present time.

We found that we would not expect a time variation of the fine–structure constant in this model, though masses (or equivalently the gravitational constant) would be expected to vary. We confirmed the presence of the attractor towards General Relativity, and found that its efficiency was strongly affected by matter content on the shadow brane. However, a full understanding of the cosmology of this model depends on understanding the nature of the spacetime singularity in the background, and may depend on a full string theory description.

In chapter 5, we used the effective theory derived from the cosmological study of our model to study the expected perturbations in the Cosmic Microwave Background radiation. We examined the effects of coupled scalar fields, both with constant coupling and with coupling functions derived from our higher-dimensional theory, and developed constraints on the parameters and initial conditions of our theory in a manner complementary to those derived in chapter 4.

We found that the observations of the Cosmic Microwave Background anisotropies provide a constraint on parameters influencing constant coupling of the same order as those from current Solar System gravity experiments. When the coupling function is not constant, however, local experiments only provide a constraint on its value today; the observations of the CMB, reflecting as they do the conditions holding at very early times in the Universe's evolution, give limits on field values at that time, constraining the state at the end of inflation more strongly than with other observations alone.

## 6.2 Further work

While we have performed an initial investigation into the effect of coupled scalar fields on the CMB anisotropies in chapter 5, a more complete analysis would involve computing the marginalized likelihood functions for the various cosmological parameters; in particular, this would expose possible degeneracies of the effect of the scalar fields with other parameters. This would be a continuation of the investigation in [133], which derived – from CMB observations in conjunction with other priors – bounds on the dark energy equation of state under the assumption that the field couples only to dark matter. Since this is not the case in our model, we anticipate that the bounds from this investigation would be correspondingly tighter.

As a further extension to our work, there has recently been proposed [134, 135] a mechanism whereby the stringent bounds derived in chapters 3 and 4 on the parameters and current field values of our theory might be evaded or weakened. The mechanism can be described as the addition of a runaway potential for the scalar field to the action (equation 5.5) of chapter 5. The result of this is that the scalar field couples to an effective potential

$$V_{\text{eff}}(\phi) = V(\phi) + \beta\rho e^{\beta\phi}, \tag{6.1}$$

where $V(\phi)$ can be taken as being, for example, of inverse power law form,

$$V(\phi) = M^4\phi^{-n}. \tag{6.2}$$

There is then a minimum of the effective potential for the scalar field $\phi$, which is dependent on the local matter density; consequently, the expectation values of the scalar field and its local mass are dependent on the matter density of the surroundings. This in turn means that measurements of gravitational effects in an Earth-based experiment can be largely unaffected by the existence of this scalar field, while still allowing significant Equivalence Principle violations in a small satellite such as the forthcoming SEE [136] or STEP [137] experiments.

This difference can come about because above a certain size, objects exhibit a thin–shell effect, such that the field outside a large object is almost entirely determined by the contribution from a shell at the object's exterior, with interior contributions being exponentially suppressed by the larger mass of the field within the body.

There is a wide range of parameter space (about four orders of magnitude in the mass scale) allowed by current local and cosmological measurements as discussed in [135]. However, no calculation of the effect of this field on the Cosmic Microwave Background Radiaton anisotropies has yet been made. Given the similarity of this scenario to the model considered in chapter 5 (related simply by the addition of a runaway potential), it should be straightforward to investigate the CMB effects, with a view to providing tighter bounds on the parameters than are available from local measurements.

# Bibliography


[1] R. P. Feynman, *QED: The Strange Theory of Light and Matter.* Princeton University Press, 1985.

[2] A. S. Eddington, *The total eclipse of 1919 May 29 and the influence of gravitation on light*, *Observatory* **42** (1919) 119–122.

[3] A. S. Eddington, *Displacement of solar lines and the Einstein effect*, *Observatory* **43** (1920) 228–229.

[4] E. Hubble, *A Relation between Distance and Radial Velocity among Extra-Galactic Nebulae*, *Proc. Nat. Acad. Sci.* **15** (1929) 168.

[5] T. Kaluza, *Zum Unitätsproblem der Physik*, *Sitz. Preuss. Akad. Wissen.* **96** (1921) 69.

[6] O. Klein, *Quantentheorie und fünfdimensionale Relativitätstheorie*, *Zeit. fur Physik* **37** (1926) 895–906.

[7] A. A. Penzias and R. W. Wilson, *A Measurement of Excess Antenna Temperature at 4080 mc/s*, *Ap. J.* **142** (1965) 419–421.

[8] G. F. Smoot *et. al.*, *Structure in the COBE differential microwave radiometer first-year maps*, *Ap. J.* **396** (1992) L1–L5.

[9] C. Brans and R. H. Dicke, *Mach's principle and a relativistic theory of gravitation*, *Phys. Rev.* **124** (1961) 925–935.

[10] C. Will, *Theory and Experiment in Gravitational Physics.* Cambridge University Press, 1993.

[11] Y. Fujii and K.-I. Maeda, *The Scalar–Tensor Theory of Gravitation.* Cambridge University Press, 2003.

[12] G. F. Smoot, G. M. V., and M. R. A., *Detection of anisotropy in the cosmic blackbody radiation*, *Phys. Rev. Lett.* **39** (1977) 898.

[13] R. Durrer, *Physics of Cosmic Microwave Background anisotropies and primordial fluctuations*, `astro-ph/0109274`.

[14] M. Zaldarriga, *The Polarization of the Cosmic Microwave Background*, astro-ph/0305272.

[15] W. Hu, *CMB Temperature and Polarization Anisotropy Fundamentals*, *Annals Phys.* (2003) [astro-ph/0210696].

[16] E. L. Wright, *Theoretical Overview of Cosmic Microwave Background Anisotropy*, astro-ph/0305591.

[17] P. J. Steinhardt and M. S. Turner, *Prescription for Successful New Inflation*, *Phys. Rev.* **D29** (1984) 2162.

[18] A. J. Tolley, N. Turok, and P. J. Steinhardt, *Cosmological Perturbations in a Big Crunch/Big Bang Space-time*, hep-th/0306109.

[19] U. Seljak and M. Zaldarriaga, *A line of sight integration approach to Cosmic Microwave Background Anisotropies*, *Ap. J.* **469** (1996) 437–444, [astro-ph/9603033].

[20] C. L. Bennett, M. Halpern, G. Hinshaw, N. Jarosik, A. Kogut, M. Limon, S. S. Meyer, L. Page, D. N. Spergel, G. S. Tucker, E. Wollack, E. L. Wright, C. Barnes, M. R. Greason, R. S. Hill, E. Komatsu, M. R. Nolta, N. Odegard, H. Peiris, L. Verde, and J. L. Weiland, *First Year Wilkinson Microwave Anisotropy Probe (WMAP) Observations: Preliminary Maps and Basic Results*, *Ap. J. Suppl.* **148** (2003) 1, [astro-ph/0302207].

[21] E. M. Leitch, J. M. Kovac, C. Pryke, B. Reddall, E. S. Sandberg, M. Dragovan, J. E. Carlstrom, N. W. Halverson, and W. L. Holzapfel, *Measuring Polarization with DASI*, *Nature* **420** (2002) 763–771, [astro-ph/0209476].

[22] R. V. Wagoner, *Big bang nucleosynthesis revisited*, *Ap. J.* **179** (1973) 343–360.

[23] S. Weinberg, *Gravitation and Cosmology.* John Wiley & Sons, 1972.

[24] E. W. Kolb and M. S. Turner, *The Early Universe.* Addison Wesley Publishing Company, 1990.

[25] C. J. Hogan, *Big bang nucleosynthesis and the observed abundances of light elements*, in *Critical Dialogues in Cosmology* (N. Turok, ed.), Singapore: World Scientific, 1997.

[26] P. Hořava and E. Witten, *Heterotic and Type I String Dynamics from Eleven Dimensions*, *Nucl. Phys.* **B460** (1996) 506–524, [hep-th/9510209].

[27] P. Hořava and E. Witten, *Eleven-Dimensional Supergravity on a Manifold with Boundary*, *Nucl. Phys.* **B475** (1996) 94–114, [hep-th/9603142].

[28] A. Lukas, B. A. Ovrut, and D. Waldram, *Cosmological Solutions of Hořava-Witten Theory*, *Phys. Rev.* **D60** (1999) 086001, [hep-th/9806022].

[29] N. Arkani-Hamed, S. Dimopoulos, and G. Dvali, *The Heirarchy Problem and New Dimensions at a Millimeter*, *Phys. Lett.* **B429** (1998) 263–272, [hep-ph/9803315].

[30] I. Antoniadis, N. Arkani-Hamed, S. Dimopoulos, and G. Dvali, *New Dimensions at a Millimeter to a Fermi and Superstrings at a TeV*, *Phys. Lett.* **B436** (1998) [hep-ph/9804398].

[31] N. Arkani-Hamed, S. Dimopoulos, and G. Dvali, *Phenomenology, Astrophysics and Cosmology of Theories with Sub-Millimeter Dimensions and TeV Scale Quantum Gravity*, *Phys. Rev.* **D59** (1999) [hep-ph/9807344].

[32] G. Landsberg, *Mini-review on extra dimensions*, in *Proceedings of the XXXth International Conference on High Energy Physics*, ICHEP, 2000. hep-ex/0009038.

[33] The OPAL Collaboration, *Photonic events with missing energy in $e^+e^-$ collisions at $\sqrt{s} = 189 GeV$*, *Eur. Phys. J.* **C18** (2000) 253–272, [hep-ex/0005002].

[34] V. A. Rubakov and M. E. Shaposnikov, *Do we live inside a domain wall?*, *Phys. Lett.* **B125** (1983) 136.

[35] V. A. Rubakov and M. E. Shaposnikov, *Extra space-time dimensions: towards a solution to the cosmological constant problem*, *Phys. Lett.* **B125** (1983) 139.

[36] E. Squires, *Dimensional Reduction caused by a cosmological constant*, *Phys. Lett.* **B167** (1986) 286.

[37] M. Visser, *An exotic class of Kaluza-Klein models*, *Phys. Lett.* **B159** (1985) 22, [hep-th/9910093].

[38] L. Randall and R. Sundrum, *A Large Mass Hierarchy from a Small Extra Dimension*, *Phys. Rev. Lett.* **83** (1999) 3370–3373, [hep-th/9905221].

[39] L. Randall and R. Sundrum, *An Alternative to Compactification*, *Phys. Rev. Lett.* **83** (1999) 4690–4693, [hep-th/9906064].

[40] R. Kallosh and A. Linde, *Supersymmetry and the Brane World*, JHEP **0002** (2000) 005, [hep-th/0001071].

[41] E. Bergshoeff, R. Kallosh, and A. van Proyen, *Supersymmetry in Singular Spaces*, JHEP **0010** (2000) 033, [hep-th/0007044].

[42] P. Brax and A.-C. Davis, *Cosmological Solutions of Supergravity in Singular Spaces*, *Phys. Lett.* **B497** (2001) 289–295, [hep-th/0011045].

[43] P. Binétruy, C. Deffayet, and D. Langlois, *Non-conventional cosmology from a brane-universe*, *Nucl. Phys.* **B565** (2000) 269–287, [hep-th/9905012].

[44] A.-C. Davis, I. Vernon, S. C. Davis, and W. B. Perkins, *Brane World Cosmology Without the $Z_2$ Symmetry*, *Phys. Lett.* **B504** (2000) 254–261, [hep-th/0008132].

[45] C. Csáki, M. Graesser, C. Kolda, and J. Terning, *Cosmology of One Extra Dimension with Localized Gravity*, *Phys. Lett.* **B462** (1999) 34–40, [hep-ph/9906513].

[46] P. Brax and A.-C. Davis, *Cosmological Evolution on Self-Tuned Branes and the Cosmological Constant*, JHEP **0105** (2001) 008, [hep-th/0104023].

[47] D. J. H. Chung and K. Freese, *Can Geodesics in Extra Dimensions Solve the Cosmological Horizon Problem?*, *Phys. Rev.* **D62** (2000) 063513, [hep-ph/9910235].

[48] P. Brax, C. van de Bruck, and A.-C. Davis, *Brane-World Cosmology, Bulk Scalars and Perturbations*, JHEP **0110** (2001) 026, [hep-th/0108215].

[49] H. Stoica, S.-H. H. Tye, and I. Wasserman, *Cosmology in the Randall-Sundrum Brane World Scenario*, *Phys. Lett.* **B482** (2000) 205–212, [hep-th/0004126].

[50] N. Deruelle and T. Dolezel, *Brane versus shell cosmologies in Einstein and Einstein-Gauss-Bonnet theories*, *Phys. Rev.* **D62** (2000) 103502, [gr-qc/0004021].

[51] B. Carter and J. Uzan, *Reflection symmetry breaking scenarios with minimal gauge form coupling in brane world cosmology*, *Nucl. Phys.* **B606** (2001) 45–58, [gr-qc/0101010].

[52] R. A. Battye and B. Carter, *Generic junction conditions in brane-world scenarios*, *Phys. Lett.* **B509** (2001) 331–336, [hep-th/0101061].

[53] R. A. Battye, B. Carter, A. Mennim, and J.-P. Uzan, *Einstein equations for an asymmetric brane-world*, *Phys. Rev.* **D64** (2001) 124007, [hep-th/0105091].

[54] W. Mück, K. S. Viswanathan, and I. V. Volovich, *Geodesics and Newton's Law in Brane Backgrounds*, *Phys. Rev.* **D62** (2000) 105019, [hep-th/0002132].

[55] R. Caldwell and D. Langlois, *Shortcuts in the fifth dimension*, *Phys. Lett.* **B511** (2001) 129–135, [gr-qc/0103070].

[56] C. Csáki, J. Erlich, and C. Grojean, *Gravitational Lorentz Violations and Adjustment of the Cosmological Constant in Asymmetrically Warped Spacetimes*, *Nucl. Phys.* **B604** (2001) 312–342, [hep-th/0012143].

[57] P. Binétruy, C. Deffayet, and D. Langlois, *The Radion in Brane Cosmology*, *Nucl. Phys.* **B615** (2001) 219–236, [hep-th/0101234].

[58] P. Binétruy, C. Deffayet, U. Ellwanger, and D. Langlois, *Brane cosmological evolution in a bulk with cosmological constant*, *Phys. Lett.* **B477** (2000) 285–291, [hep-th/9910219].

[59] C. Charmousis, R. Gregory, and V. A. Rubakov, *Wave function of the radion in a brane world*, *Phys. Rev.* **D62** (2000) 067505, [hep-th/9912160].

[60] T. Tanaka and X. Montes, *Gravity in the brane-world for two-branes model with stabilized modulus*, *Nucl. Phys.* **B582** (2000) 259–276, [hep-th/0001092].

[61] U. Gen and M. Sasaki, *Radion on the de Sitter brane*, *Prog. Theor. Phys.* **105** (2001) 591–606, [gr-qc/0011078].

[62] A. Karch and L. Randall, *Locally Localized Gravity*, JHEP **0105** (2001) 008, [hep-th/0011156].

[63] A. Hebecker and J. March-Russell, *Randall-Sundrum II Cosmology, AdS/CFT, and the Bulk Black Hole*, hep-ph/0103214.

[64] C. Csáki, J. Erlich, T. J. Hollowood, and Y. Shirman, *Universal Aspects of Gravity Localized on Thick Branes*, *Nucl. Phys.* **B581** (2000) 309–338, [hep-th/0001033].

[65] L. Pilo, R. Rattazzi, and A. Zaffaroni, *The Fate of the Radion in Models with Metastable Graviton*, JHEP **0007** (2000) 056, [hep-th/0004028].

[66] J. Garriga, O. Pujolas, and T. Tanaka, *Radion effective potential in the Brane-World*, *Nucl. Phys.* **B605** (2001) 192–214, [hep-th/0004109].

[67] U. Gen and M. Sasaki, *Radion on the de Sitter brane*, *Prog. Theor. Phys.* **105** (2001) 591–606, [gr-qc/0011078].

[68] I. Kogan, S. Mouslopoulos, A. Papazoglou, and L. Pilo, *Radion in Multibrane World*, *Nucl. Phys.* **B625** (2002) 179–197, [hep-th/0105255].

[69] T. Wiseman, *Strong Brane Gravity and the Radion at Low Energies*, *Class. Quant. Grav.* **19** (2002) 3083–3106, [hep-th/0201127].

[70] J. E. Kim, B. Kyae, and H. M. Lee, *Wave function of the radion in the brane background with a massless scalar field and a self-tuning problem*, *Phys. Rev.* **D66** (2002) 106004, [hep-th/0110103].

[71] T. Chiba, *Scalar-Tensor Gravity in Two 3-brane System*, *Phys. Rev.* **D62** (2000) 021502, [gr-qc/0001029].

[72] I. Antoniadis, J. Iliopoulos, and T. N. Tomaras, *One-loop effective action around de Sitter space*, *Nucl. Phys.* **B462** (1996) 437–452, [hep-th/9510112].

[73] P. Brax and A.-C. Davis, *On Brane Cosmology and Naked Singularities*, *Phys. Lett.* **B513** (2001) 156–162, [hep-th/0105269].

[74] J. Garriga and T. Tanaka, *Gravity in the Randall-Sundrum Brane World*, *Phys. Rev. Lett.* **84** (2000) 2778–2781, [hep-th/9911055].

[75] T. Damour and K. Nordtvedt, *Tensor-scalar cosmological models and their relaxation toward general relativity*, *Phys. Rev.* **D48** (1993) 3436.

[76] J. Khoury and R.-J. Zhang, *On the Friedmann Equation in Brane-World Scenarios*, *Phys. Rev. Lett.* **89** (2002) 061302, [hep-th/0203274].

[77] S. Kanno and J. Soda, *Brane World Effective Action at Low Energies and the AdS/CFT Correspondence*, *Phys. Rev.* **D66** (2002) 043526, [hep-th/0205188].

[78] S. Kanno and J. Soda, *Radion and Holographic Brane Gravity*, *Phys. Rev.* **D66** (2002) 083506, [hep-th/0207029].

[79] K. Choi, H. B. Kim, and H. Kim, *Moduli Stabilization in Heterotic M-theory*, *Mod. Phys. Lett.* **A14** (1999) 125–134, [hep-th/9808122].

[80] T. Barreiro, B. de Carlos, and E. J. Copeland, *Stabilizing the Dilaton in Superstring Cosmology*, *Phys. Rev.* **D58** (1998) 083513, [hep-th/9805005].

[81] P. J. Steinhardt, *General considerations of the cosmological constant and the stabilization of moduli in the brane-world picture*, *Phys. Lett.* **B462** (1999) 41–47, [hep-th/9907080].

[82] G. Huey, P. J. Steinhardt, B. A. Ovrut, and D. Waldram, *A Cosmological Mechanism for Stabilizing Moduli*, *Phys. Lett.* **B476** (2000) 379–386, [hep-th/0001112].

[83] D. I. Santiago, D. Kalligas, and R. V. Wagoner, *Scalar-Tensor Cosmologies and their Late Time Evolution*, *Phys. Rev.* **D58** (1998) 124005, [gr-qc/9805044].

[84] T. Damour and K. Nordtvedt, *General Relativity as a cosmological attractor of tensor-scalar theories*, *Phys. Rev. Lett.* **70** (1993) 2217–2219.

[85] J. K. Webb, V. V. Flambaum, C. W. Churchill, M. J. Drinkwater, and J. D. Barrow, *A Search for Time Variation of the Fine Structure Constant*, *Phys. Rev. Lett.* **82** (1999) 884–887, [astro-ph/9803165].

[86] J. K. Webb, M. T. Murphy, V. V. Flambaum, V. A. Dzuba, J. D. Barrow, C. W. Churchill, J. X. Prochaska, and A. M. Wolfe, *Further Evidence for Variation of the Fine Structure Constant*, *Phys. Rev. Lett.* **87** (2001) 091301, [astro-ph/0012539].

[87] J. Garriga, O. Pujolas, and T. Tanaka, *Moduli effective action in warped brane world compactifications*, *Nucl. Phys.* **B655** (2003) 127–169, [hep-th/0111277].

[88] G. Cynolter, *Wave function of the radion with BPS branes*, `hep-th/0209152`.

[89] A. Lukas, B. A. Ovrut, and D. Waldram, *Boundary Inflation*, *Phys. Rev.* **D61** (2000) 023506, [`hep-th/9902071`].

[90] J. M. Cline and J. Vinet, *Order $\rho^2$ Corrections to Randall-Sundrum I Cosmology*, JHEP **0202** (2002) 042, [`hep-th/0201041`].

[91] J. Khoury, B. A. Ovrut, P. Steinhardt, and N. Turok, *The Ekpyrotic Universe: Colliding Branes and the Origin of the Hot Big Bang*, *Phys. Rev.* **D64** (2001) 123522, [`hep-th/0103239`].

[92] P. Steinhardt and N. Turok, *Cosmic Evolution in a Cyclic Universe*, *Phys. Rev.* **D65** (2002) 126003, [`hep-th/0111098`].

[93] R. Wald, *General Relativity.* University of Chicago Press, 1984.

[94] T. Damour, G. W. Gibbons, and C. Gundlach, *Dark matter, time-varying G, and a dilaton field*, *Phys. Rev. Lett.* **64** (1990) 123–126.

[95] T. Damour and C. Gundlach, *Nucleosynthesis constraints on an extended Jordan–Brans–Dicke theory*, *Phys. Rev.* **D43** (1991) 3873–3877.

[96] P. Brax and J. Martin, *The Robustness of Quintessence*, *Phys. Rev.* **D61** (2000) 103502, [`astro-ph/9912046`].

[97] T. Damour and G. Esposito-Farese, *Tensor-multi-scalar theories of gravitation*, *Class. Quant. Grav.* **9** (1992) 2093–2176.

[98] C. Wetterich, *Cosmology and the fate of dilaton symmetry*, *Nucl. Phys.* **B302** (1988) 668–696.

[99] B. Ratra and P. J. E. Peebles, *Cosmological consequences of a rolling homogeneous scalar field*, *Phys. Rev.* **D37** (1988) 3406–3427.

[100] P. G. Ferreira and M. Joyce, *Cosmology with a Primordial Scaling Field*, *Phys. Rev.* **D58** (1998) 023503, [`astro-ph/9711102`].

[101] P. Binétruy, *Models of dynamical supersymmetry breaking and quintessence*, *Phys. Rev.* **D60** (1999) 063502, [`hep-ph/9810553`].

[102] P. Brax and J. Martin, *Quintessence and Supergravity*, *Phys. Lett.* **B468** (1999) 40–45, [`astro-ph/9905040`].

[103] E. J. Copeland, N. J. Nunes, and F. Rosati, *Quintessence models in Supergravity*, *Phys. Rev.* **D62** (2000) 123503, [`hep-ph/0005222`].

[104] R. Kallosh, A. Linde, S. Prokushkin, and M. Shmakova, *Supergravity, Dark Energy and the Fate of the Universe*, *Phys. Rev.* **D66** (2002) 123503, [hep-th/0208156].

[105] J.-P. Uzan, *The fundamental constants and their variation: observational status and theoretical motivations*, *Rev. Mod. Phys.* **75** (2003) 403, [hep-th/0205340].

[106] T. Chiba, *Constancy of the Constants of Nature*, gr-qc/0110118.

[107] G. T. Horowitz and J. Polchinksi, *Instability of Spacelike and Null Orbifold Singularities*, *Phys. Rev.* **D66** (2002) 103512, [hep-th/0206288].

[108] H. Liu, G. Moore, and N. Seiberg, *Strings in Time-Dependent Orbifolds*, JHEP **0210** (2002) 031, [hep-th/0206182].

[109] A. Lukas, B. A. Ovrut, K. S. Stelle, and D. Waldram, *Heterotic M-theory in Five Dimensions*, *Nucl. Phys.* **B552** (1999) 246–290, [hep-th/9806051].

[110] S. Kanno and J. Soda, *Low Energy Effective Action for Dilatonic Braneworld –A Formalism for Inflationary Braneworld–*, hep-th/0303203.

[111] S. Kobayashi and K. Koyama, *Cosmology with Radion and Bulk Scalar Field in Two Branes Model*, JHEP **0212** (2002) 056, [hep-th/0210029].

[112] T. Shiromizu, K. Koyama, and K. Takahashi, *Effective theory for close limit of two branes*, *Phys. Rev.* **D67** (2003) 084022, [hep-th/0212331].

[113] K. Koyama, *CMB Anisotropies in Brane Worlds*, *Phys. Rev. Lett.* **91** (2003) 221301, [astro-ph/0303108].

[114] V. Faraoni, E. Gunzig, and P. Nardone, *Conformal transformations in classical gravitational theories and in cosmology*, *Fund. Cosmic Phys.* **20** (1999) 121, [gr-qc/9811047].

[115] C. M. Will, *The Confrontation between General Relativity and Experiment*, *Living Rev. Rel.* **4** (2001) 4, [gr-qc/0103036].

[116] N. Bartolo and M. Pietroni, *Scalar-Tensor Gravity and Quintessence*, *Phys. Rev.* **D61** (1999) 023518, [hep-ph/9908521].

[117] L. Amendola, *Coupled Quintessence*, *Phys. Rev.* **D62** (2000) 043511, [astro-ph/9908023].

[118] C.-P. Ma and E. Bertschinger, *Cosmological Perturbation Theory in the Synchronous and Conformal Newtonian Gauges*, *Ap. J.* **455** (1995) 7–25.

[119] L. Amendola and D. Tocchini-Valentini, *Baryon bias and structure formation in an accelerating universe*, *Phys. Rev.* **D66** (2002) 043528, [astro-ph/0111535].

[120] R. Durrer, *The theory of CMB Anisotropies*, *J. Phys. Stud.* **5** (2001) 177–215, [astro-ph/0109522].

[121] W. Hu and S. Dodelson, *Cosmic Microwave Background Anisotropies*, *Ann. Rev. Astron. Astrophys.* (2002).

[122] S. Dodelson, *Modern Cosmology.* Academic Press, 2003.

[123] W. Hu and N. Sugiyama, *Small Scale Cosmological Perturbations: An Analytic Approach*, *Astrophys. J.* **471** (1996) 542–570, [astro-ph/9510117].

[124] A. Lewis, A. Challinor, and A. Lasenby, *Efficient computation of CMB anisotropies in closed FRW Models*, *Ap. J.* **538** (2000) 473–476, [astro-ph/9911177].

[125] A. Lewis. private communication.

[126] L. Amendola, *Perturbations in a coupled scalar field cosmology*, *Mon. Not. Roy. Astron. Soc.* **312** (2000) 521, [astro-ph/9906073].

[127] L. Amendola, M. Gasperini, D. Tocchini-Valentini, and C. Ungarelli, *Early acceleration and adiabatic matter perturbations in a class of dilatonic dark-energy models*, *Phys. Rev.* **D67** (2003) 043512, [astro-ph/0208032].

[128] S. Gratton, J. Khoury, P. J. Steinhardt, and N. Turok, *Conditions for Generating Scale-Invariant Density Perturbations*, astro-ph/0301395.

[129] R. Gregory, V. A. Rubakov, and S. M. Sibiryakov, *Opening up extra dimensions at ultra-large scales*, *Phys. Rev. Lett.* **84** (2000) 5928–5931, [hep-th/0002072].

[130] G. R. Dvali, G. Gabadadze, and M. Porrati, *Metastable Gravitons and Infinite Volume Extra Dimensions*, *Phys. Lett.* **B484** (2000) 112–118, [hep-th/0002190].

[131] G. R. Dvali, G. Gabadadze, and M. Porrati, *4D Gravity on a Brane in 5D Minkowski Space*, *Phys. Lett.* **B485** (2000) 208–214, [hep-th/0005016].

[132] P. Binétruy and J. Silk, *Probing large distance higher-dimensional gravity with cosmic microwave background measurements*, *Phys. Rev. Lett.* **87** (2001) 031102, [astro-ph/0007452].

[133] L. Amendola and C. Quercellini, *Tracking and coupled dark energy as seen by WMAP*, *Phys. Rev.* **D68** (2003) 023514, [astro-ph/0303228].

[134] J. Khoury and A. Weltman, *Chameleon Fields: Awaiting Surprises for Tests of Gravity in Space*, astro-ph/0309300.

[135] J. Khoury and A. Weltman, *Chameleon Cosmology*, astro-ph/0309411.

[136] A. J. Sanders *et. al.*, *Project SEE (Satellite Energy Exchange): proposal for space-based gravitational measurements*, *Meas. Sci. Technol.* **10** (1999) 514–524.

[137] J. Mester *et. al.*, *The STEP mission: principles and baseline design*, *Class. Quant. Grav.* **18** (2001) 2475–2486.